



The gamma-ray galactic center excess with multi-messenger observations

Focus on recent work with:

IC, Zhong, McDermott, Surdutovich, PRD **105**, 103023 (2022)

McDermott, Zhong, **IC** MNRAS Letters, **522**, L21-L25 (2023)

Also ongoing work in Zhong, **IC** (in prep)

(will mention other works with Tim Linden and Dan Hooper as well)



THE INSTITUTE
FOR UNDERGROUND SCIENCE
AT SURF

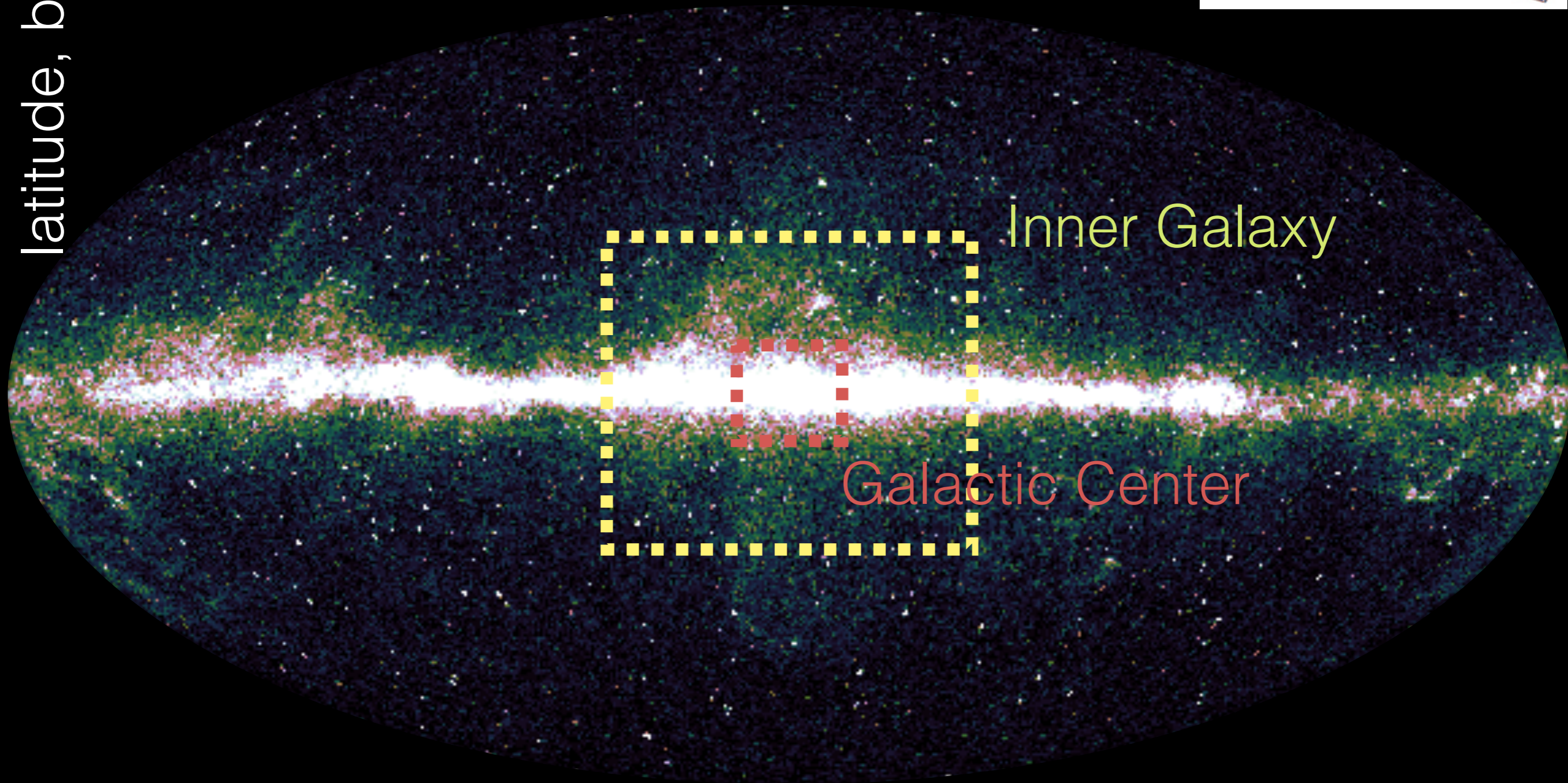
Ilias Cholis, 6/28/2023

third dimension (not shown) — energy

The Fermi-LAT Gamma-ray SKY



latitude, b ↑



Inner Galaxy

Galactic Center

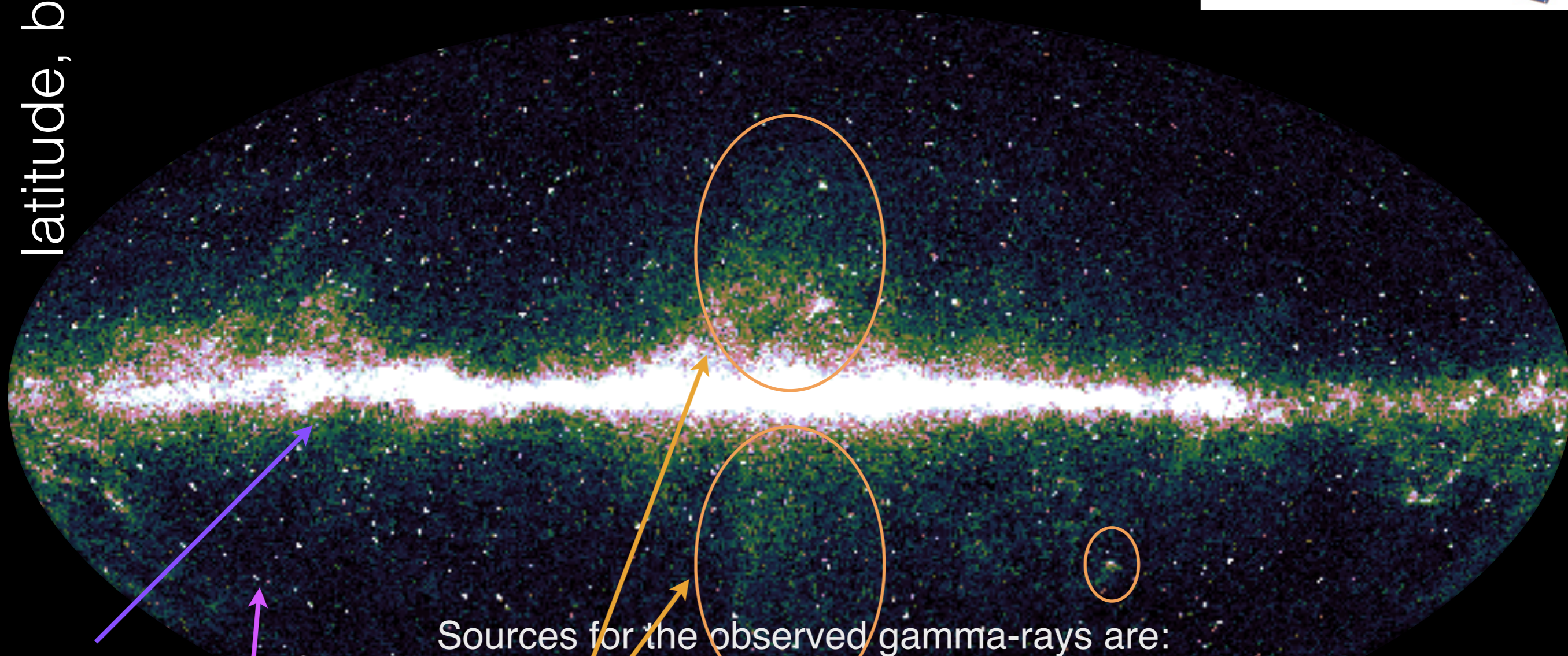
← Galactic longitude, l

third dimension (not shown) — energy

The Fermi-LAT Gamma-ray SKY



latitude, b ↑



Sources for the observed gamma-rays are:

- i) **Galactic Diffuse Emission**: decay of π^0 s (and other mesons) from pp (NN) collisions in the ISM, **bremsstrahlung radiation** off CR e, **Inverse Compton scattering**: up-scattering of CMB and IR/optical photons from CR e
- ii) from **point sources** (galactic or extra galactic)
- iii) **Extragalactic Isotropic**
- iv) **"extended sources"** (Fermi Bubbles, Geminga, Vela ...)
- iv) **misidentified CRs** (isotropic due to diffusion of CRs in the Galaxy)

Modeling the ISM galactic production and propagation uncertainties for cosmic rays

$$\begin{aligned} \frac{\partial \psi(r, p, t)}{\partial t} = & \overset{\text{sources}}{q(r, p, t)} + \overset{\text{diffusion}}{\vec{\nabla} \cdot (D_{xx} \vec{\nabla} \psi)} \\ & + \underset{\text{re-acceleration}}{\frac{\partial}{\partial p} \left[p^2 D_{pp} \frac{\partial}{\partial p} \left(\frac{\psi}{p^2} \right) \right]} + \underset{\text{convection}}{\frac{\partial}{\partial p} \left[\frac{p}{3} (\vec{\nabla} \cdot \vec{V}) \psi \right]} \end{aligned}$$

Voyager 1

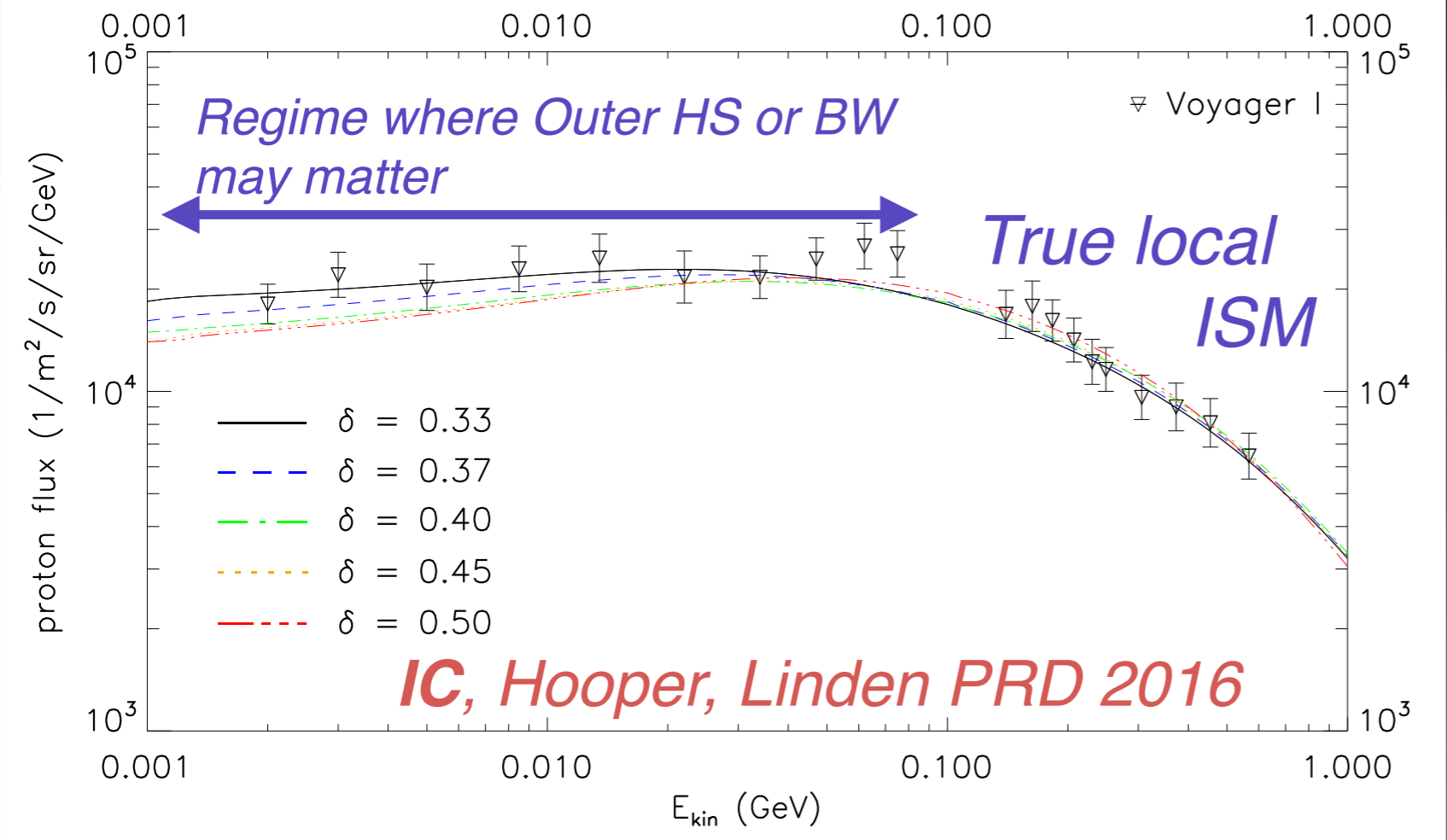


Modeling the ISM galactic production and propagation uncertainties for cosmic rays

$$\begin{aligned}
 \frac{\partial \psi(r, p, t)}{\partial t} &= \overset{\text{sources}}{q(r, p, t)} + \overset{\text{diffusion}}{\vec{\nabla} \cdot (D_{xx} \vec{\nabla} \psi)} \\
 &+ \overset{\text{re-acceleration}}{\frac{\partial}{\partial p} \left[p^2 D_{pp} \frac{\partial}{\partial p} \left(\frac{\psi}{p^2} \right) \right]} + \overset{\text{convection}}{\frac{\partial}{\partial p} \left[\frac{p}{3} (\vec{\nabla} \cdot \vec{V}) \psi \right]}
 \end{aligned}$$

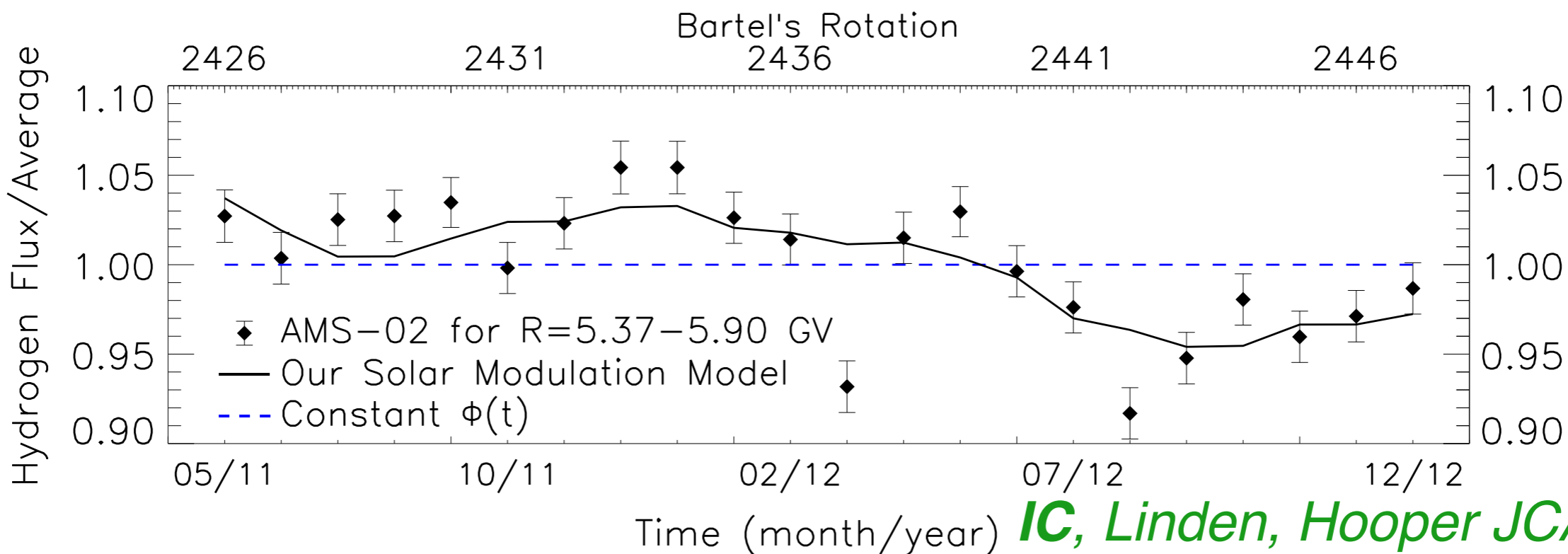
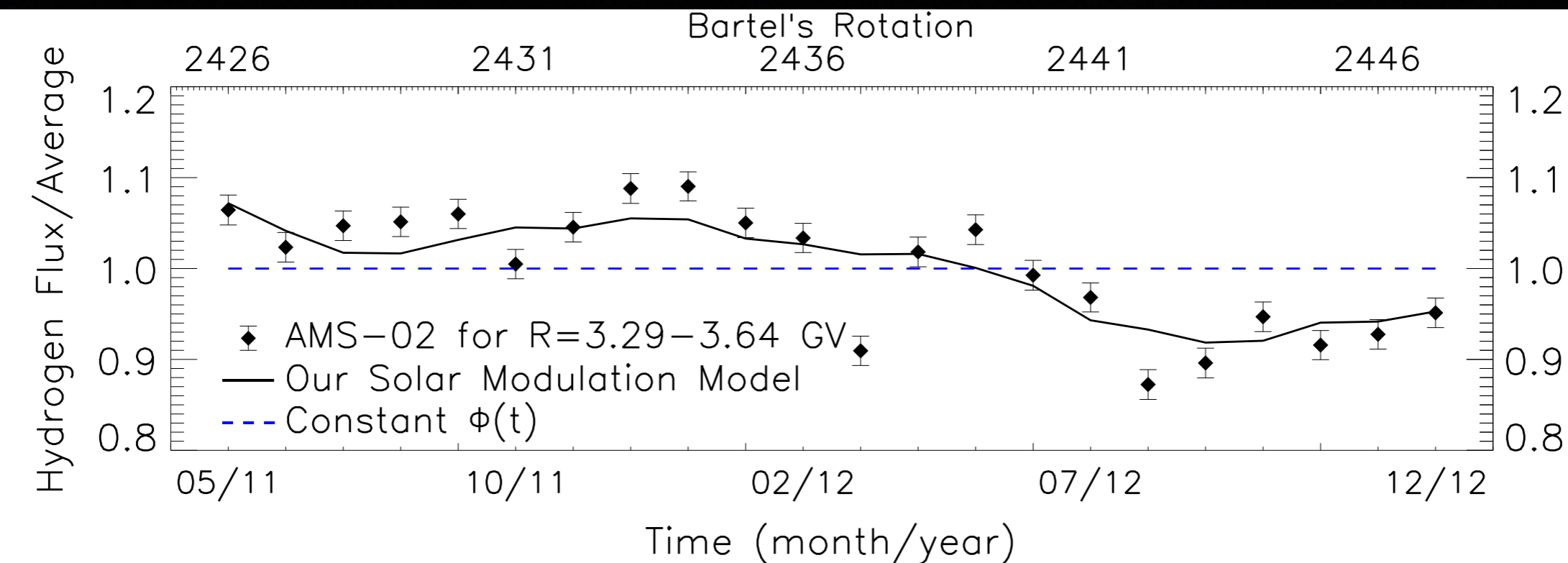


Voyager 1 (ISM) proton flux:



We use GALPROP a numerical solver build by Moskalenko, Strong et al. as a starting point and build several models that are in agreement with CR measurements

Cross-checking with the PROTON data that account for the majority of observed cosmic rays; monthly AND total (i.e ISM & Solar Modulation):

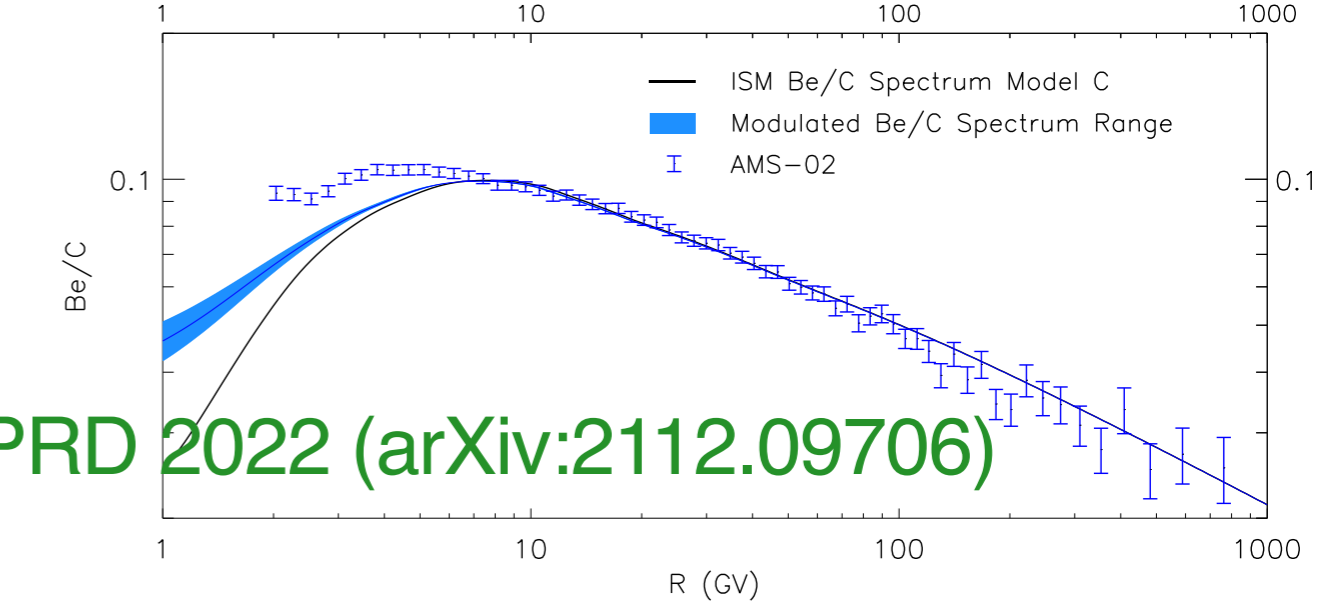
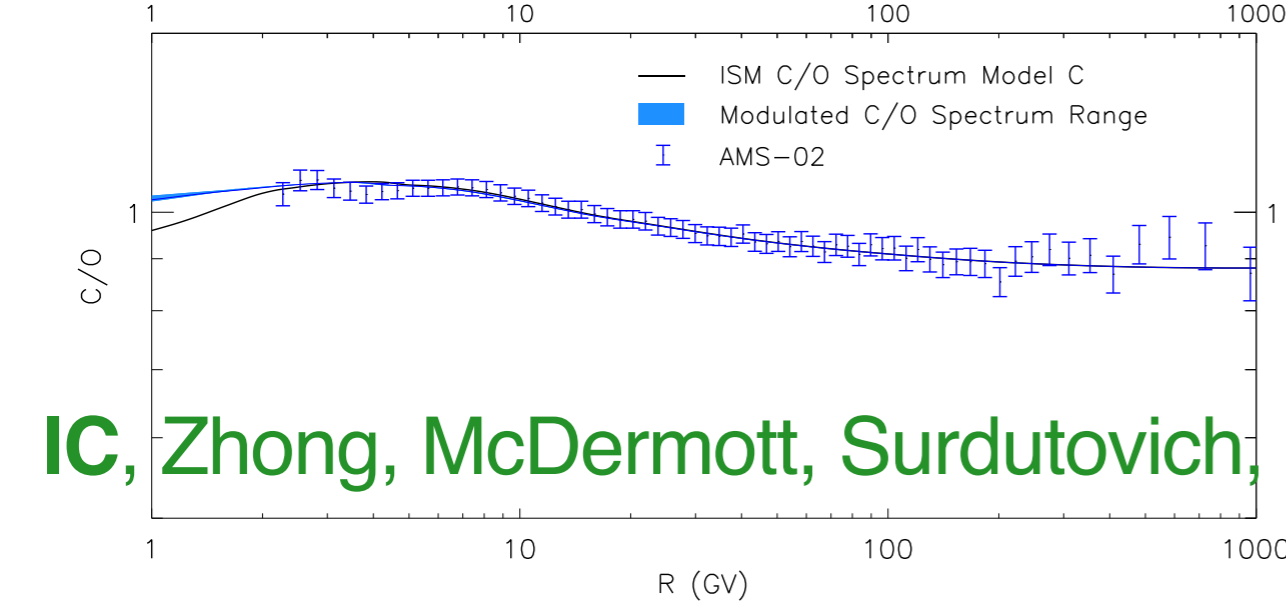
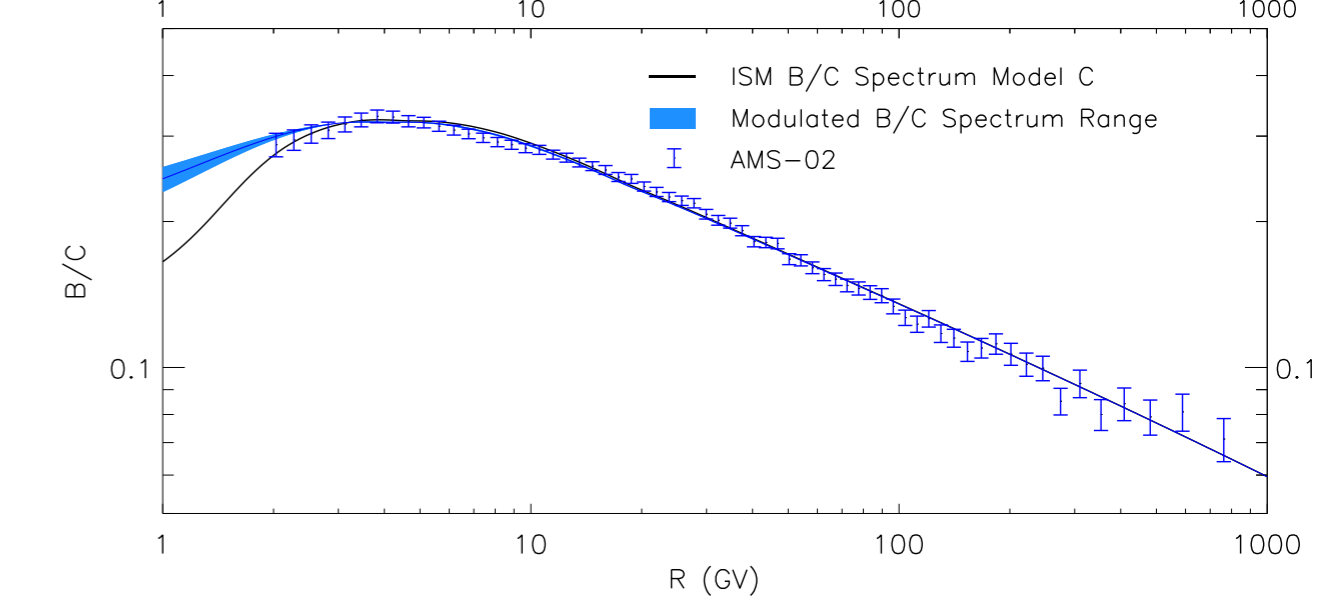
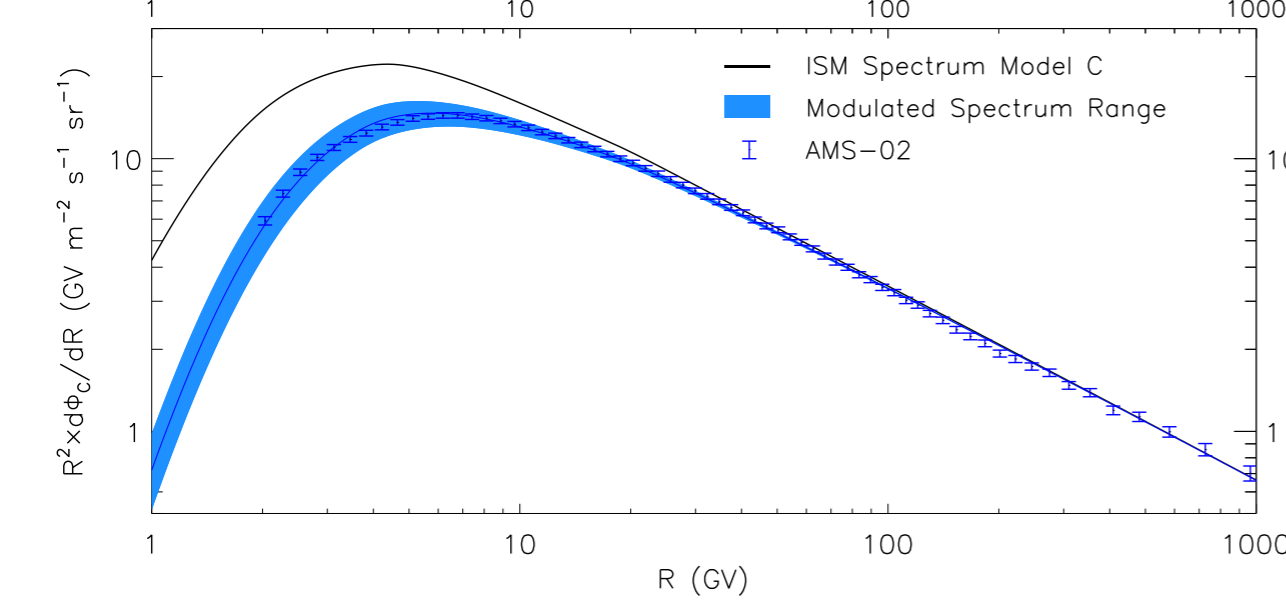
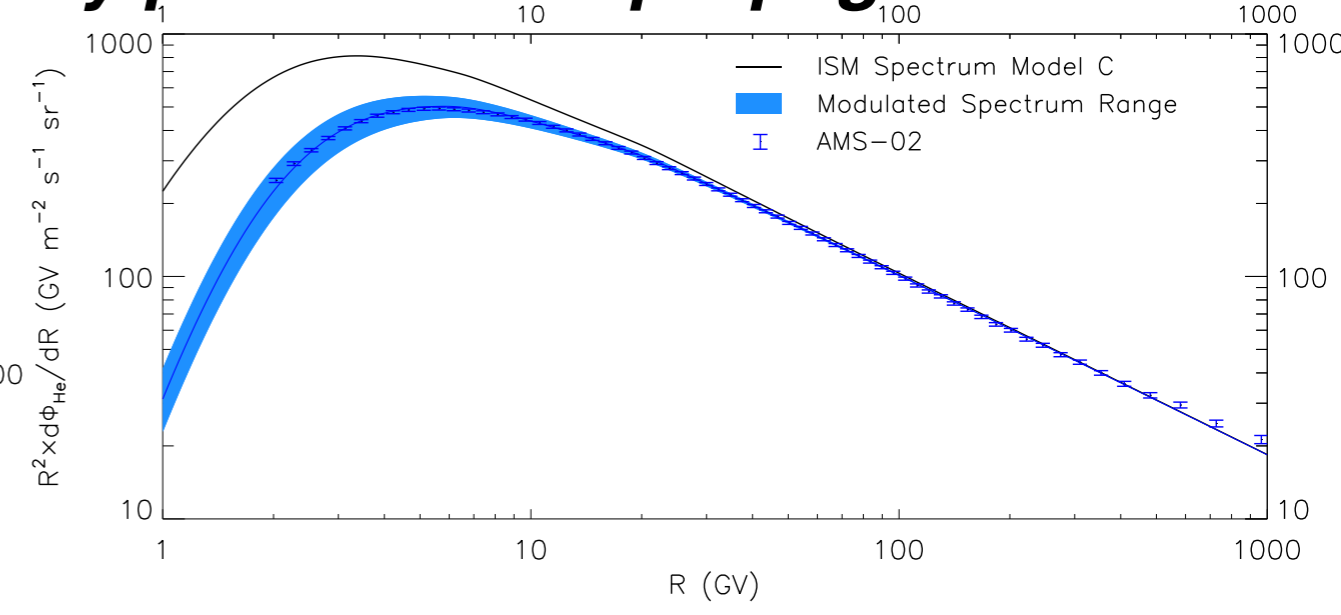
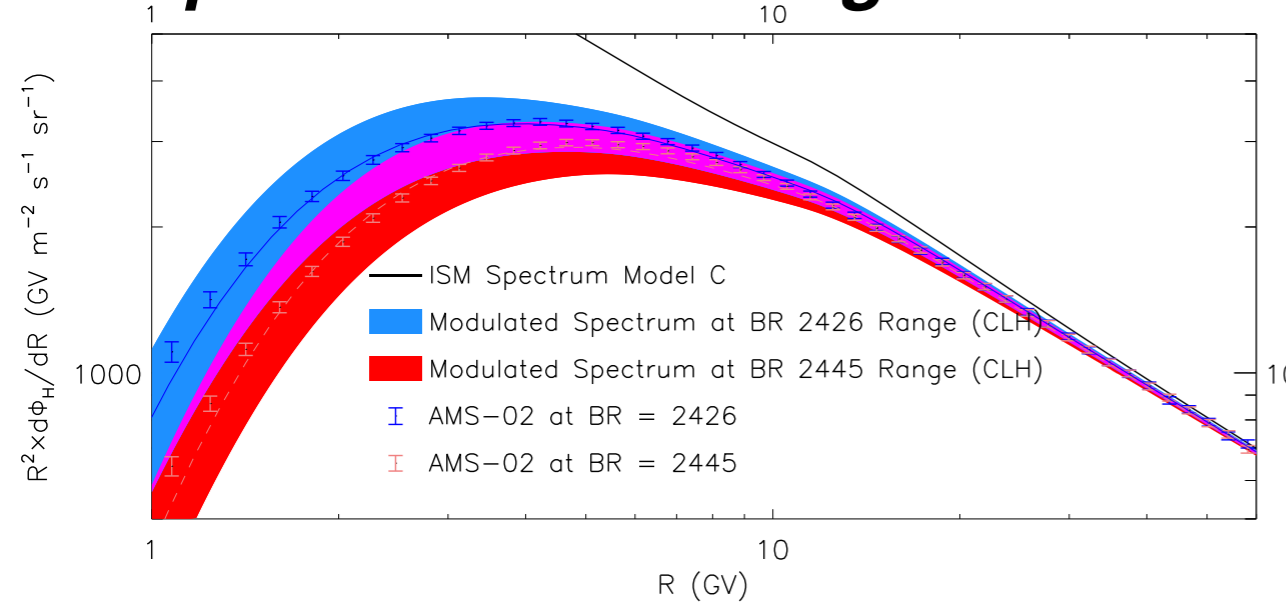


IC, Linden, Hooper JCAP 2022

Constraining the form of the Modulation potential and the ISM p spectrum in a recursive manner.

Also IC, McKinnon PRD 106, 063021 2022

Repeating for multiple Cosmic-Ray species we can constrain the physical processes affecting the cosmic-ray production & propagation



IC, Zhong, McDermott, Surdutovich, PRD 2022 (arXiv:2112.09706)

The ISM propagation conditions that fit the local spectra

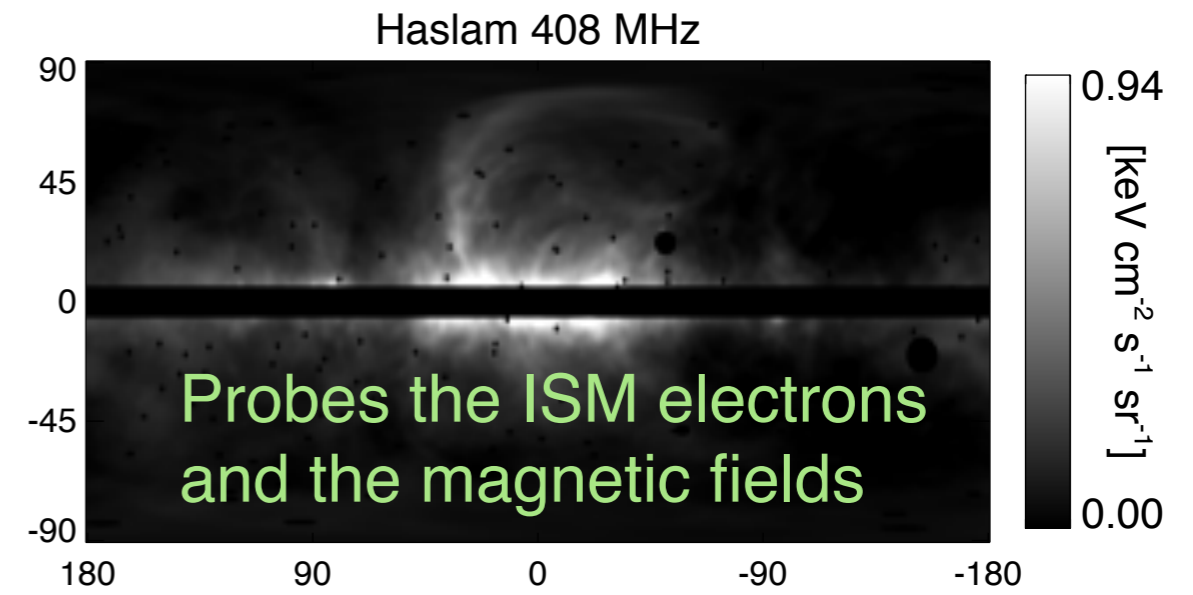
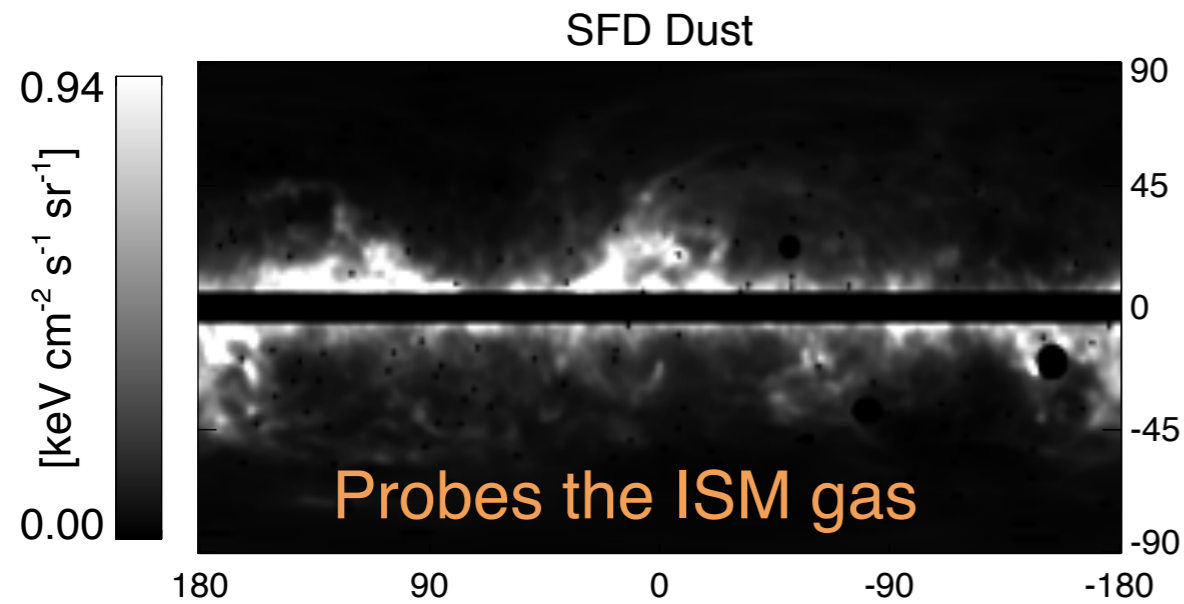
TABLE I. The cosmic-ray propagation assumptions (CR model), determined by the diffusion index δ , the diffusion scale height z_L , the normalization of the diffusion co-efficient D_0 , the Alfvén velocity v_A , the galactic convection gradient dv_c/dv , the injection indices α_1 , α_2 , α_3 , and the rigidity breaks R_{br_1} and R_{br_2} for cosmic-ray hydrogen and helium isotopes. In the last five columns, the first values refer to hydrogen injection properties and the second values to helium.

CR model	δ	z_L (kpc)	$D_0 \times 10^{28}$ (cm ² /s)	v_A (km/s)	$dv_c/d z $ (km/s/kpc)	α_1 H/He	R_{br_1} H/He (GV)	α_2 H/He	R_{br_2} H/He (GV)	α_3 H/He
A	0.33	5.7	6.70	30.0	0	1.74/1.70	6.0/7.4	2.04/2.16	14.0/21.5	2.41/2.39
B	0.37	5.5	5.50	30.0	2	1.72/1.74	6.0/8.0	2.00/2.14	12.4/21.0	2.38/2.375
C	0.40	5.6	4.85	24.0	1	1.69/1.65	6.0/6.7	2.00/2.13	12.4/20	2.38/2.355
D	0.45	5.7	3.90	24.0	5.5	1.69/1.68	6.0/7.0	1.99/2.12	12.4/18.7	2.355/2.34
E	0.50	6.0	3.10	23.0	9	1.71/1.68	6.0/7.2	2.02/2.14	11.2/17.5	2.38/2.33
F	0.43	3.0	1.85	20.0	2	1.68/1.74	6.0/10.5	2.08/2.09	13.0/21.0	2.41/2.33

This is a **starting point**.

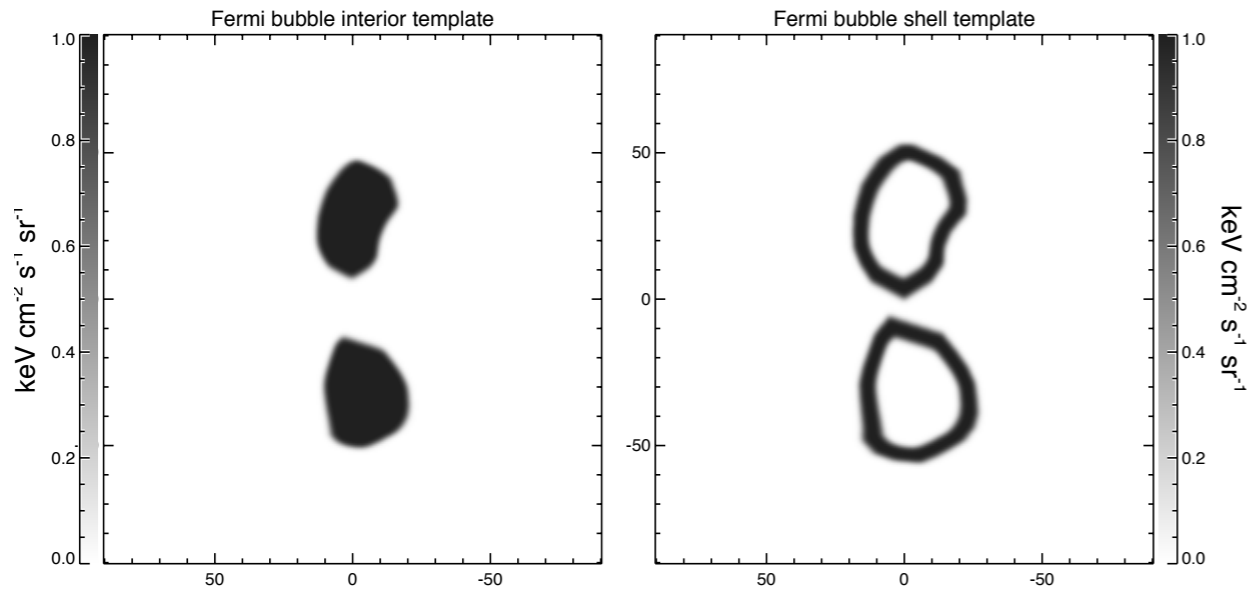
Using templates on Gamma-ray maps → It's first use led to the discovery of the Fermi(Haze)-Bubbles

Dobler, Finkbeiner, **IC**, Slatyer, Weiner, ApJ, 2010

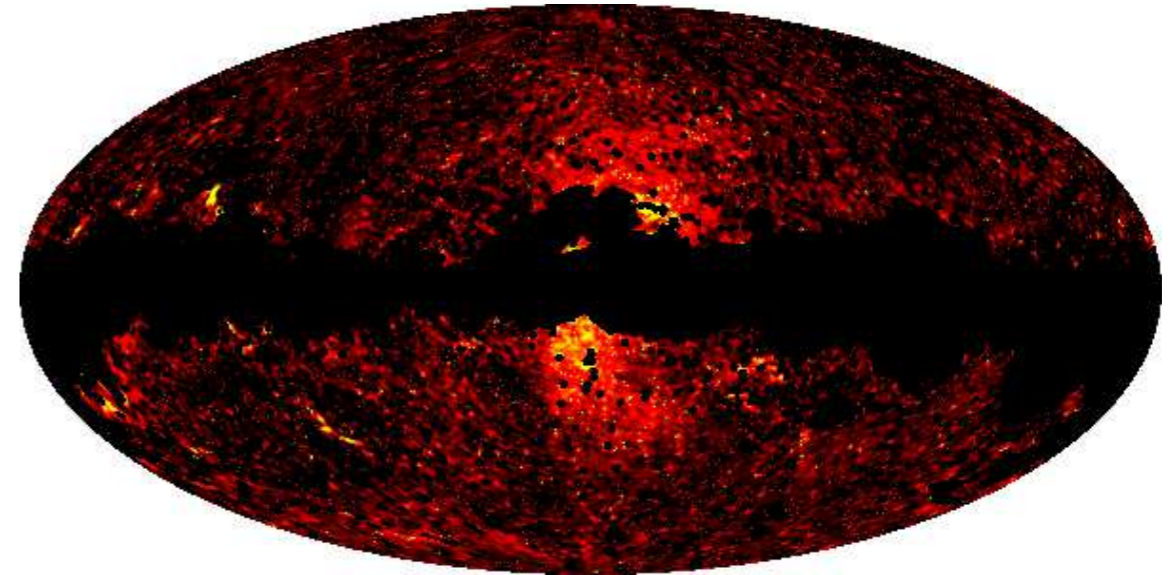


Fermi Bubbles

Su et al. ApJ 724, 1044 (2010)



Planck intermediate results. IX. Detection of the Galactic haze with Planck



Discovery of **edges** on the emission.

Planck Coll. A&A 2013

Residual intensity, $E = 10 - 500$ GeV

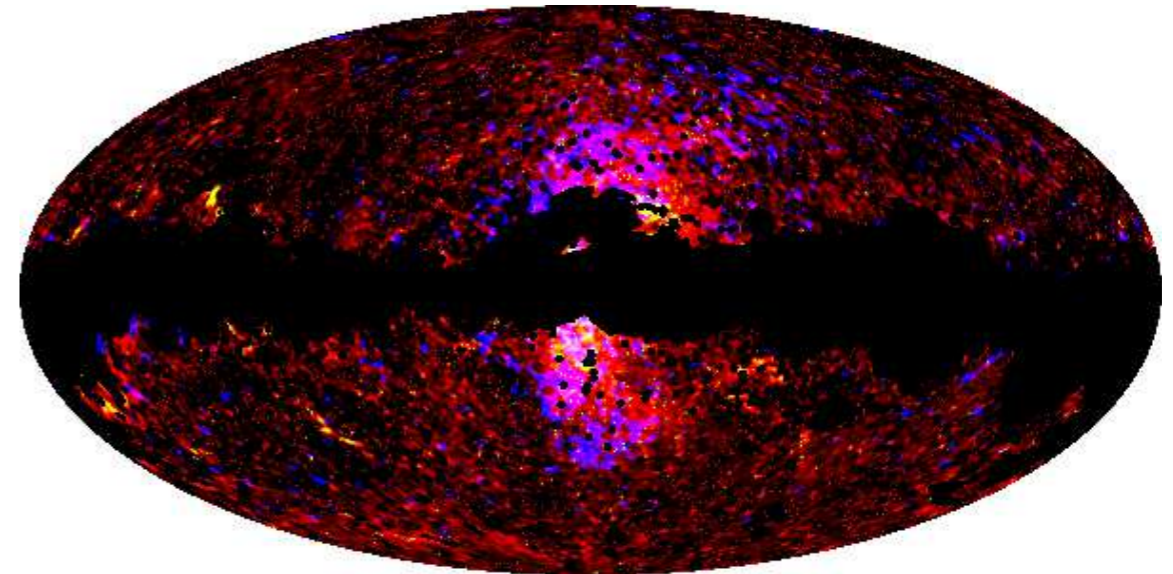
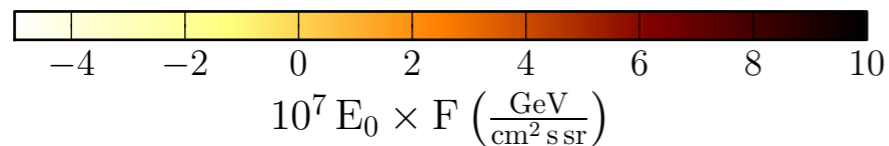
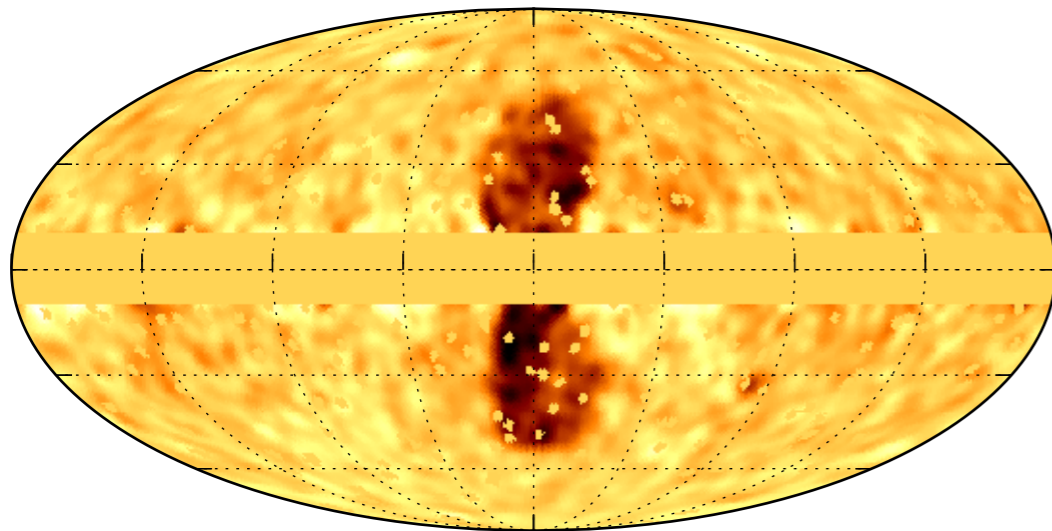
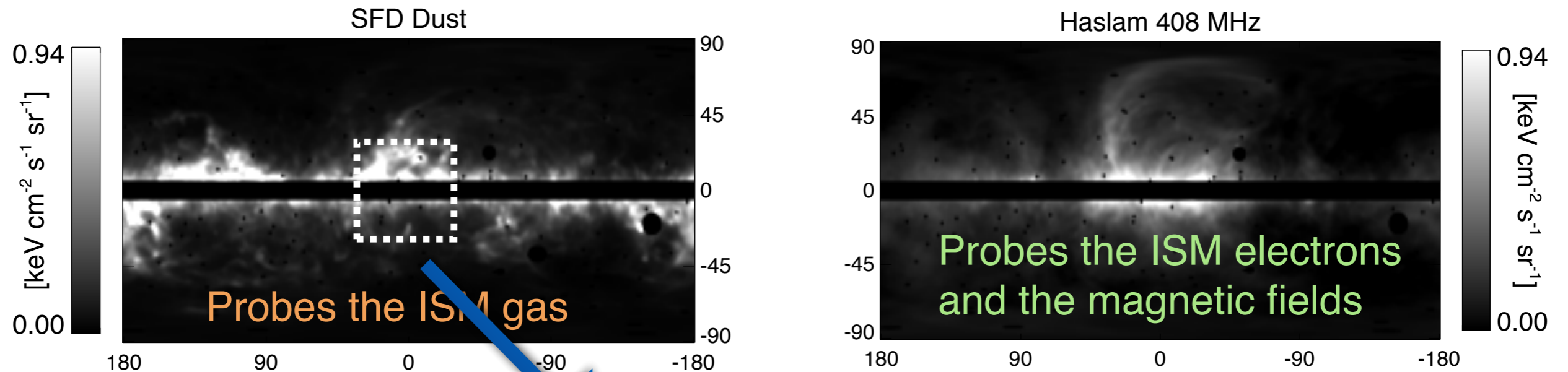


Fig.9. Top: The microwave haze at Planck 30 GHz (red, $-12 \mu\text{K} < \Delta T_{\text{CMB}} < 30 \mu\text{K}$) and 44 GHz (yellow, $12 \mu\text{K} < \Delta T_{\text{CMB}} < 40 \mu\text{K}$). Bottom: The same but including the Fermi 2-5 GeV haze/bubbles of [Dobler et al. \(2010\)](#) (blue, $1.05 < \text{intensity} [\text{keV cm}^{-2} \text{s}^{-1} \text{sr}^{-1}] < 1.25$; see their Fig. 11). The spatial correspondence between the two is excellent, particularly at low southern Galactic latitude, suggesting that this is a multi-wavelength view of the same underlying physical mechanism.

Fermi-LAT Collaboration
Result ApJ 2014

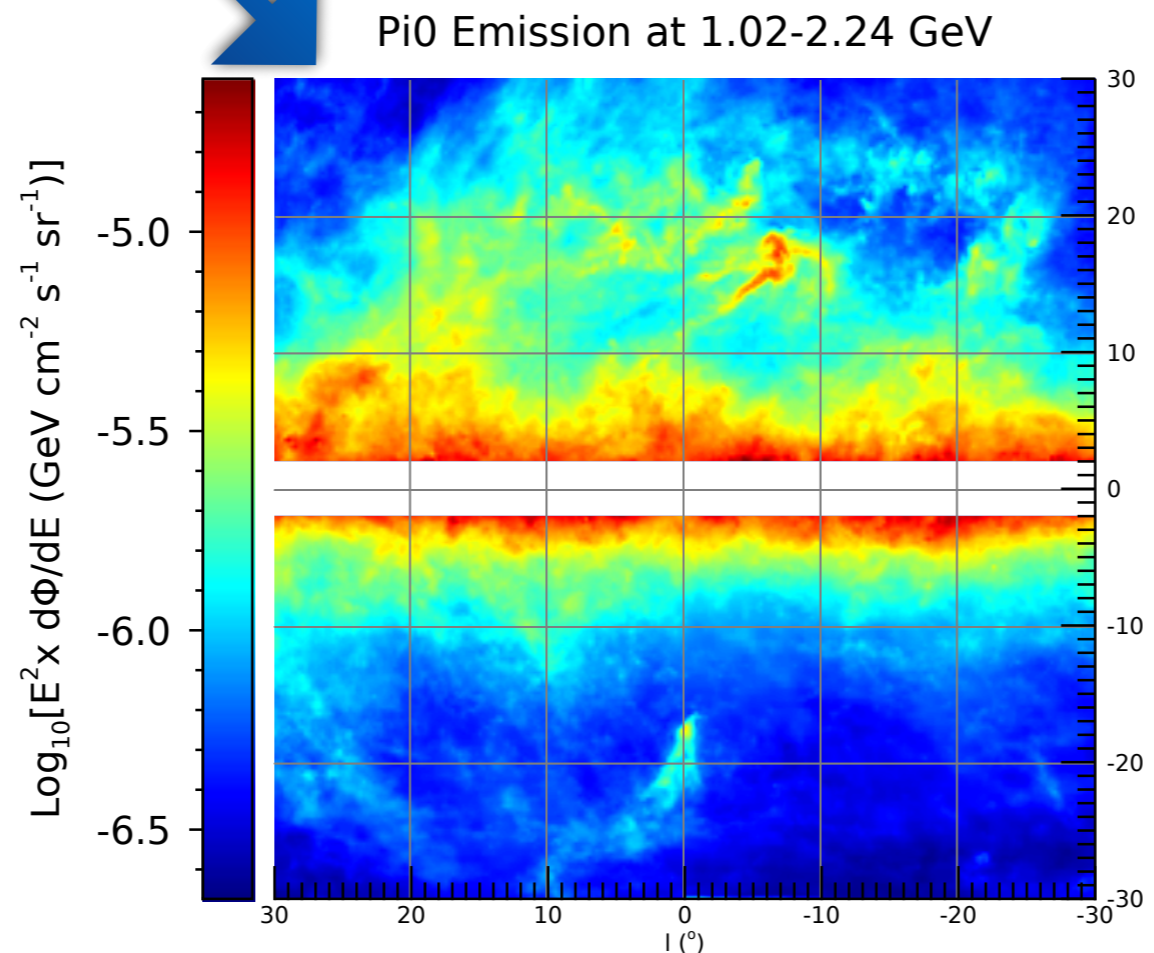
Using templates on Gamma-ray maps

Dobler, Finkbeiner, IC, Slatyer, Weiner, ApJ, 2010



Adding ISM physics, cosmic-ray observations and running an array of Milky Way simulations

...



60 degrees in latitude

The ISM propagation conditions that fit the local spectra

TABLE I. The cosmic-ray propagation assumptions (CR model), determined by the diffusion index δ , the diffusion scale height z_L , the normalization of the diffusion co-efficient D_0 , the Alfvén velocity v_A , the galactic convection gradient dv_c/dv , the injection indices α_1 , α_2 , α_3 , and the rigidity breaks R_{br_1} and R_{br_2} for cosmic-ray hydrogen and helium isotopes. In the last five columns, the first values refer to hydrogen injection properties and the second values to helium.

CR model	δ	z_L (kpc)	$D_0 \times 10^{28}$ (cm ² /s)	v_A (km/s)	$dv_c/d z $ (km/s/kpc)	α_1 H/He	R_{br_1} H/He (GV)	α_2 H/He	R_{br_2} H/He (GV)	α_3 H/He
A	0.33	5.7	6.70	30.0	0	1.74/1.70	6.0/7.4	2.04/2.16	14.0/21.5	2.41/2.39
B	0.37	5.5	5.50	30.0	2	1.72/1.74	6.0/8.0	2.00/2.14	12.4/21.0	2.38/2.375
C	0.40	5.6	4.85	24.0	1	1.69/1.65	6.0/6.7	2.00/2.13	12.4/20	2.38/2.355
D	0.45	5.7	3.90	24.0	5.5	1.69/1.68	6.0/7.0	1.99/2.12	12.4/18.7	2.355/2.34
E	0.50	6.0	3.10	23.0	9	1.71/1.68	6.0/7.2	2.02/2.14	11.2/17.5	2.38/2.33
F	0.43	3.0	1.85	20.0	2	1.68/1.74	6.0/10.5	2.08/2.09	13.0/21.0	2.41/2.33

This is a **starting point**. For the inner galaxy we allow for **greater ranges** to account for uncertainties on the ISM conditions of the inner galaxy. As:

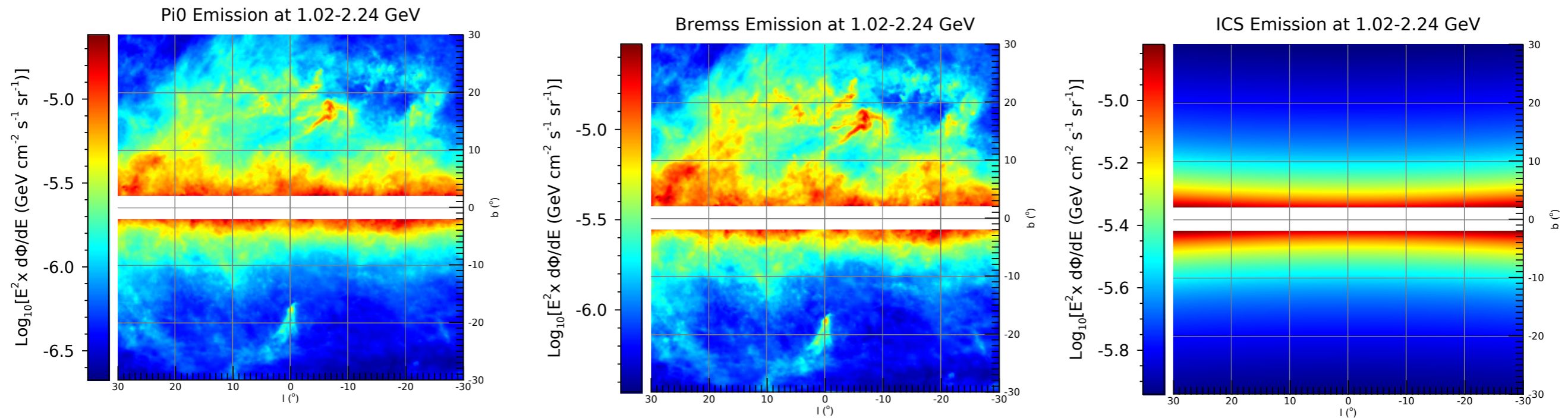
TABLE II. Galactic diffuse model parameters z_L is in kpc, D_0 is in $\times 10^{28}$ cm²/s, v_A is in km/s, $dv_c/d|z|$ is in km/s/kpc. N^p and N^e are the cosmic-ray proton and electron differential flux dN/dE normalizations at the galactocentric distance of 8.5 kpc. They are defined at 100 and 34.5 GeV for the protons and electrons respectively and are in units of $\times 10^{-9}$ cm⁻² s⁻¹ sr⁻¹ MeV⁻¹. See text for full details.

Name	z_L	D_0	δ	v_A	$dv_c/d z $	S^N/S^e	α_1^p/α_2^p	α_1^e/α_2^e	N^p/N^e	B-field	ISRF	H2	HI	HII
I	4.0	5.00	0.33	32.7	55	Pul/Pul	1.35/2.33	1.5/2.25	4.13/3.33	200030050	1.36,1.36,1.0	9	5	1
II	6.0	7.1	0.33	50.0	0	Pul/SNR	1.89/2.30	1.40/2.10	2.40/2.20	050100020	1.0,1.0,1.0	2*	1	1
III	5.6	4.85	0.40	40.0	0	Pul/Pul	1.50/1.90	1.5/2.25	2.40/1.55	200050040	1.4,1.4,1.0	9	4	1
VI	6.0	2.00	0.33	0	200	Pul/SNR	1.60/2.10	1.6/2.30	2.32/5.70	200030050	1.4,1.4,1.0	9	5	1
X	10.0	8.00	0.33	32.2	50	Pul/SNR	1.40/1.80	1.4/2.35	1.90/3.20	200040050	1.4,1.4,1.0	0	5	2
XV	6.0	7.10	0.33	50.0	0	Pul/SNR	1.89/2.30	1.40/2.10	2.40/2.20	050100020	1.0,1.0,1.0	0	5	2

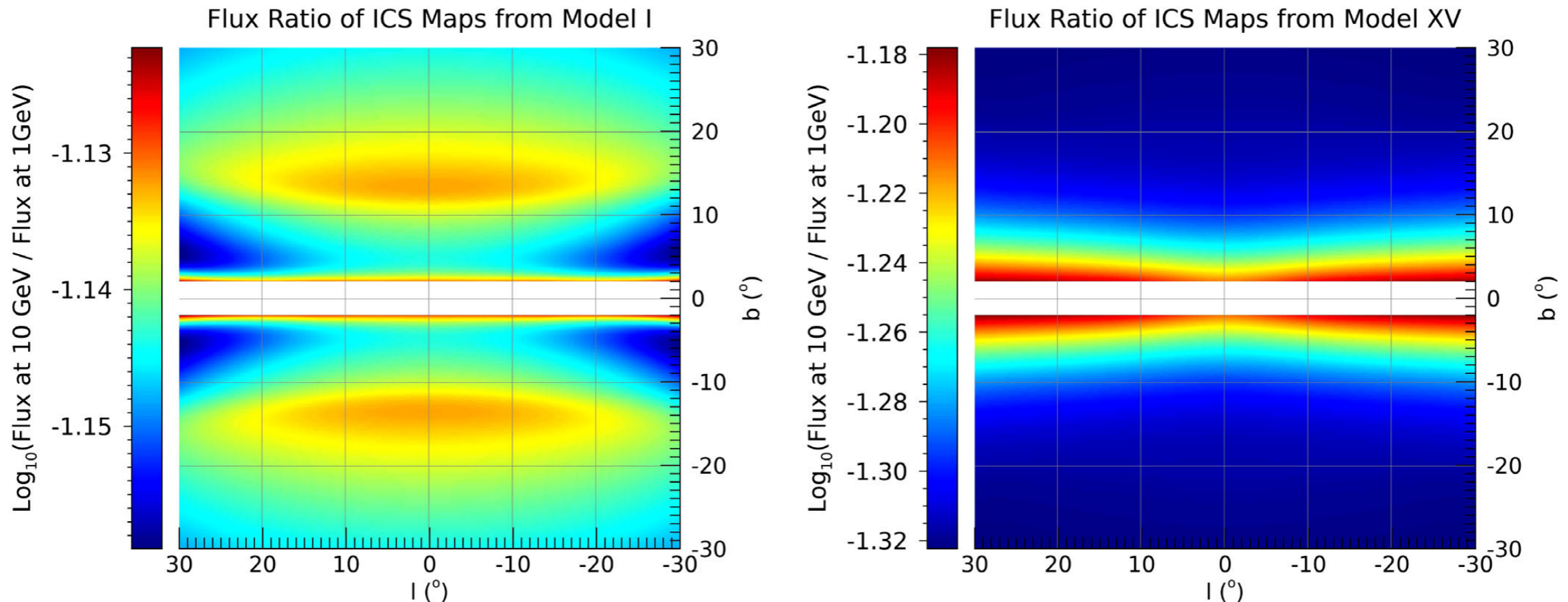
...

LXXX	5.6	4.85	0.40	40.0	0	Pul/Pul	1.50/1.90	1.5/2.25	2.40/1.55	200050040	1.4,1.4,1.0	0	4	3
------	-----	------	------	------	---	---------	-----------	----------	-----------	-----------	-------------	---	---	---

Every model predicts its own unique combination of diffuse emission maps:

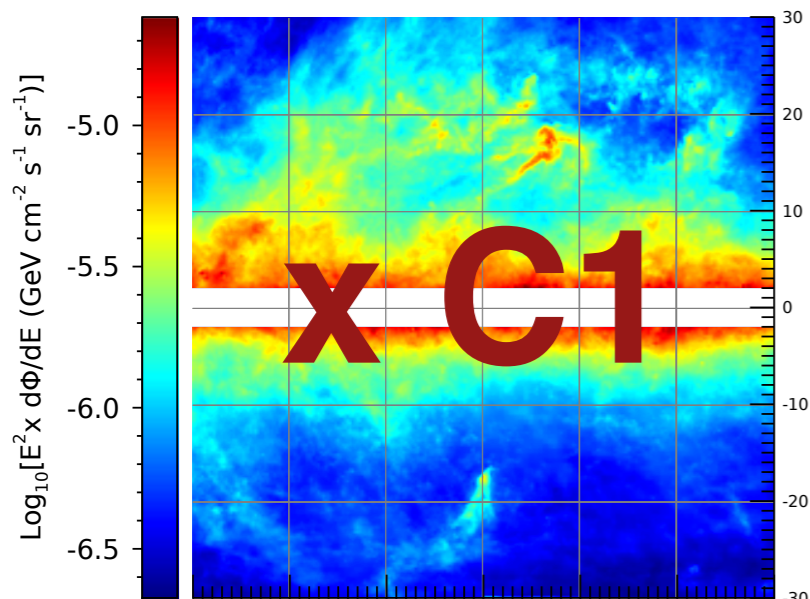


And energy evolution:

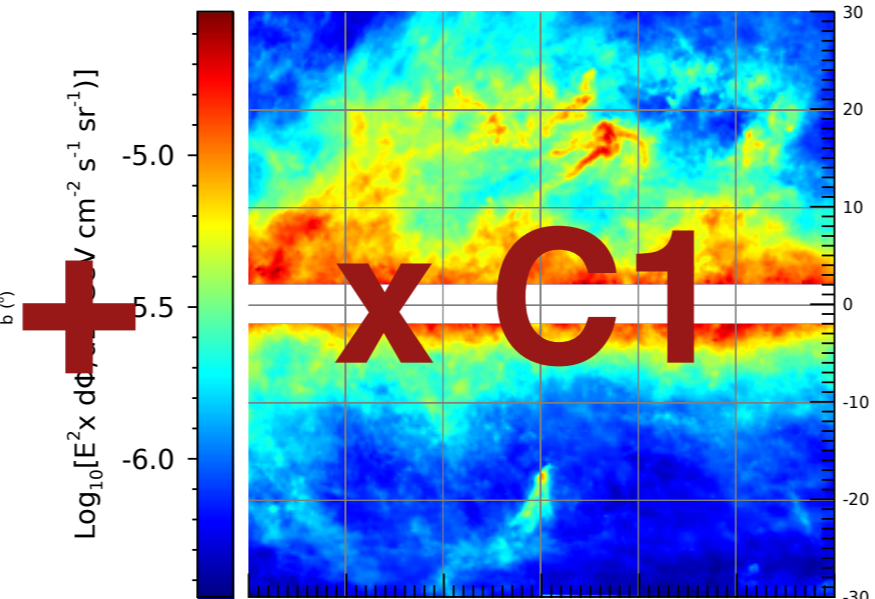


IC, Zhong, McDermott, Surdutovich, PRD 2022

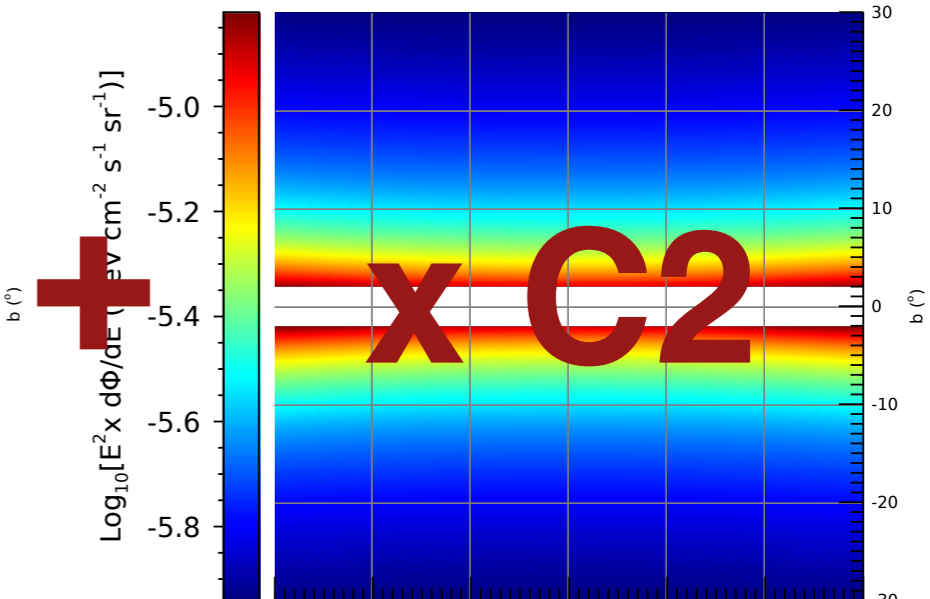
Pi0 Emission at 1.02-2.24 GeV



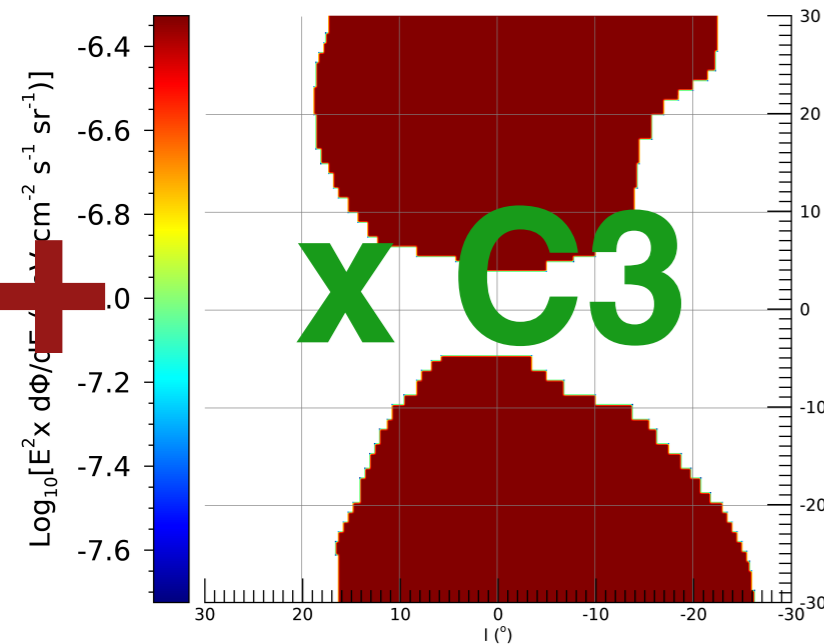
Bremss Emission at 1.02-2.24 GeV



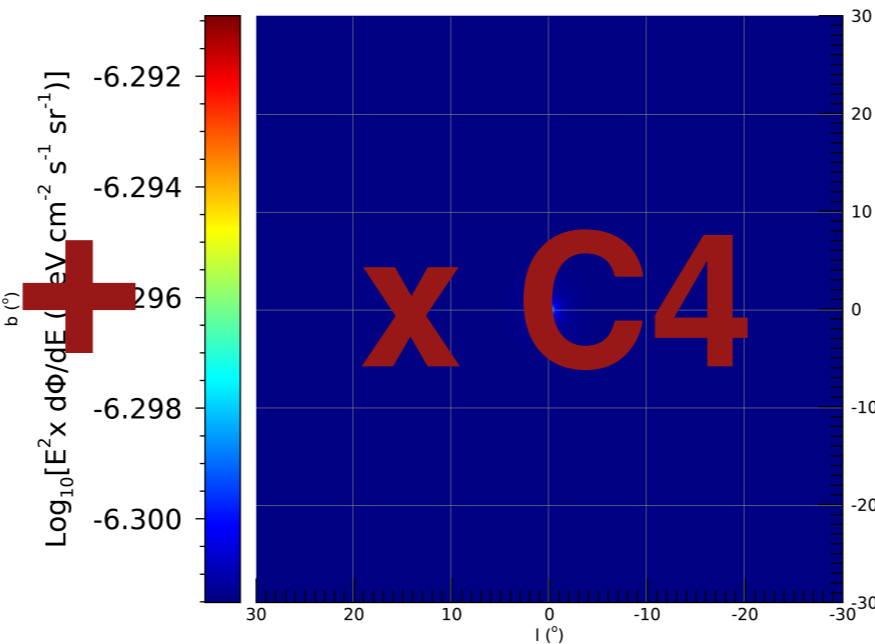
ICS Emission at 1.02-2.24 GeV



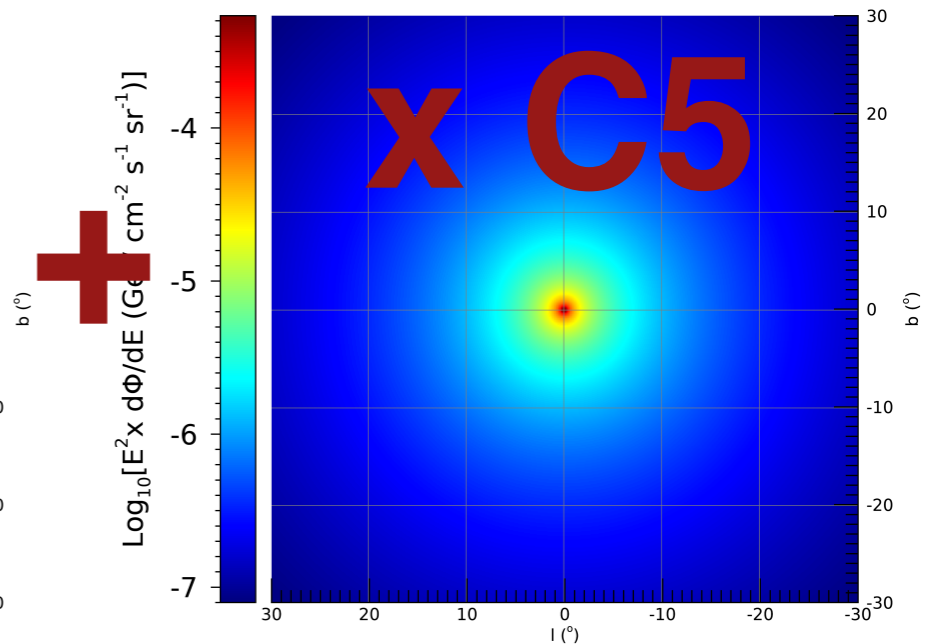
Bubbles Emission at 1.02-2.24 GeV



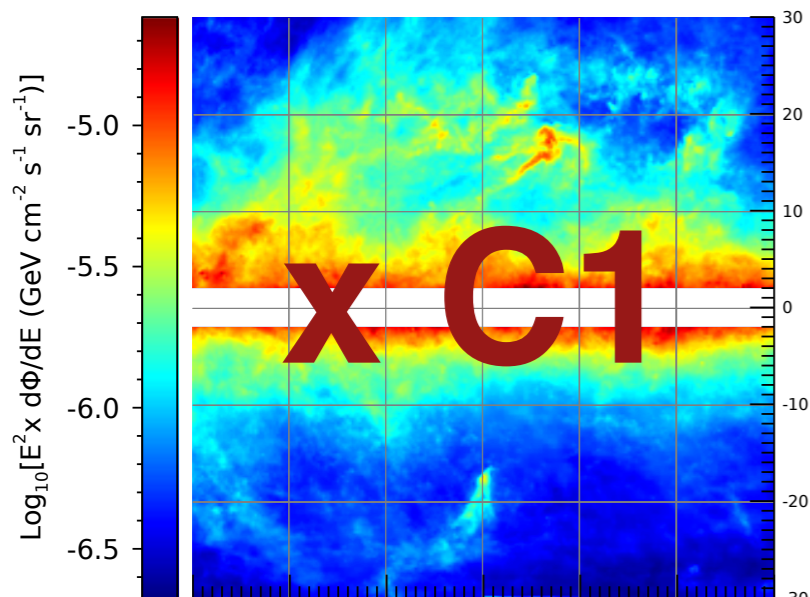
Isotropic Emission at 1.02-2.24 GeV



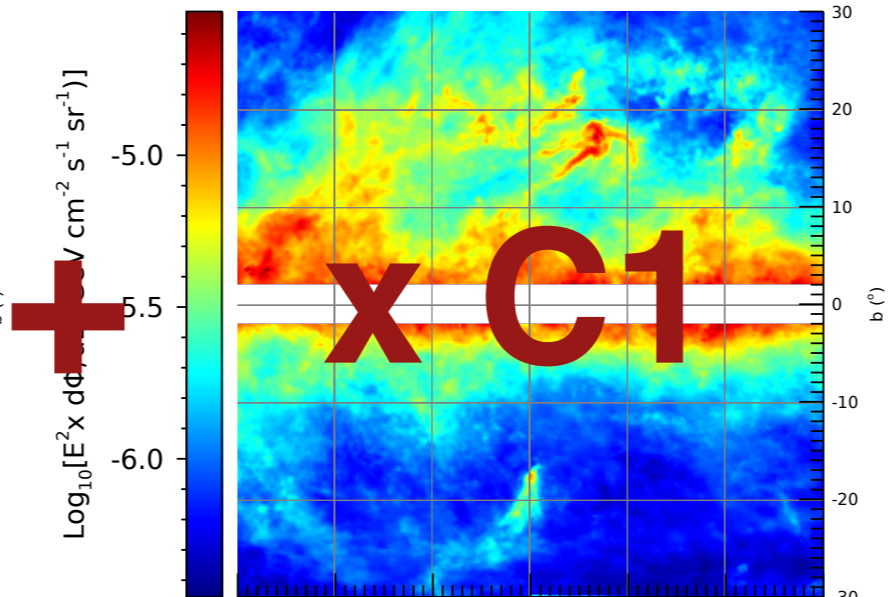
Dark Matter Emission at 1.02-2.24 GeV



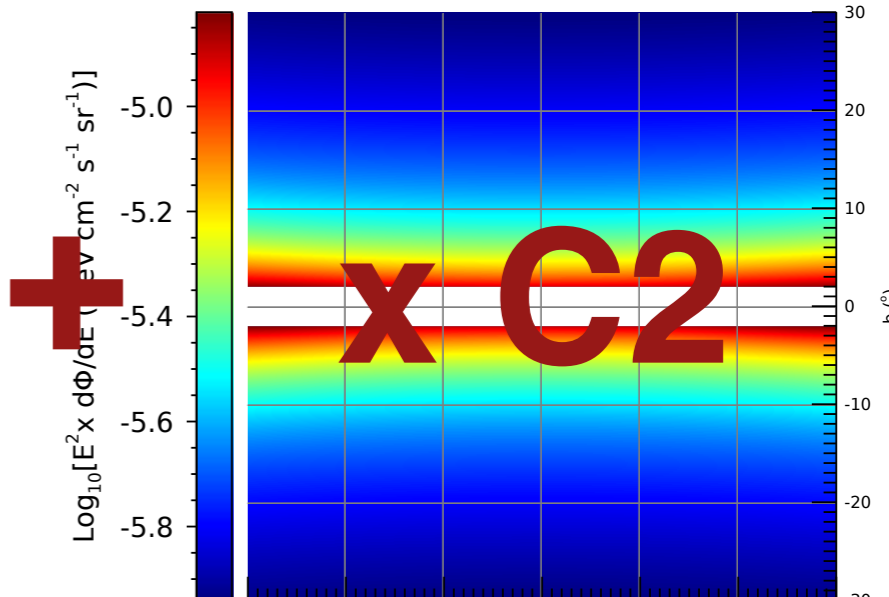
Pi0 Emission at 1.02-2.24 GeV



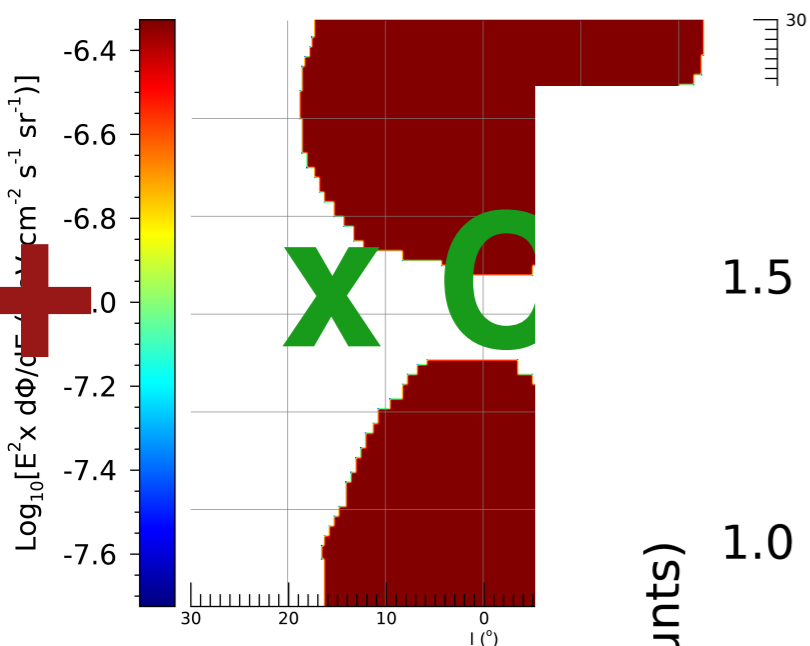
Brems Emission at 1.02-2.24 GeV



ICS Emission at 1.02-2.24 GeV



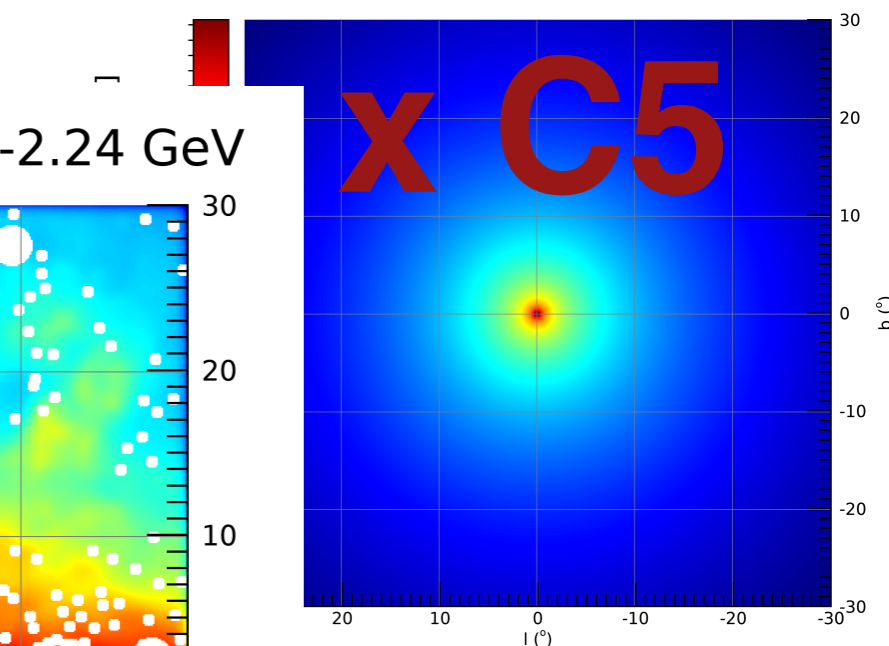
Bubbles Emission at 1.02-2.24 GeV



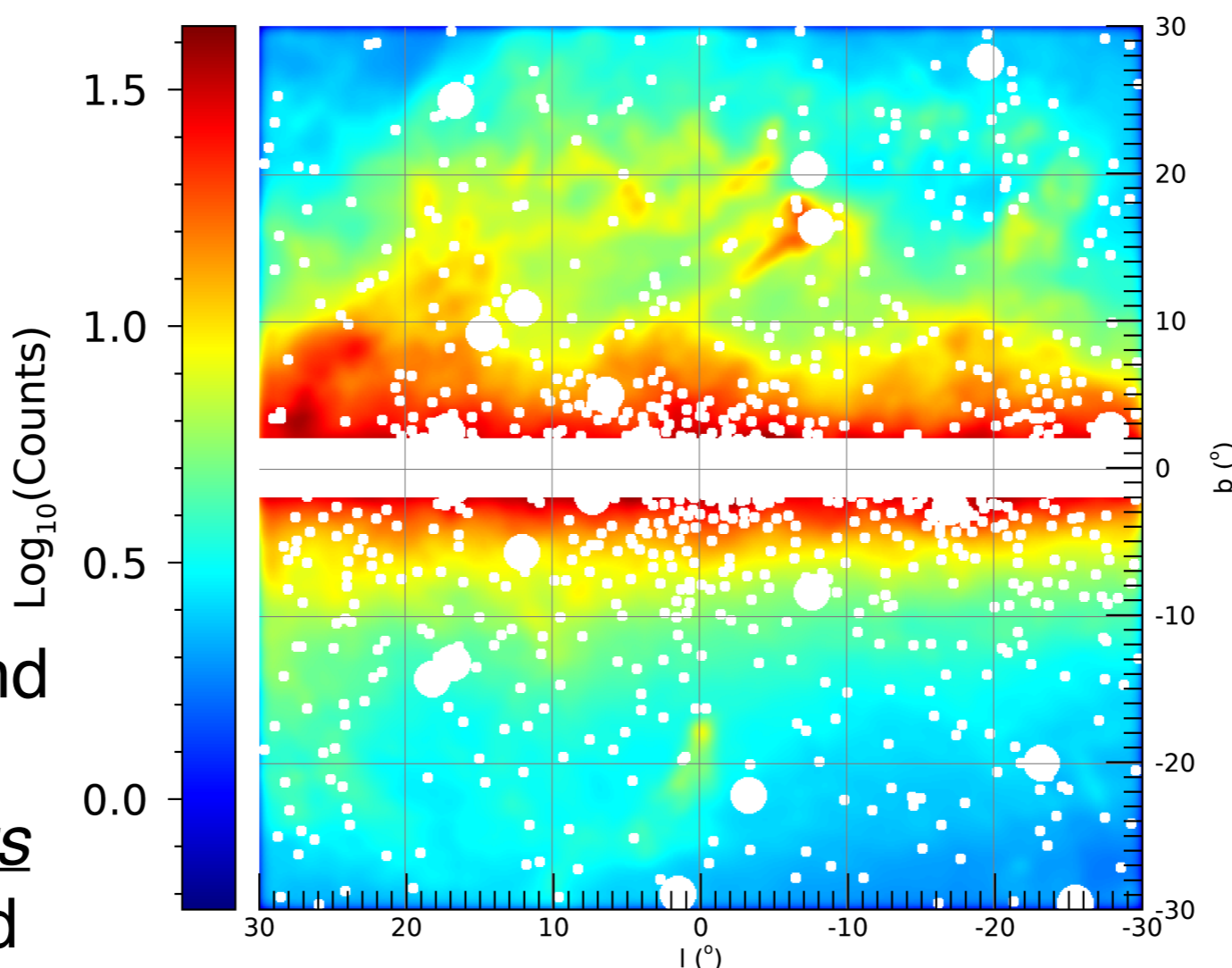
Isotropic Emission at 1.02-2.24 GeV



Dark Matter Emission at 1.02-2.24 GeV



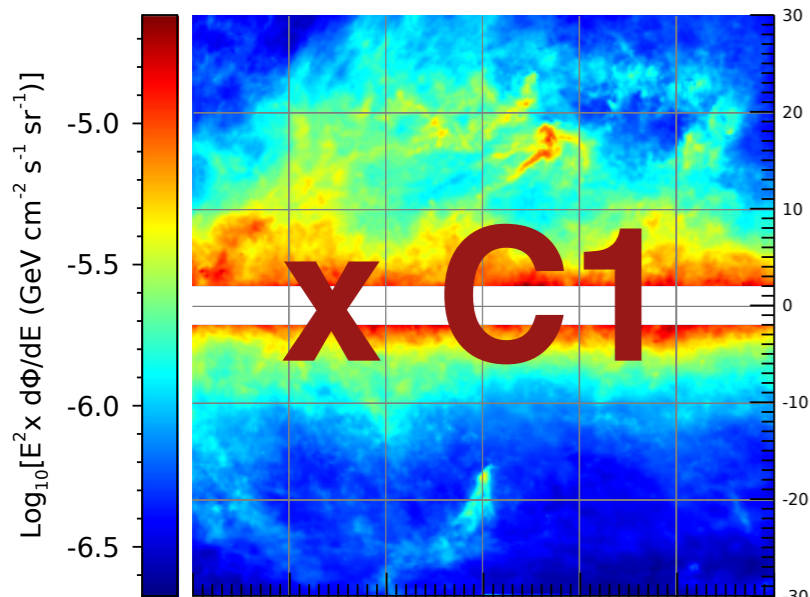
Composite Emission w PSF at 1.02-2.24 GeV



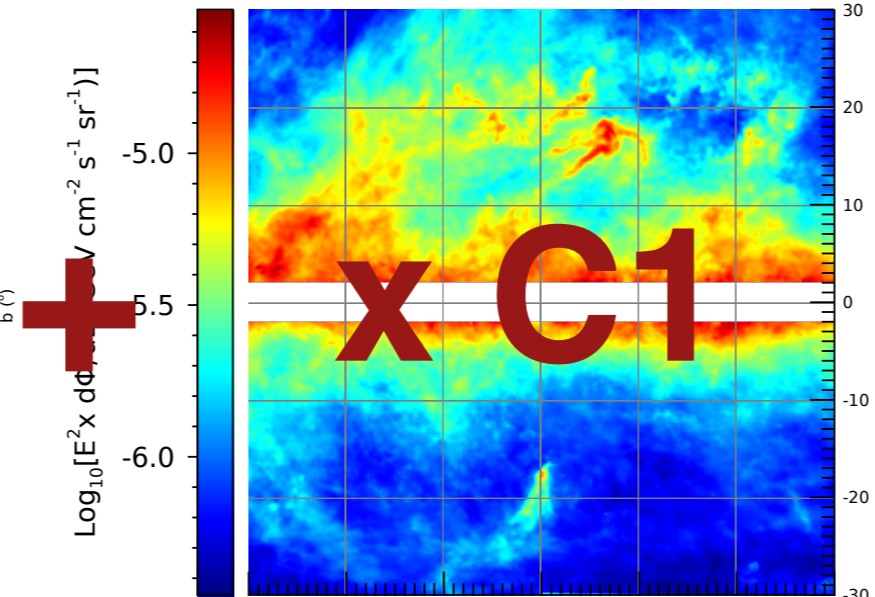
Adding properly and accounting for instrumental effects as the point spread

function and the non-uniform exposure (also masking-out bright point sources)

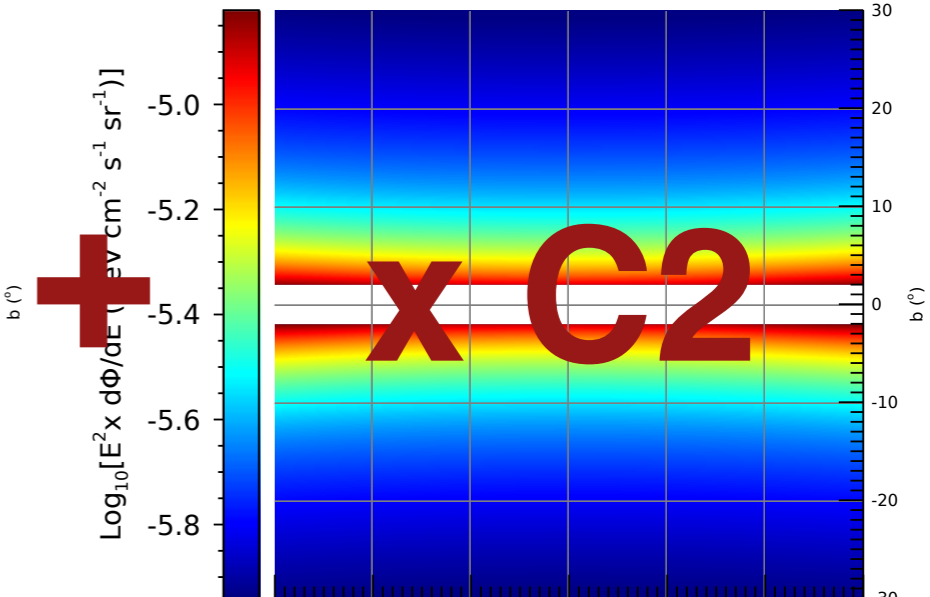
Pi0 Emission at 1.02-2.24 GeV



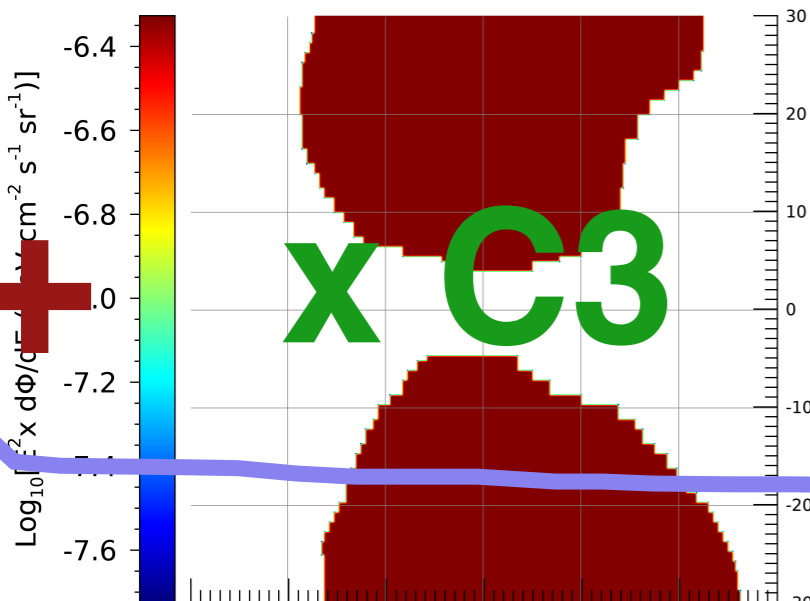
Bremss Emission at 1.02-2.24 GeV



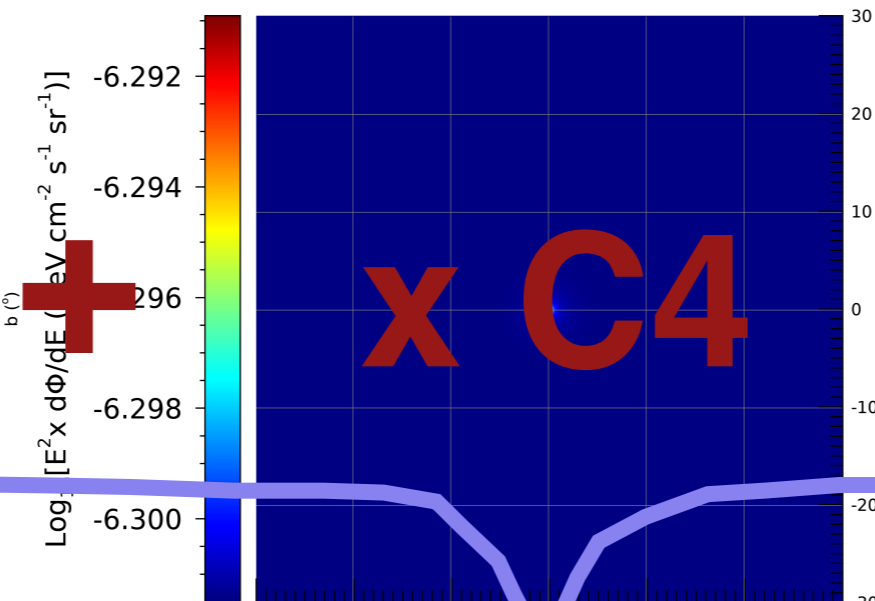
ICS Emission at 1.02-2.24 GeV



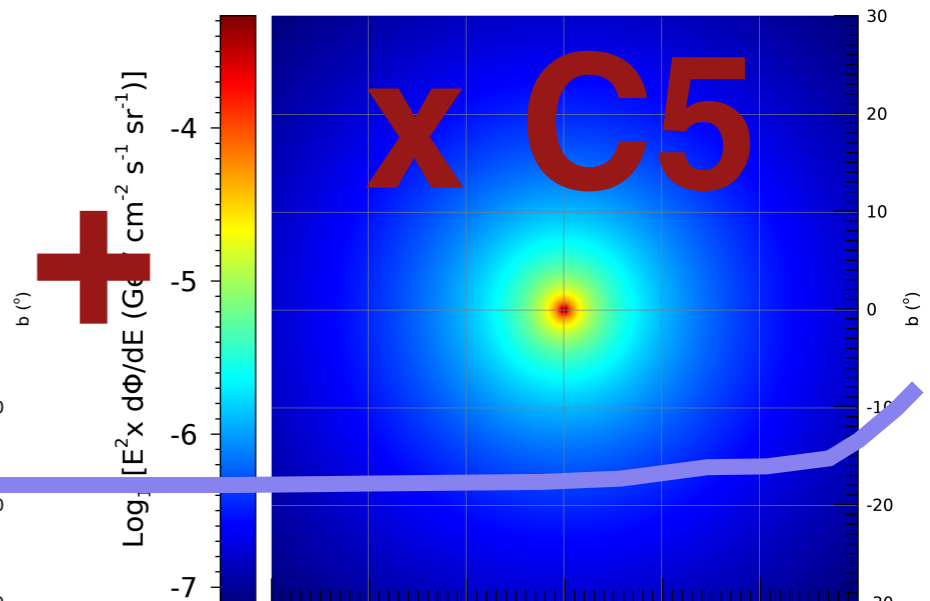
Bubbles Emission at 1.02-2.24 GeV



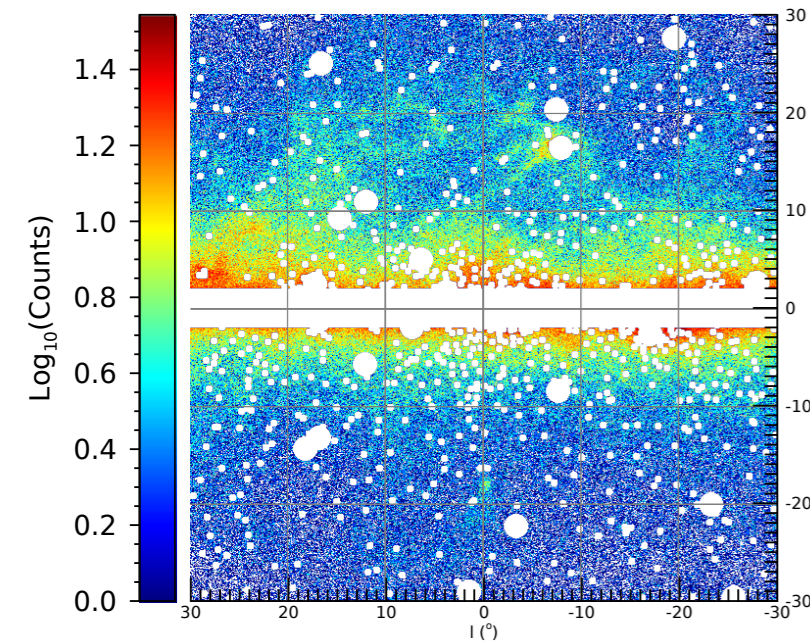
Isotropic Emission at 1.02-2.24 GeV



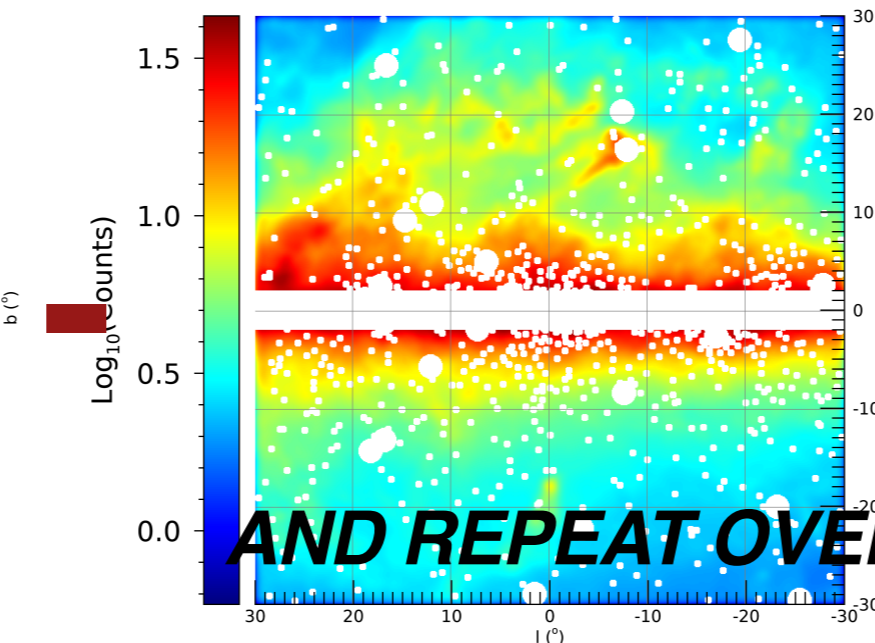
Dark Matter Emission at 1.02-2.24 GeV



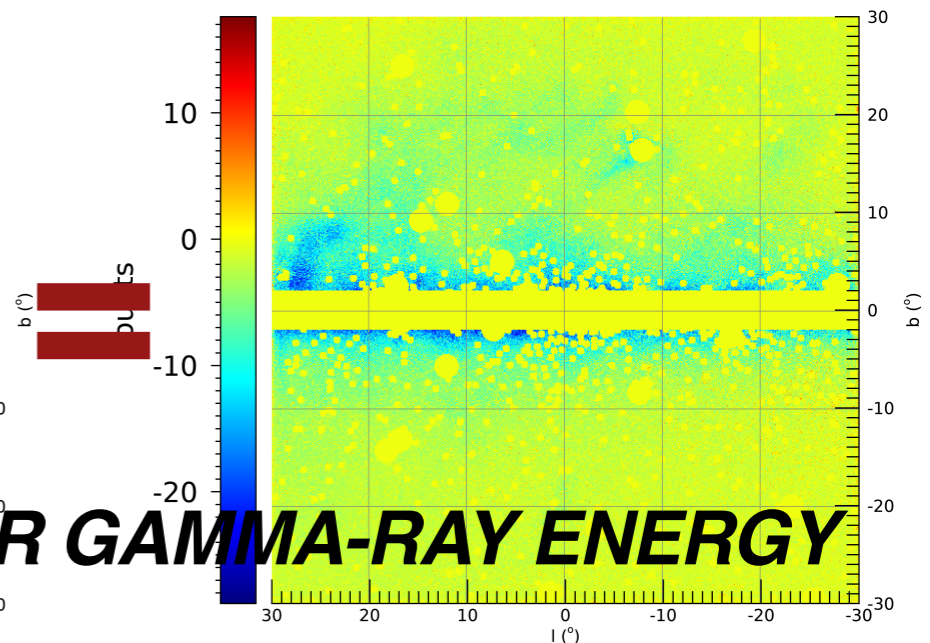
Observed Emission at 1.02-2.24 GeV



Composite Emission w/ PSF at 1.02-2.24 GeV



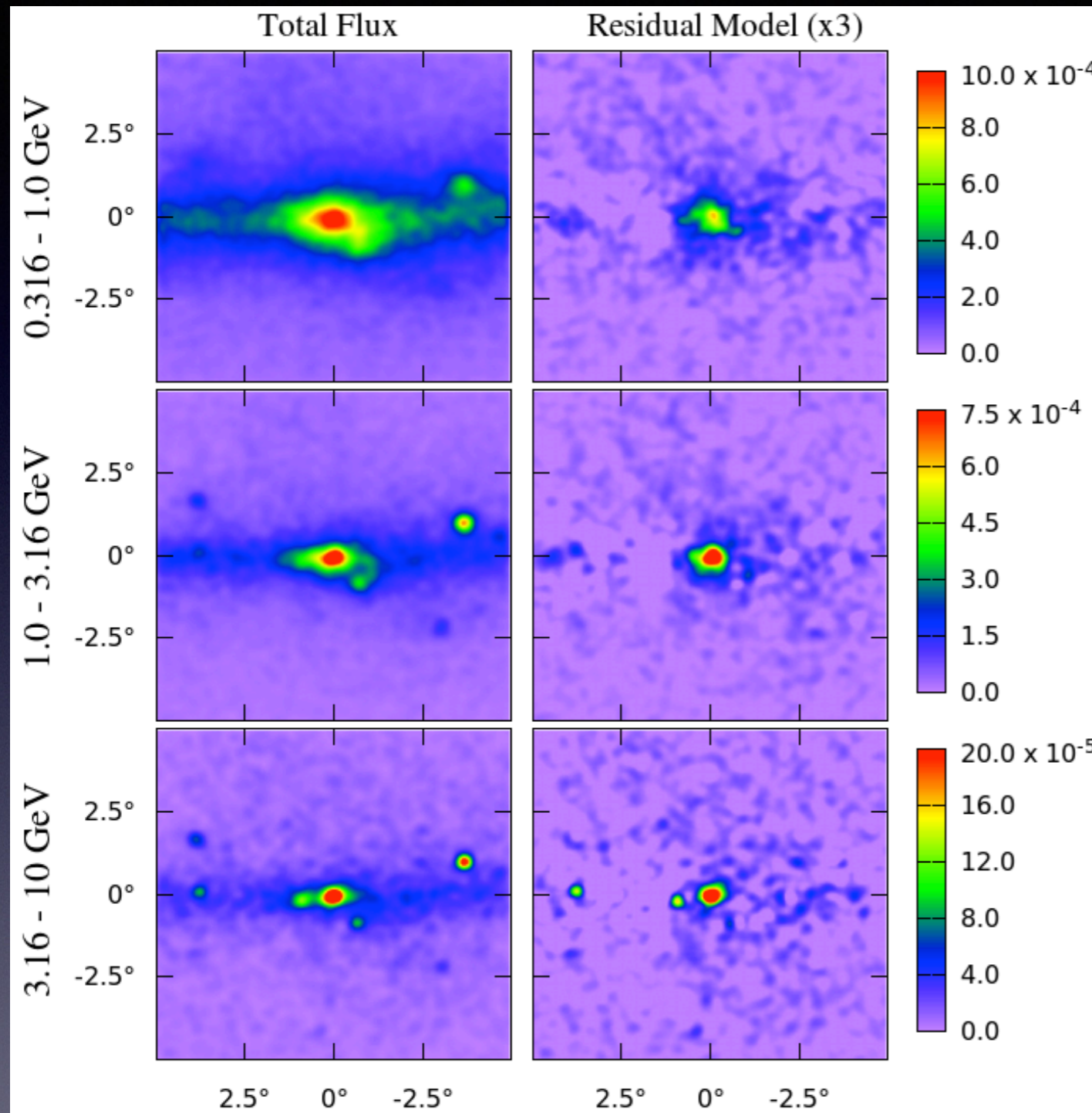
Residual Emission at 1.02-2.24 GeV



AND REPEAT OVER GAMMA-RAY ENERGY

Looking for excesses in the galactic center

Using Templates:

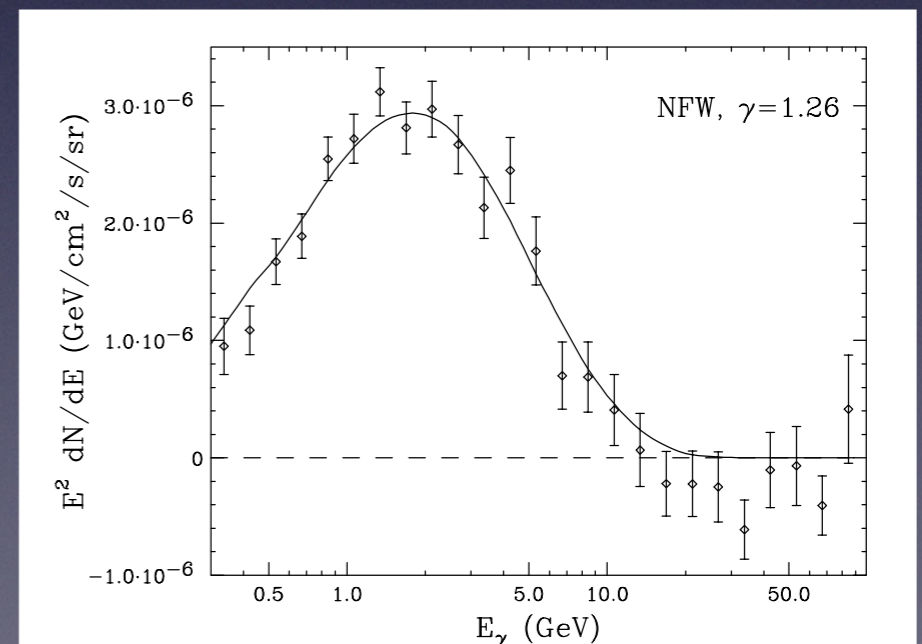


Daylan, Finkbeiner, Hooper, Linden, Portilo, Rodd, Slatyer, PoDU 2015

Claim:

- A clear **excess emission in the galactic center emerges**
- Excess emission cuts-off at ~ 10 GeV (is in some disagreement with later findings)

Will call this excess emission the **Galactic Center Excess (GCE)**

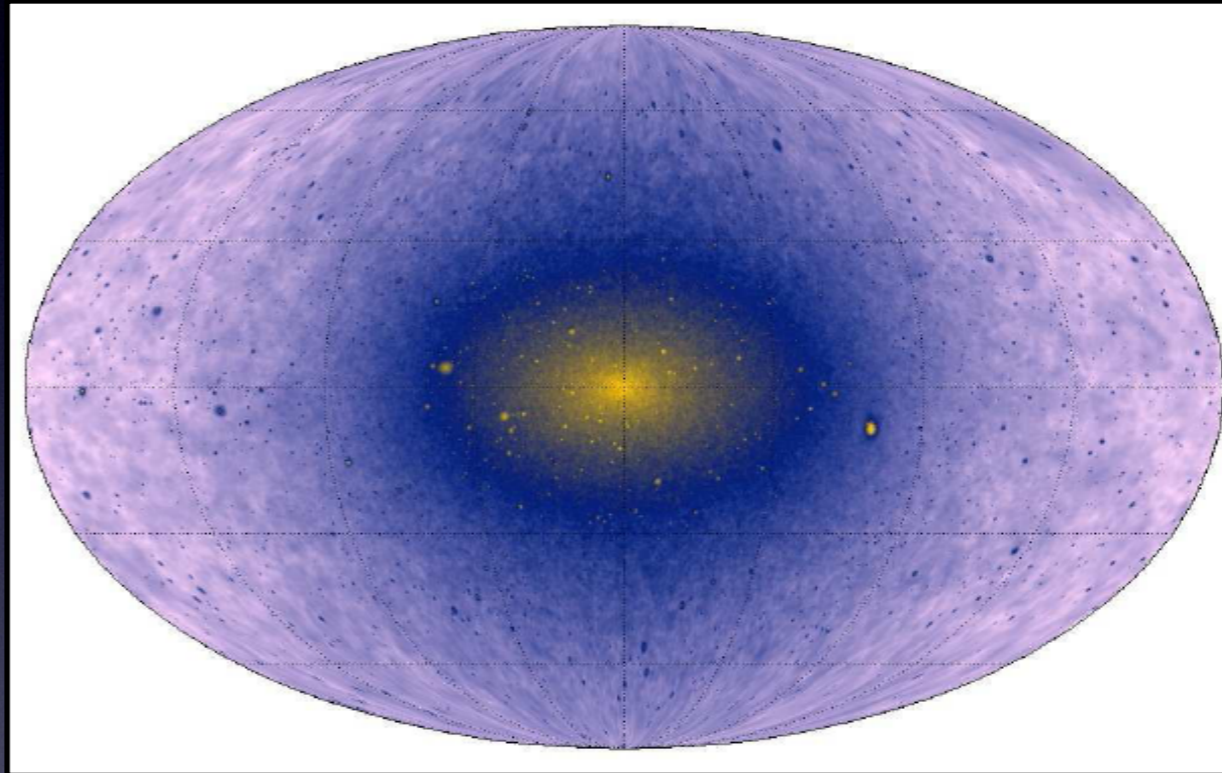


Also: Hooper & Goodenough PRL 2011, Abazajian JCAP 2011, Hooper & Linden PRD 2011, Gordon & Macias PRD 2014, Zhou et al. PRD 2015, Ajello et al. ApJ 2016

Going to High Latitudes (Inner Galaxy)

Advantages of looking further away from the center:

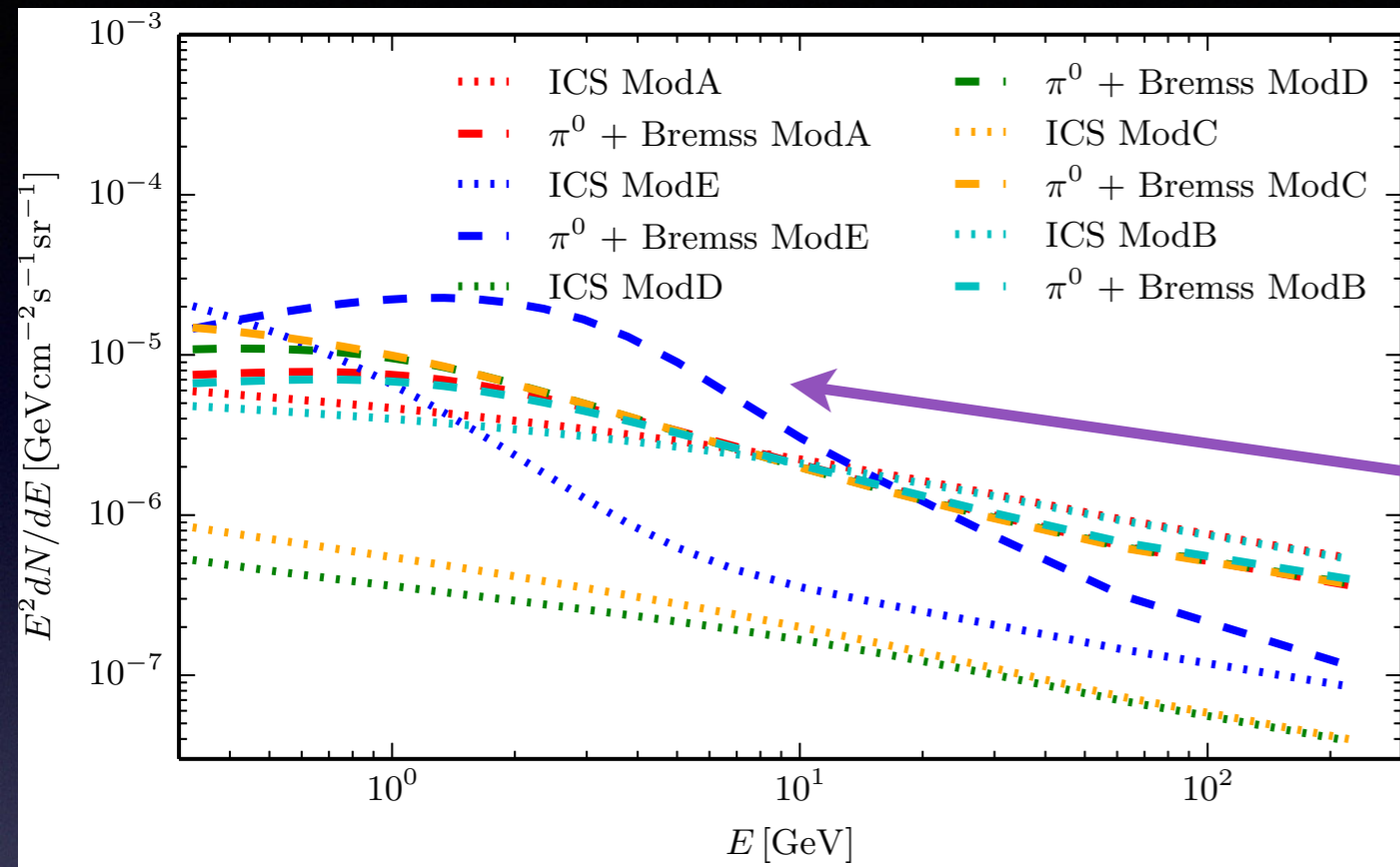
i) For a DM signal, you now have a prediction on the spectrum and its normalization based on the DM distribution.



ii) Different region on the galactic sky suffers from different uncertainties in the background gamma-ray flux.

iii) A region that does not have too many very young and energetic sources that might affect the CR propagation on a local scale. That relates to avoiding the stronger inhomogeneities in diffusion, that exist along the disk. Similar argument for the interstellar radiation field.

Modeling the background gamma-ray sky: Interplay with Cosmic-Rays & the ISM

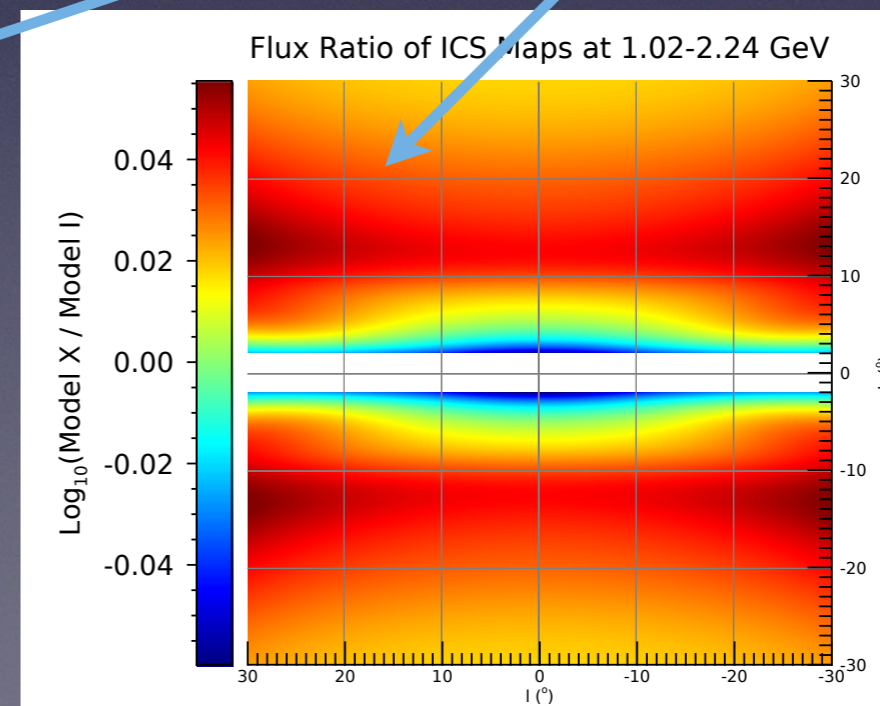
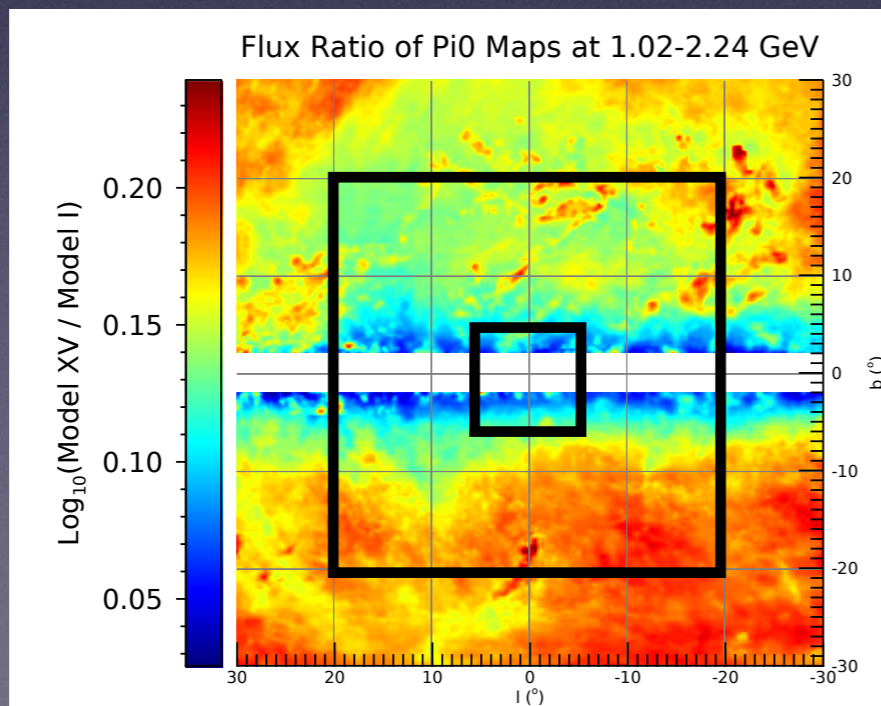


The exact **astrophysics model assumptions** can affect both the gamma-ray **background spectrum** and its **morphology** on the galactic sky.

Calore, IC, Weniger, JCAP 2015

IC, Zhong, McDermott, Surdutovich, PRD 2022

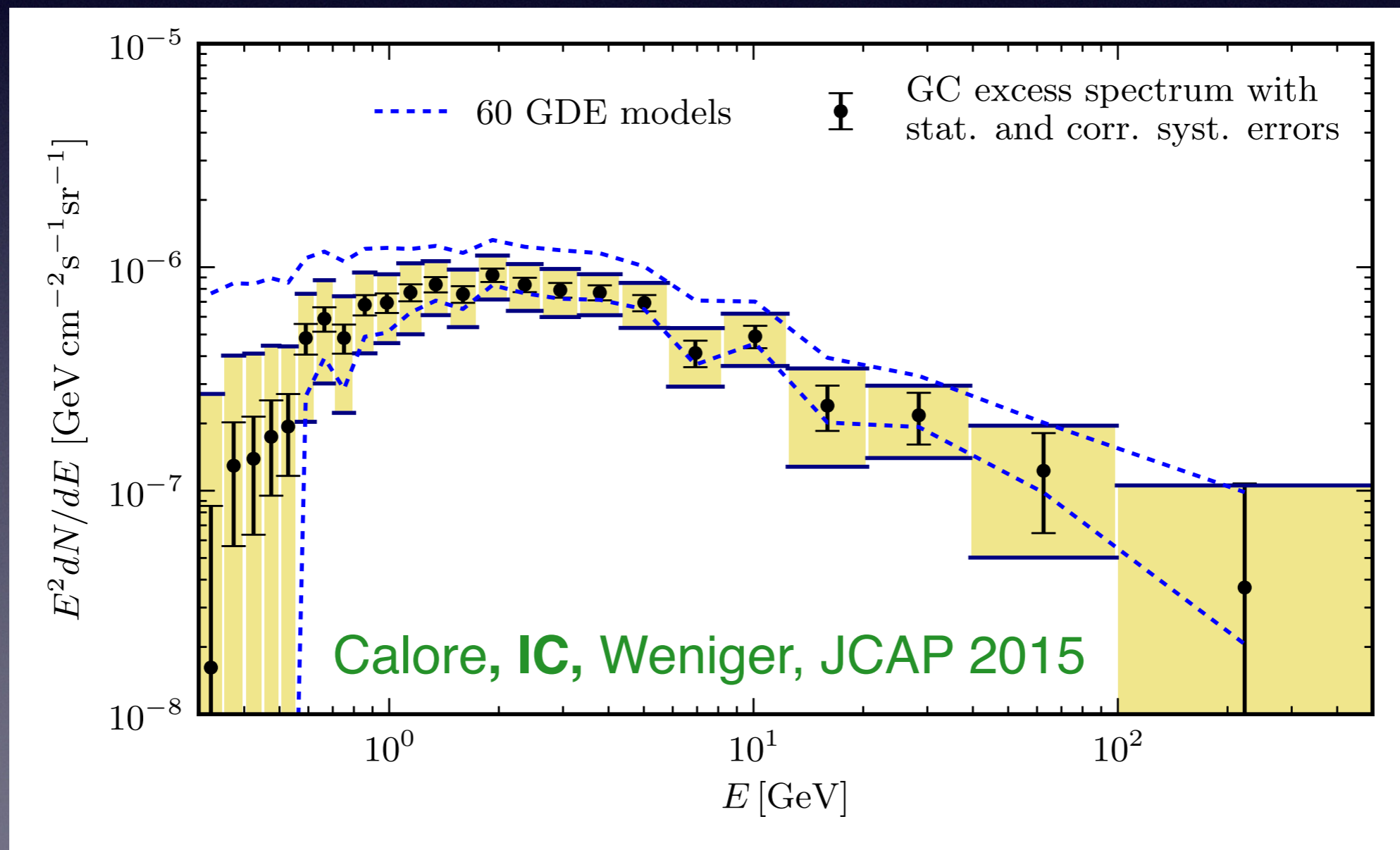
60 degrees in latitude



Accounting for the galactic diffuse emission uncertainties

We use models, accounting for **uncertainties** related to the **diffusion** of CRs, the presence of **convective winds**, diffusive **re-acceleration**, **energy losses**, **CR injection sources**, **gas** and other **interstellar medium properties**. From the existing literature and in 2015 we created our own (60) models → **6660** different Templates!

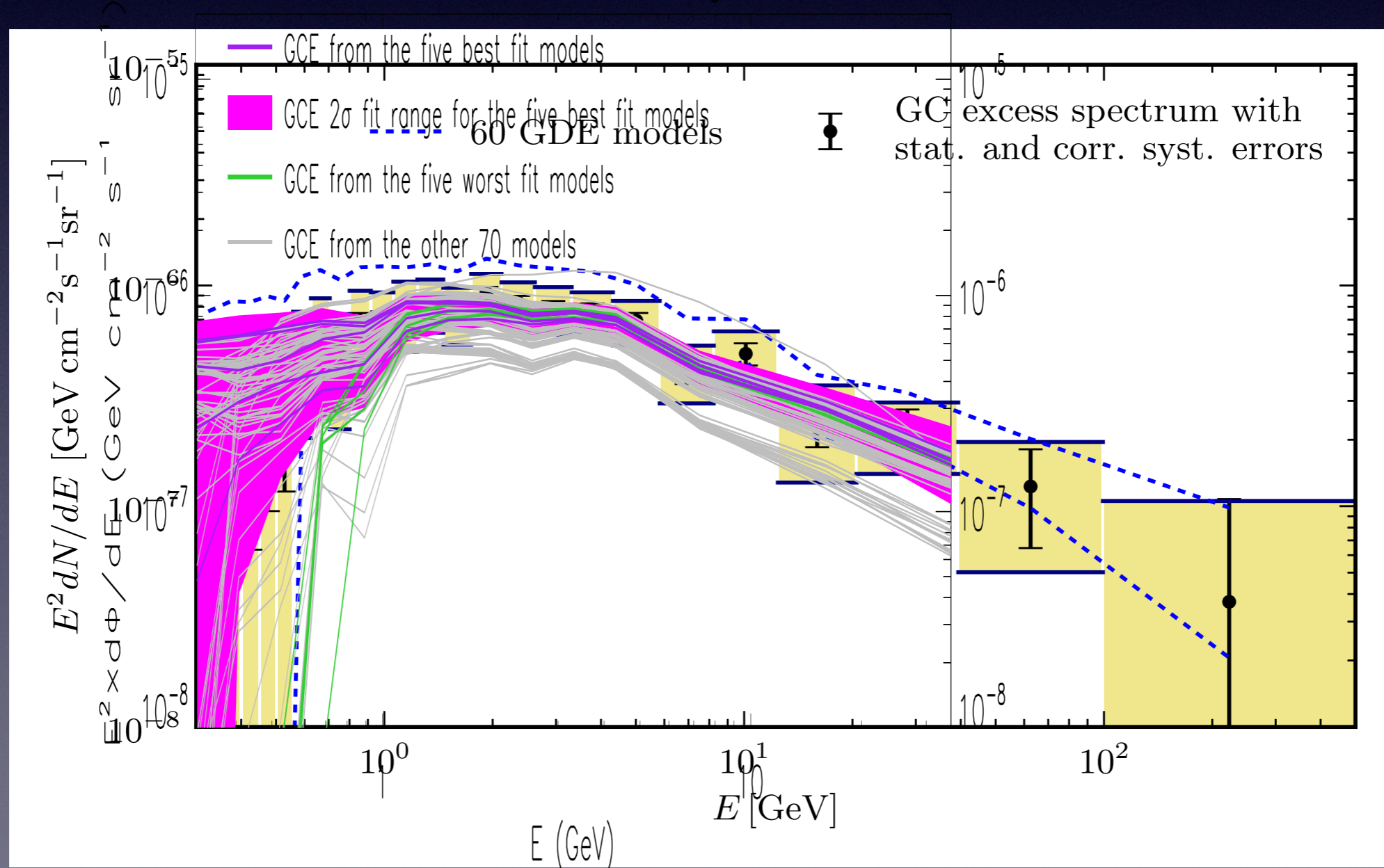
It turns out that it actually does not affect dramatically the excess spectrum:



Accounting for the galactic diffuse emission uncertainties

We use models, accounting for **uncertainties** related to the **diffusion** of CRs, the presence of **convective winds**, diffusive **re-acceleration**, **energy losses**, **CR injection sources**, **gas** and other **interstellar medium properties**. To account for new observations in 2020-2021 we created and tested 45K high resolution templates.

The GCE from all 80 diffuse background models



Maps, Astrophysical Models and Correlated Errors publicly available via Zenodo

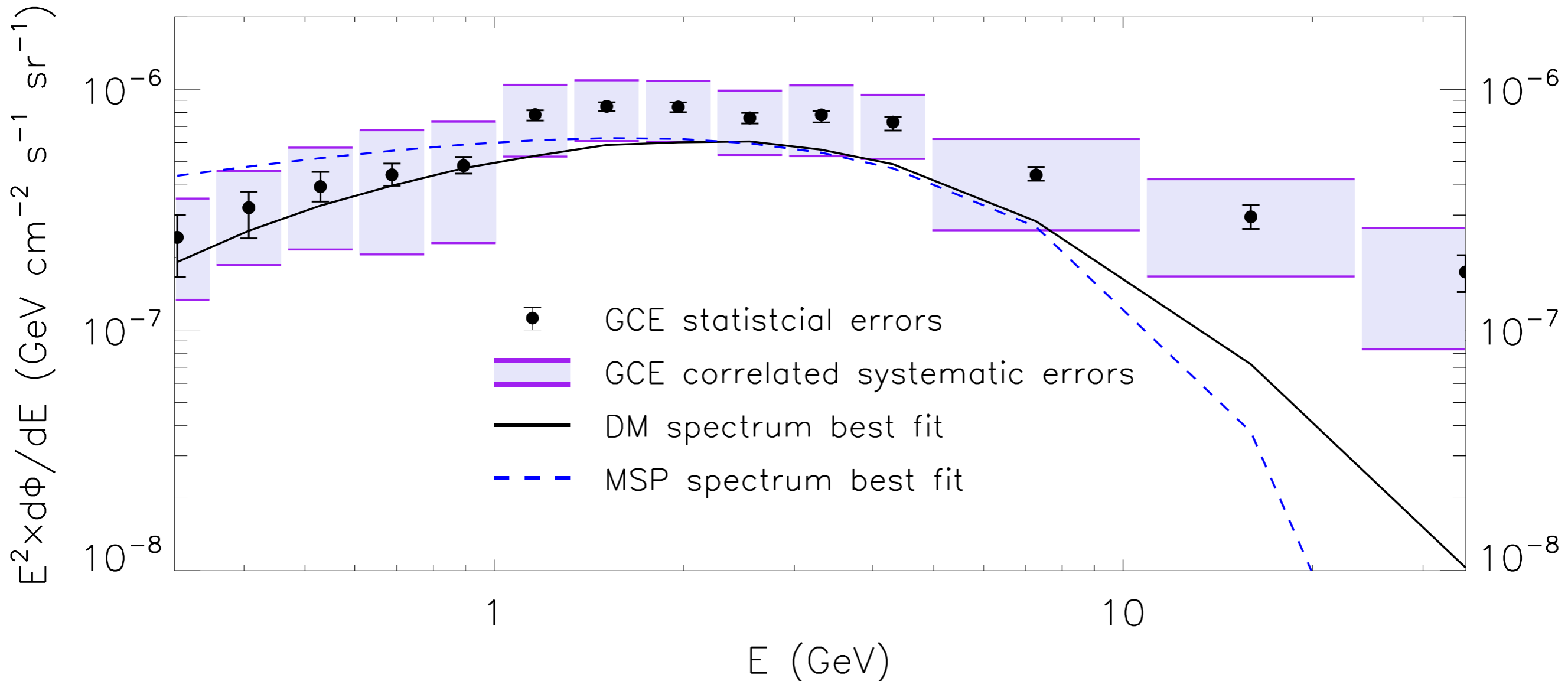
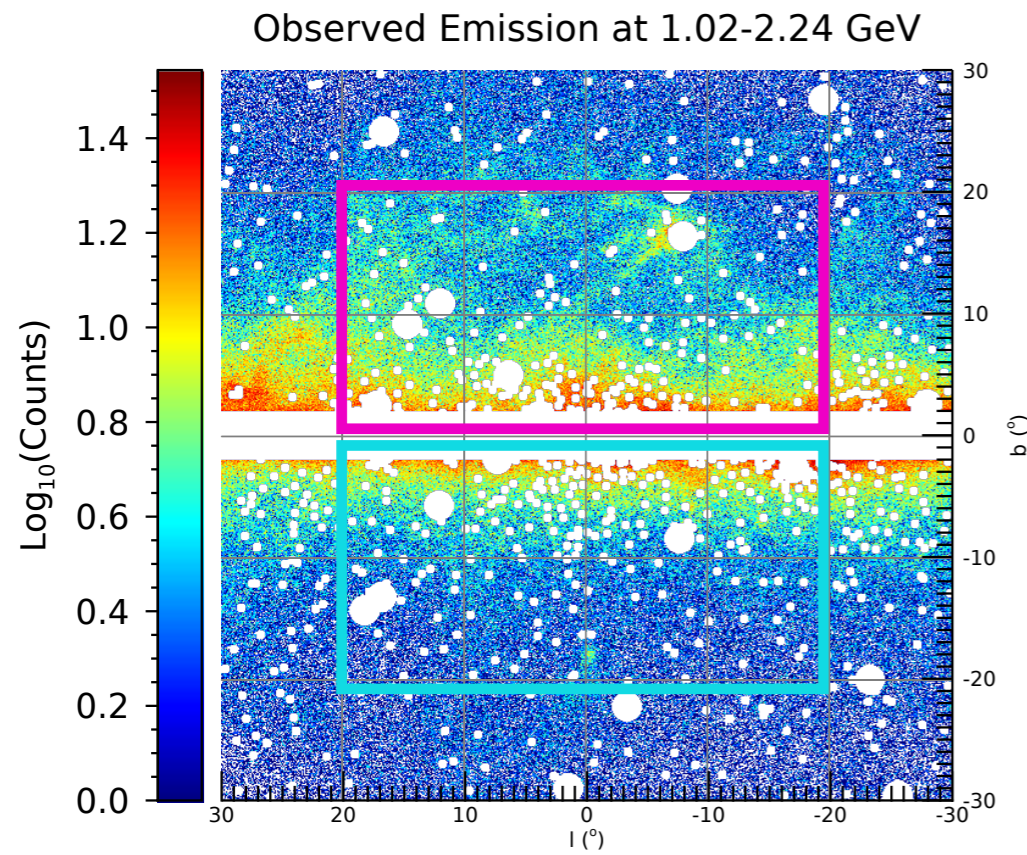


TABLE V. The first four principal components of the systematic uncertainty contribution to the covariance matrix, defined as in Eq. (16), in units of $10^{-7} \text{ GeV cm}^{-2} \text{ s}^{-1} \text{ sr}^{-1}$.

PC_i	Φ_1	Φ_2	Φ_3	Φ_4	Φ_5	Φ_6	Φ_7	Φ_8	Φ_9	Φ_{10}	Φ_{11}	Φ_{12}	Φ_{13}	Φ_{14}
PC_1	2.52	2.37	2.47	2.43	2.19	2.35	2.08	1.83	1.65	1.69	1.38	1.09	0.67	0.34
PC_2	-1.70	-1.07	-0.16	0.14	0.54	0.42	0.40	0.31	0.58	0.41	0.56	0.48	0.41	0.33
PC_3	0.27	0.06	-0.53	-0.22	-0.21	-0.18	-0.08	0.25	0.04	0.45	0.23	0.24	0.20	0.24
PC_4	0.20	-0.15	0.15	-0.14	0.06	-0.04	-0.04	-0.27	0.08	-0.25	0.11	0.25	0.27	0.17

The profile for the GCE. Does it look like a DM signal?

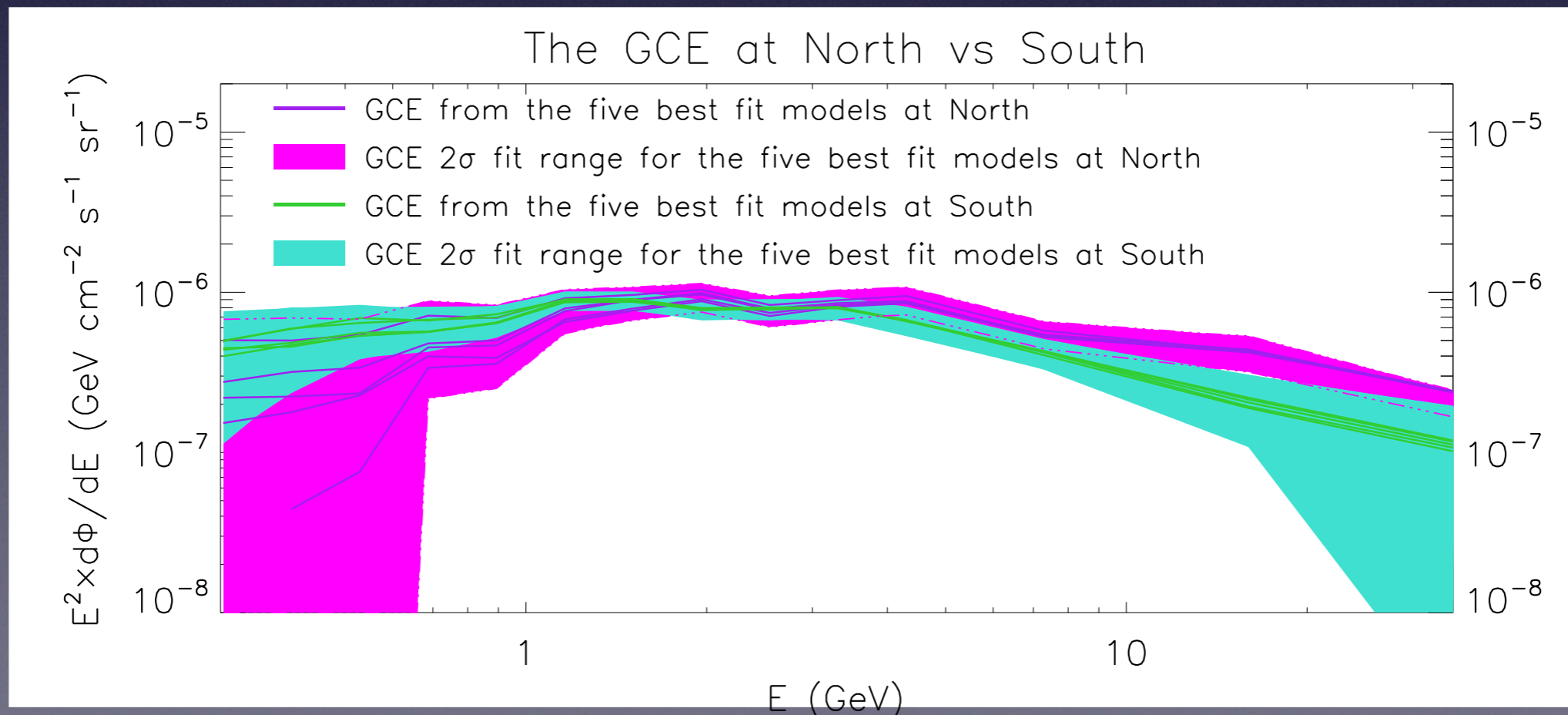
IC, Zhong, McDermott, Surdutovich, PRD 2022



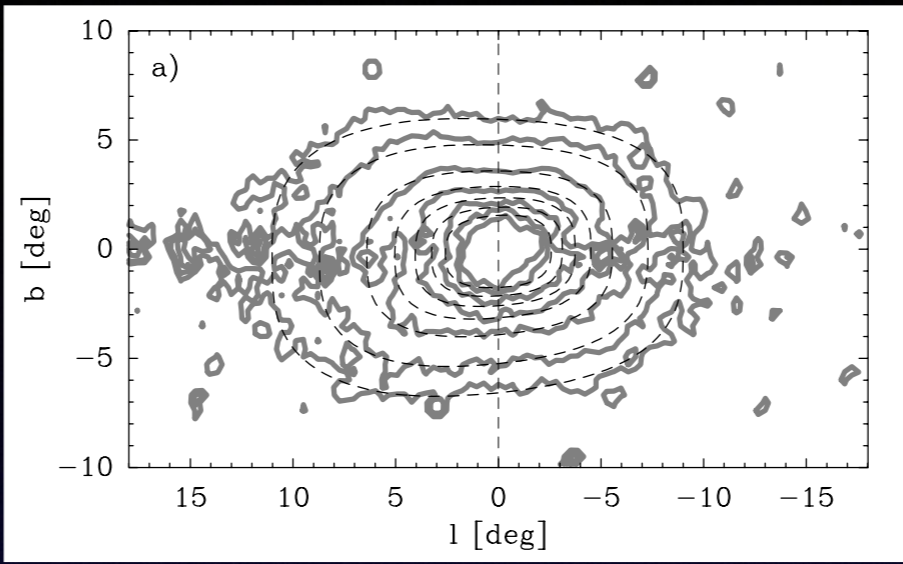
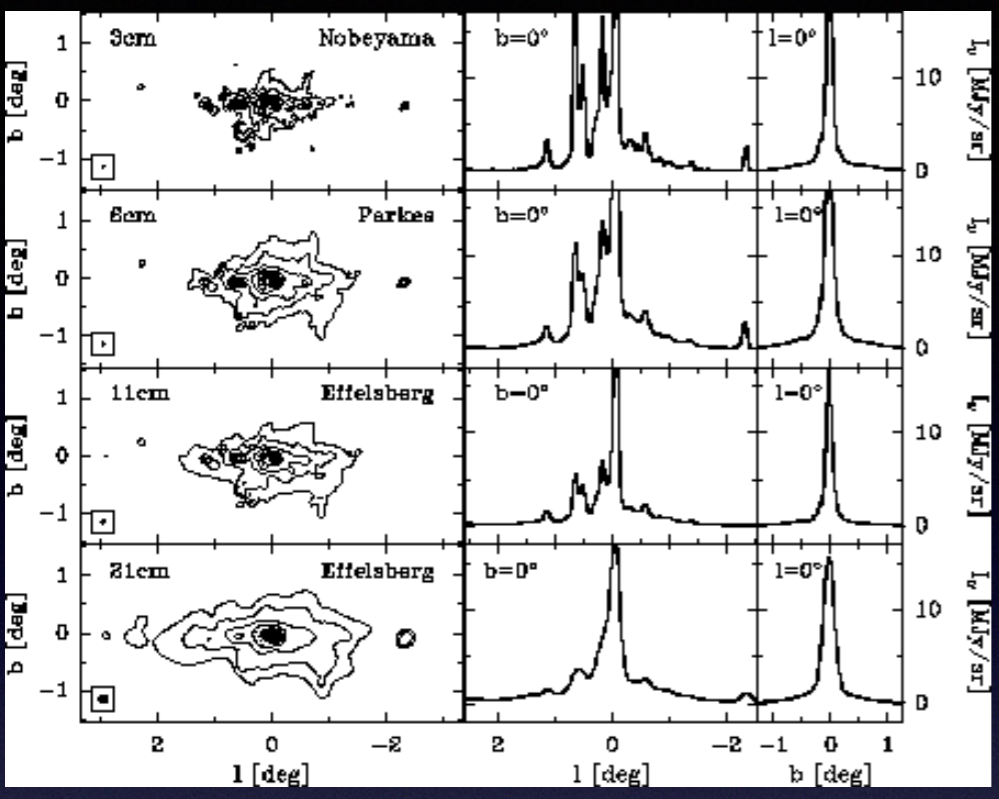
North

South

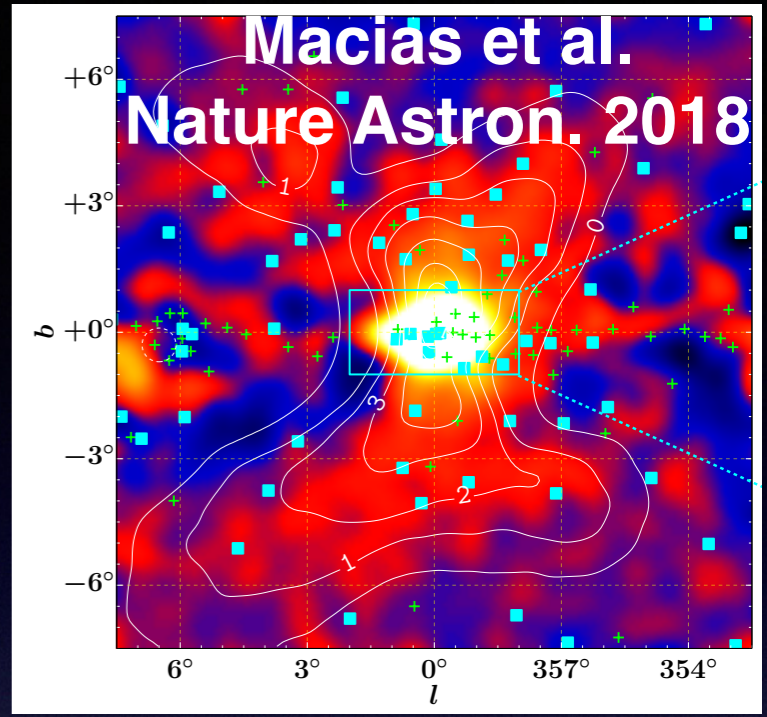
Roughly consistent between southern and northern galactic hemisphere as expected from dark matter



The profile for the GCE. Does it look like a DM signal?



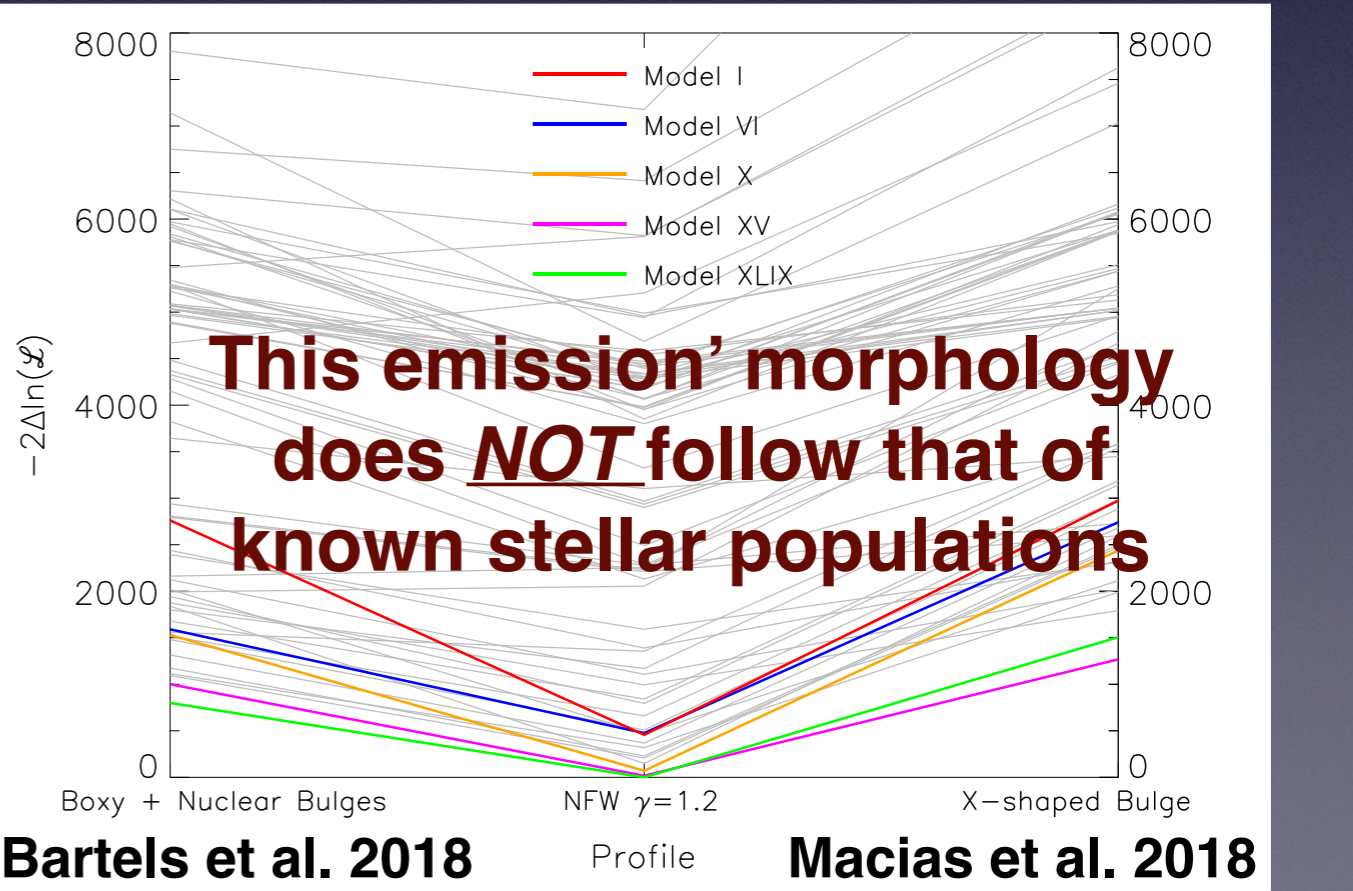
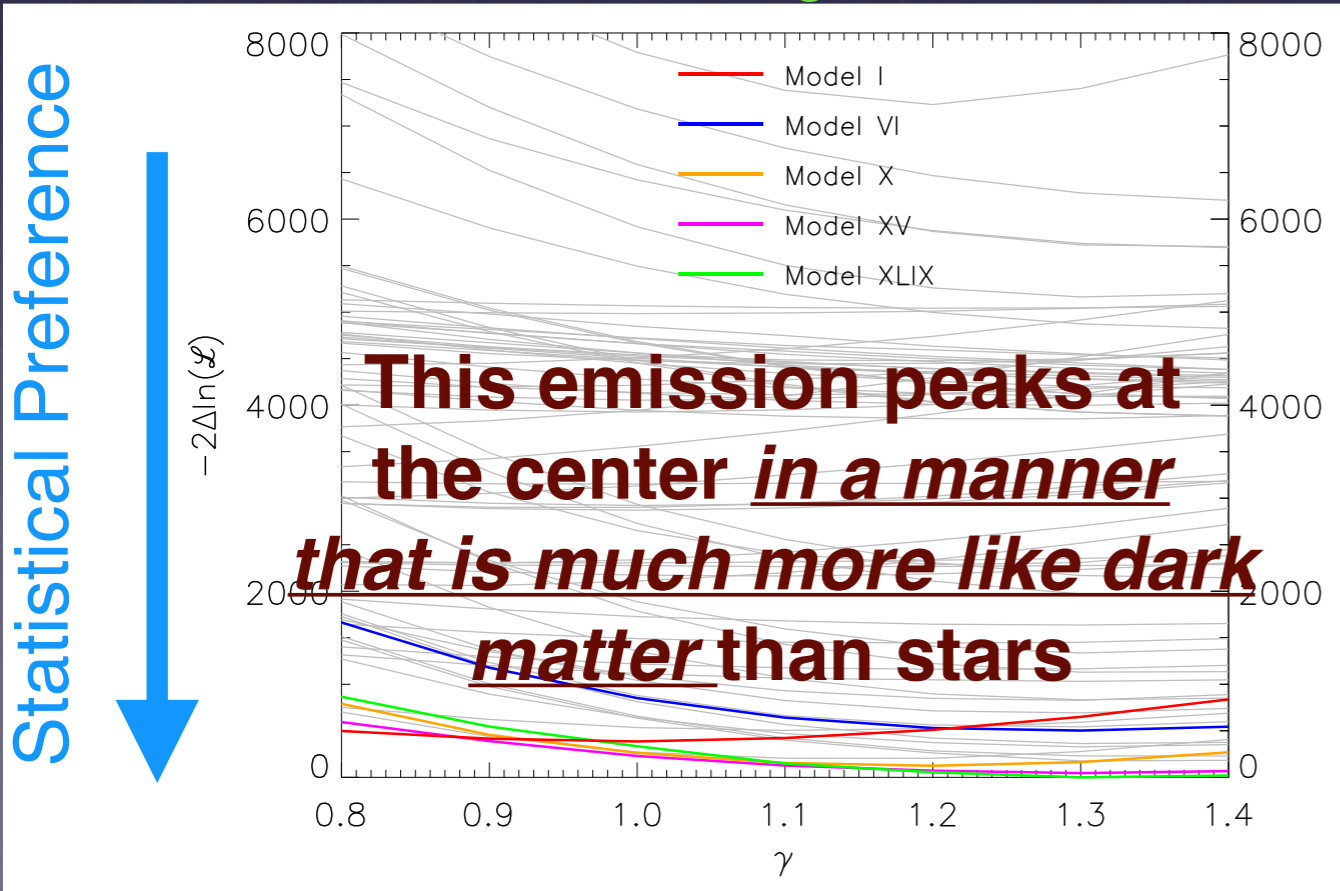
Boxy Bulge @ 2-5 μm
 Launhardt et al. A&A 2002



X-shaped Bulge @ "low" gamma-rays
 Macias et al. Nature Astron. 2018

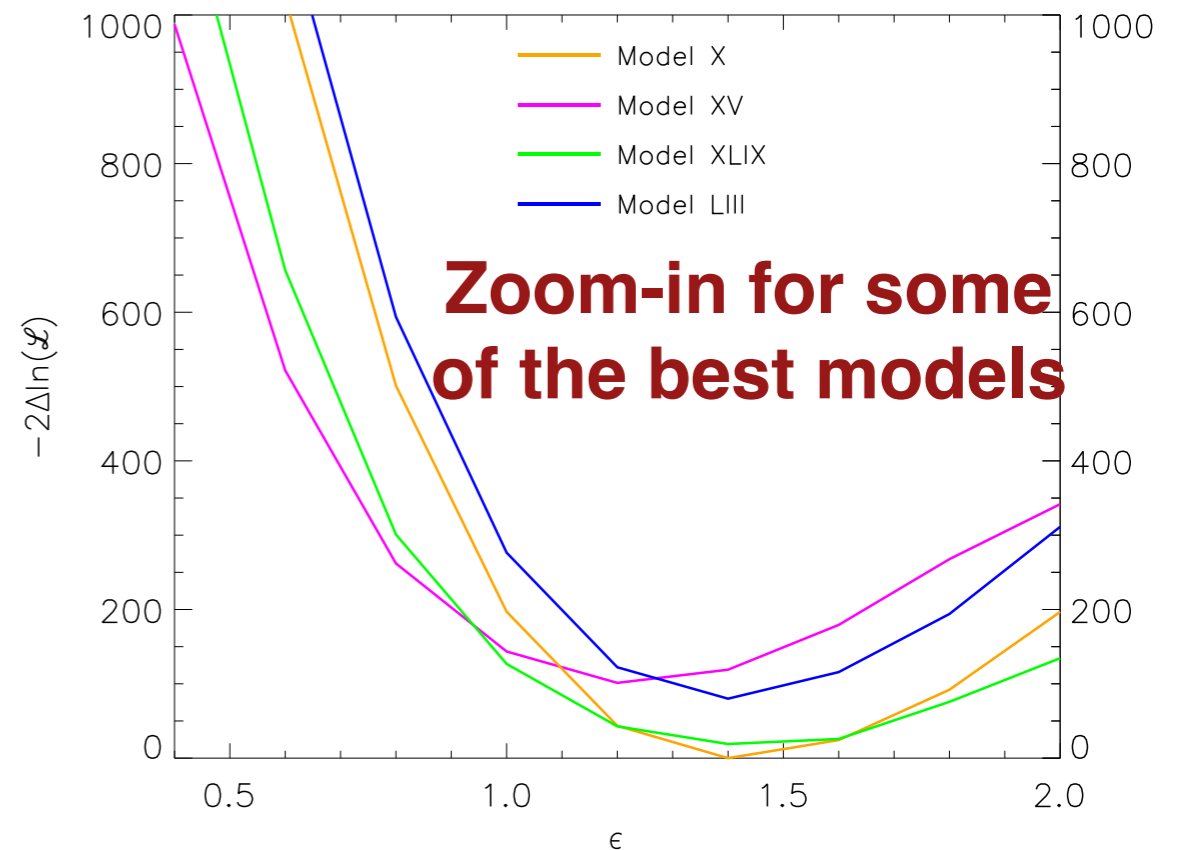
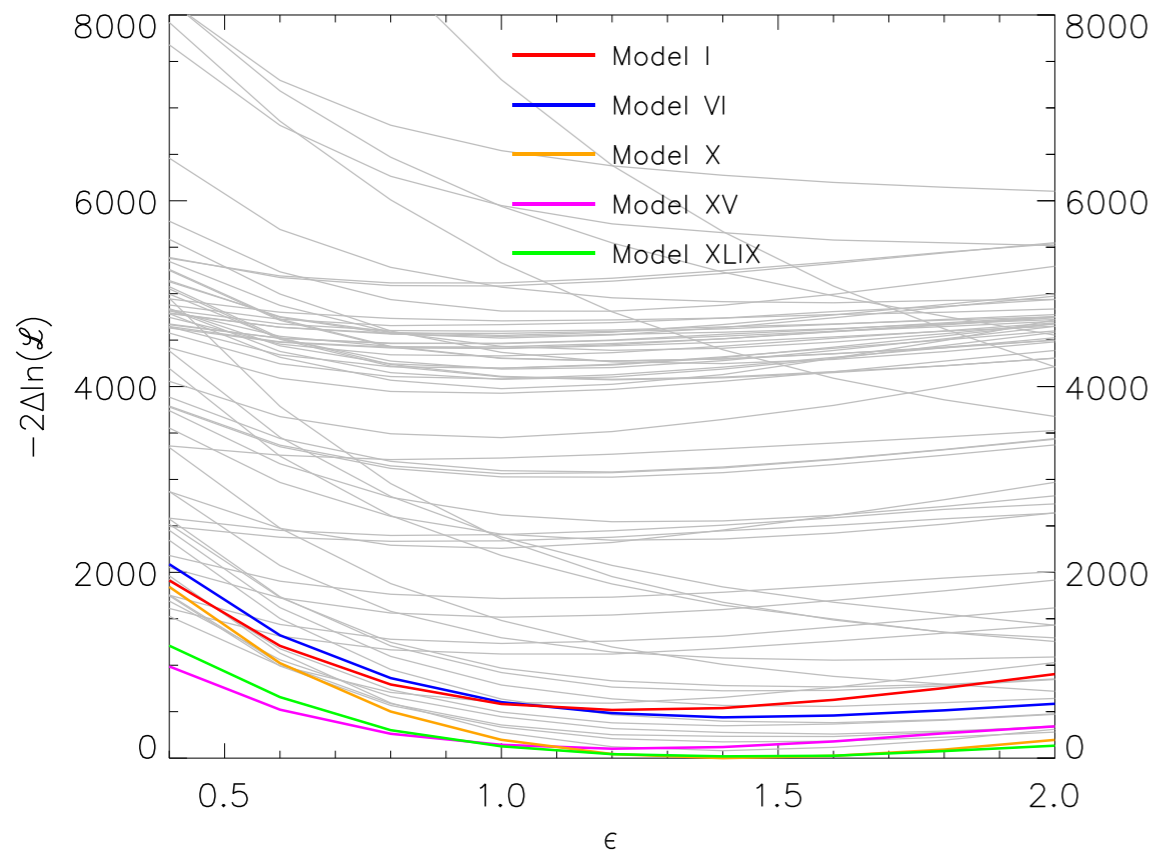
Nuclear Bulge @ Radio

IC, Zhong, McDermott, Surdutovich, PRD 2022



Bartels et al. 2018

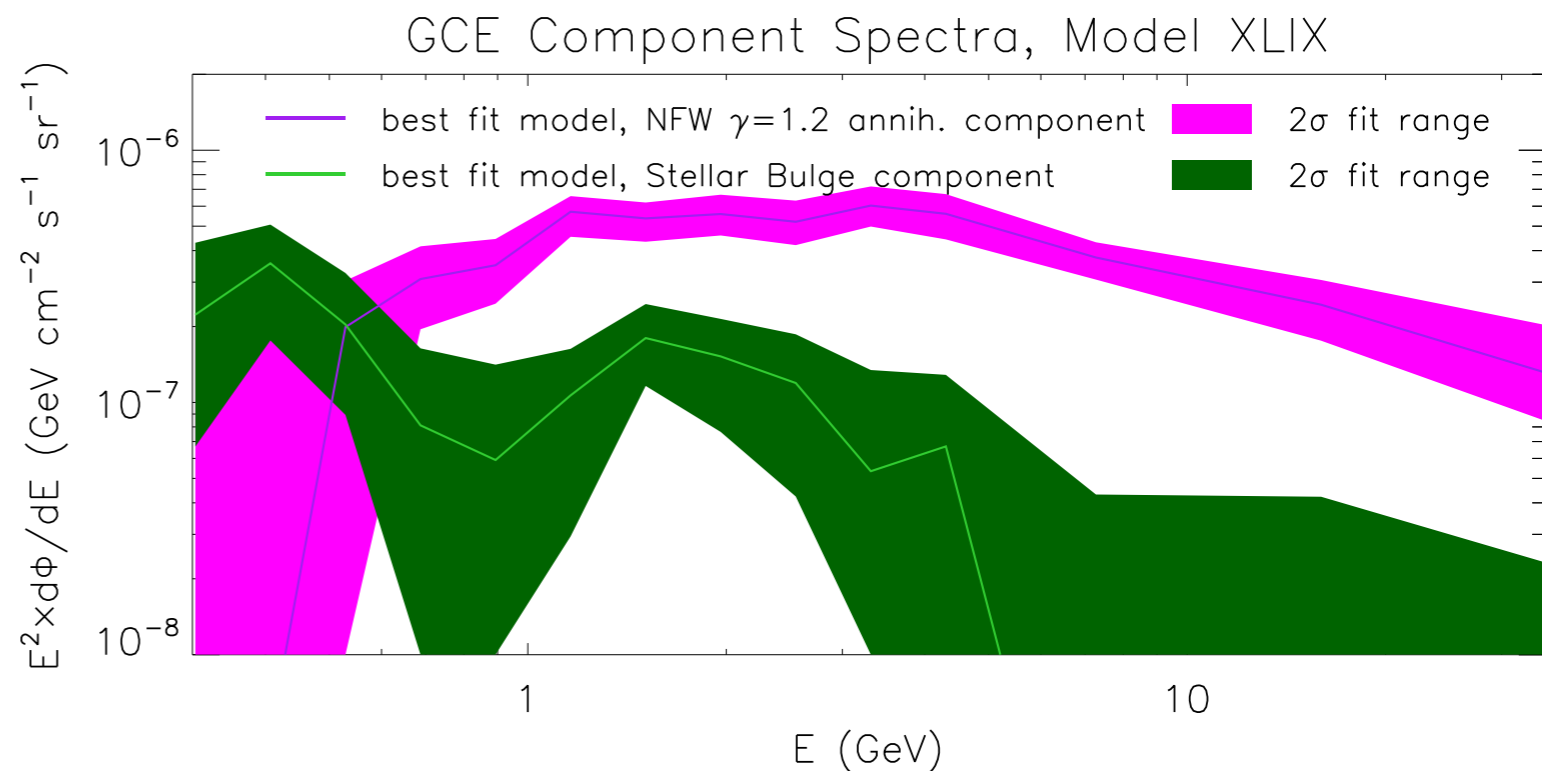
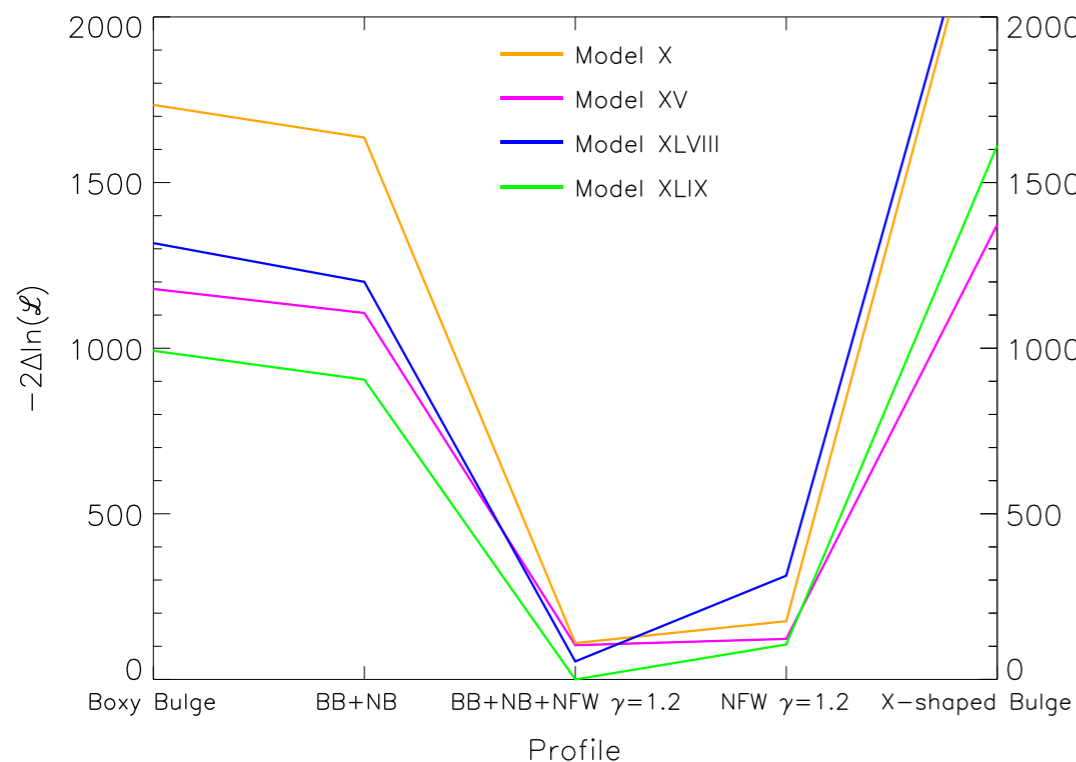
Macias et al. 2018



Results do not change substantively between 4FGL, 4FGL-DR2 (and also 4FGL-DR3) point source catalogues

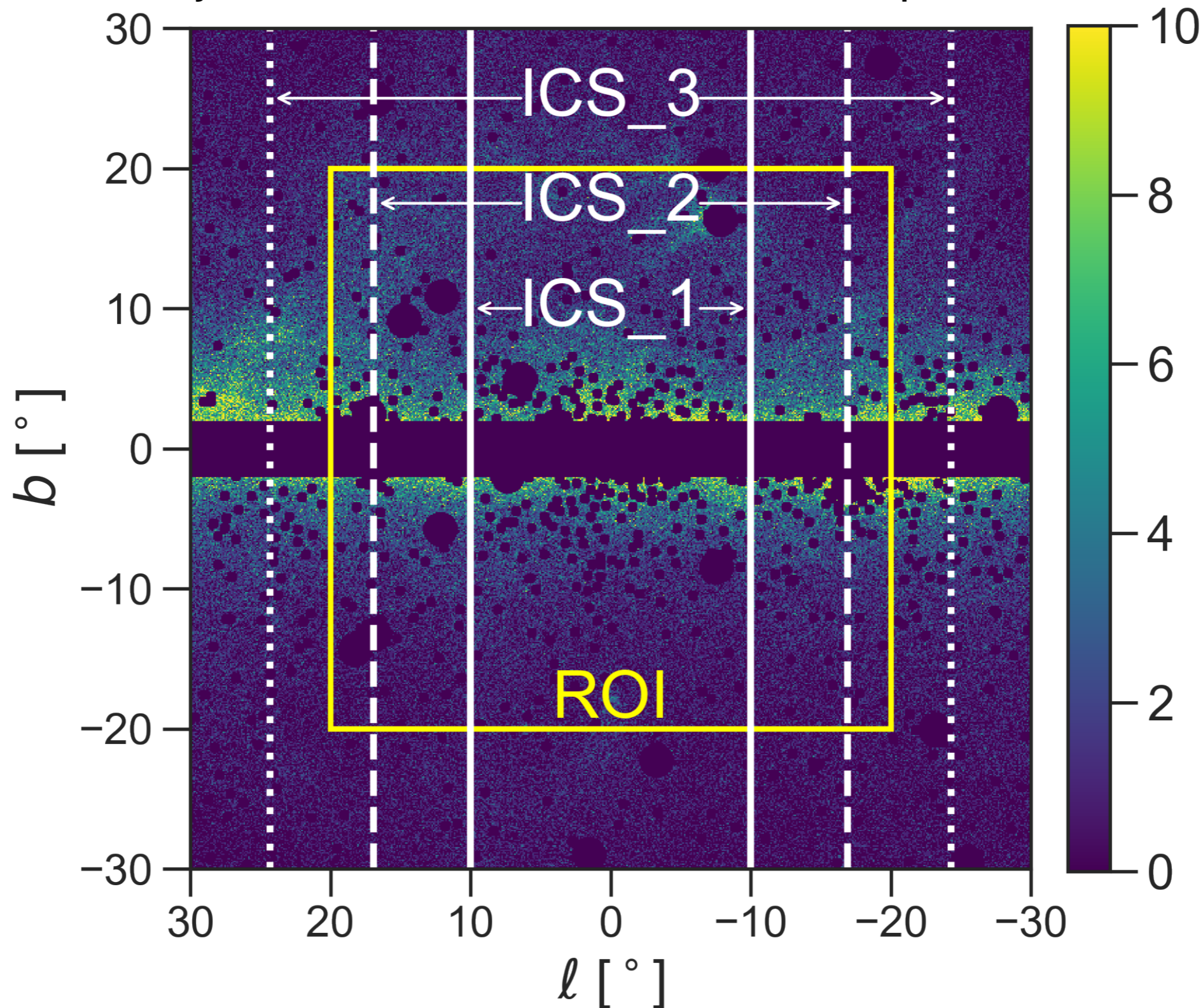
IC, Zhong, McDermott, Surdutovich, PRD 2022

Even when we allow for an additional **stellar bulge component** (probing MSPs) component, we still get **preference for a dominant cuspy NFW-like profile**



Comparison with other recent results that come to different conclusions. The ring-based approach

Works: Macias et al. Nature Astron. 2018, Macias et al. JCAP 2019, Abazajian et al. PRD 2020, Pohl et al. ApJ 2022




The background assumptions on the galactic diffuse emission affect the derived conclusions on the GCE.

McDermott, Zhong, **IC MNRAS Letters 2023** Comparing astrophysically motivated templates (IC et al. 2022) vs ring-based templates (Pohl et al. 2022).

Table 1. Comparison of models of the GCE. The first six results, generated in this work, rely on the ring-based method of Pohl et al. (2022) to describe astrophysical emission. The final three results utilize best fit template model XLIX from Cholis et al. (2022).

Excess Model	Bgd. Templates	$-2\Delta\ln \mathcal{L}$	$\Delta\ln \mathcal{B}$
No Excess	ring-based	0	0
X-Shaped Bulge	ring-based	+30	-190
Dark Matter	ring-based	-237	+12
Boxy & X-Shaped Bulges	ring-based	-634	+178
Boxy Bulge	ring-based	-724	+228
Boxy Bulge “plus”	ring-based	-765	+311
Boxy Bulge “plus” & DM	ring-based	-817	+316
No Excess	astrophysical	-4539	+2933
Boxy Bulge	astrophysical	-6398	+3814
Boxy Bulge “plus”	astrophysical	-6477	+3853
Dark Matter	astrophysical	-7288	+4268
Boxy Bulge “plus” & DM	astrophysical	-7401	+4298

The statistically best models give preference for a more spherical GCE morphology



The background assumptions on the galactic diffuse emission affect the derived conclusions on the GCE.

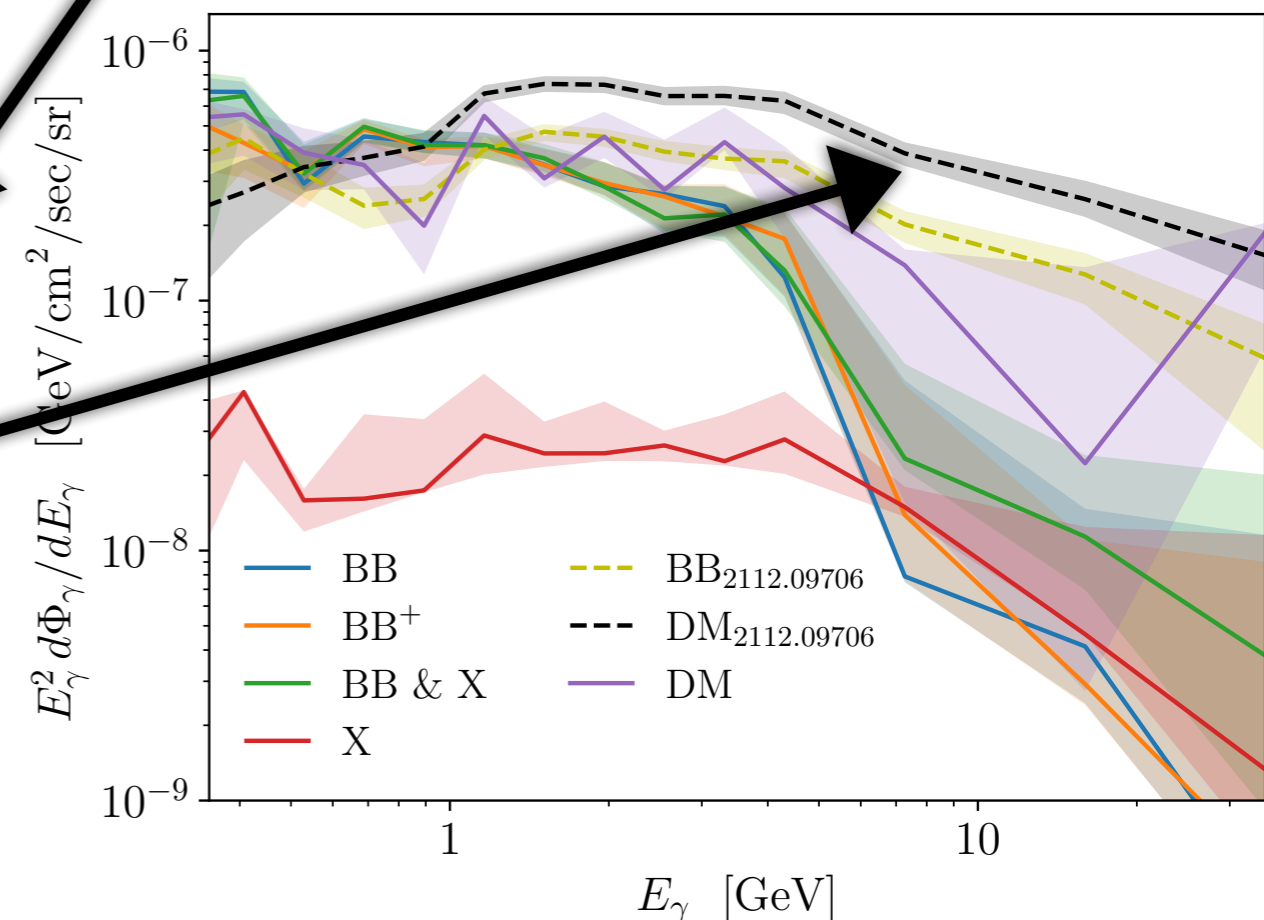
McDermott, Zhong, IC MNRAS Letters 2023 Comparing astrophysically motivated templates (IC et al. 2022) vs ring-based templates (Pohl et al. 2022).

Table 1. Comparison of models of the GCE. The first six results, generated in this work, rely on the ring-based method of Pohl et al. (2022) to describe astrophysical emission. The final three results utilize best fit template model XLIX from Cholis et al. (2022).

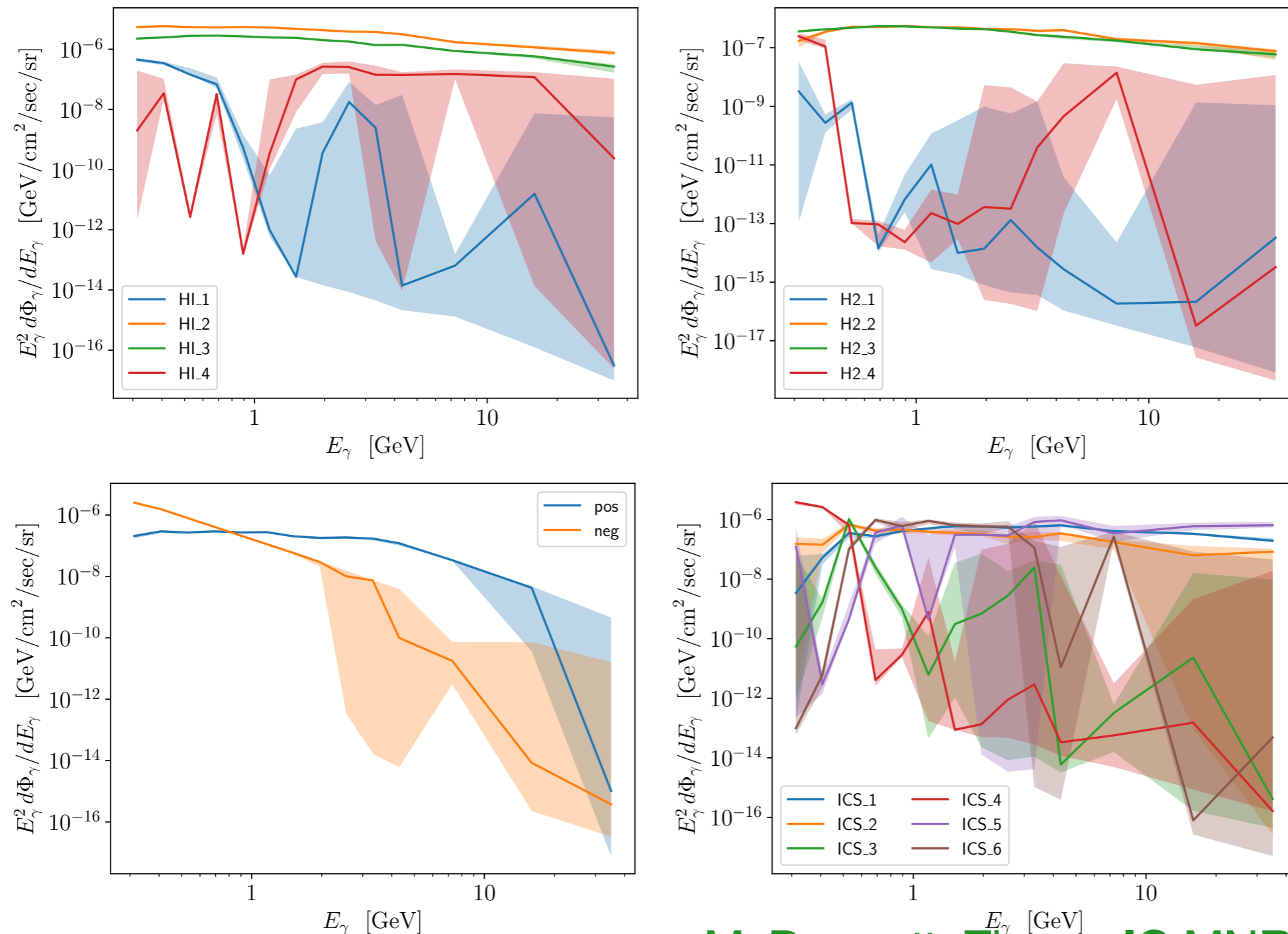
Excess Model	Bgd. Templates	$-2\Delta\ln \mathcal{L}$	$\Delta\ln \mathcal{B}$
No Excess	ring-based	0	0
X-Shaped Bulge	ring-based	+30	-190
Dark Matter	ring-based	-237	+12
Boxy & X-Shaped Bulges	ring-based	-634	+178
Boxy Bulge	ring-based	-724	+228
Boxy Bulge “plus”	ring-based	-765	+311
Boxy Bulge “plus” & DM	ring-based	-817	+316
No Excess	astrophysical	-4539	+2933
Boxy Bulge	astrophysical	-6398	+3814
Boxy Bulge “plus”	astrophysical	-6477	+3853
Dark Matter	astrophysical	-7288	+4268
Boxy Bulge “plus” & DM	astrophysical	-7401	+4298

The statistically best models give preference for a more spherical GCE morphology

And also a preference for a harder GCE spectrum at higher energies (and also a smoother spectrum).



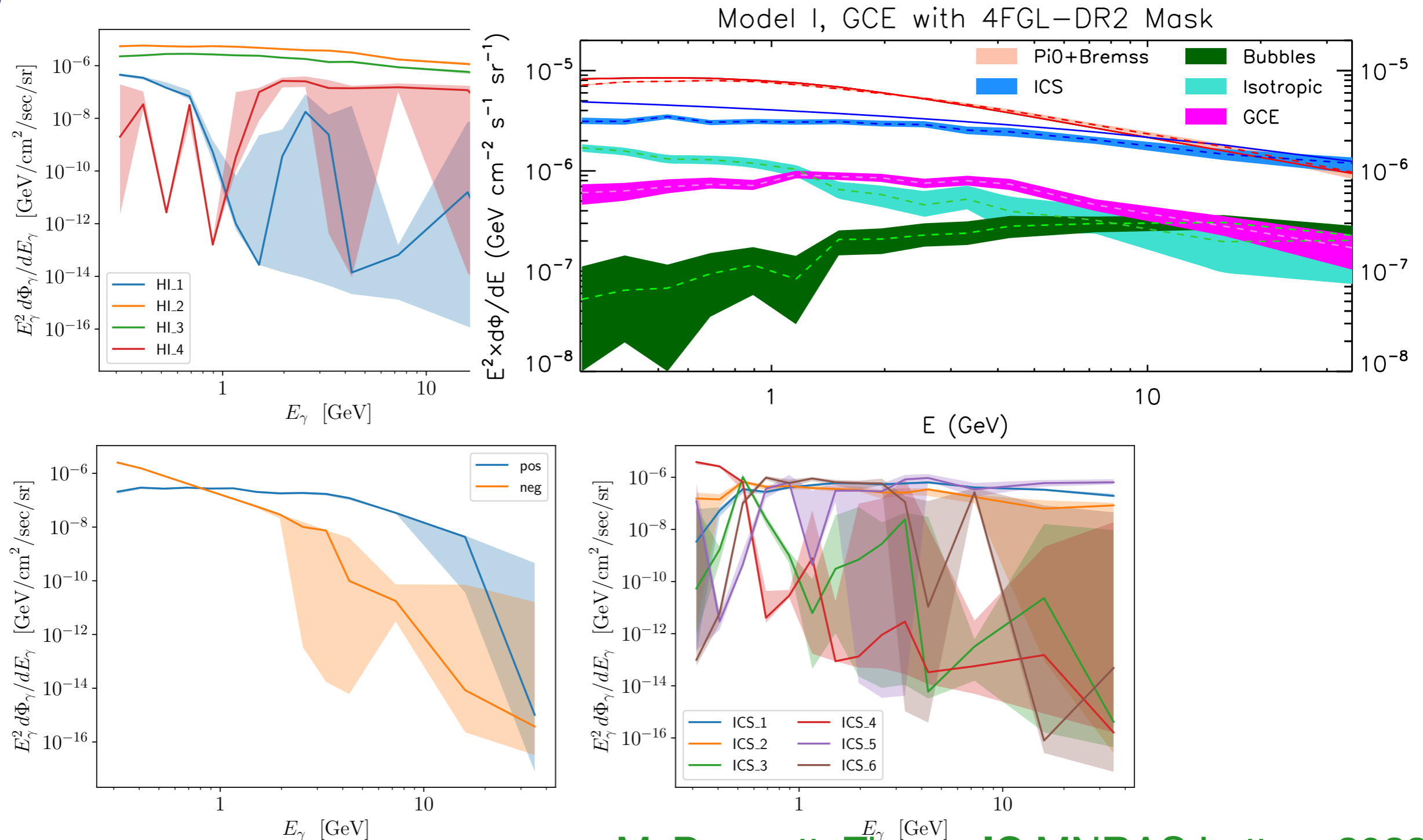
We also find unphysical spectral variations/breaks in the individual flux components associated to the separate rings.



McDermott, Zhong, IC MNRAS Letters 2023

Figure 2. Best-fit spectra and 95% credible intervals of the flux of the ring-based templates that were fit alongside the boxy bulge excess template. For the negative residual component, we show its absolute value in the lower left panel.

We also find unphysical spectral variations/breaks in the individual flux components associated to the separate rings. This never happens with the modeled astrophysical assumption-based templates.

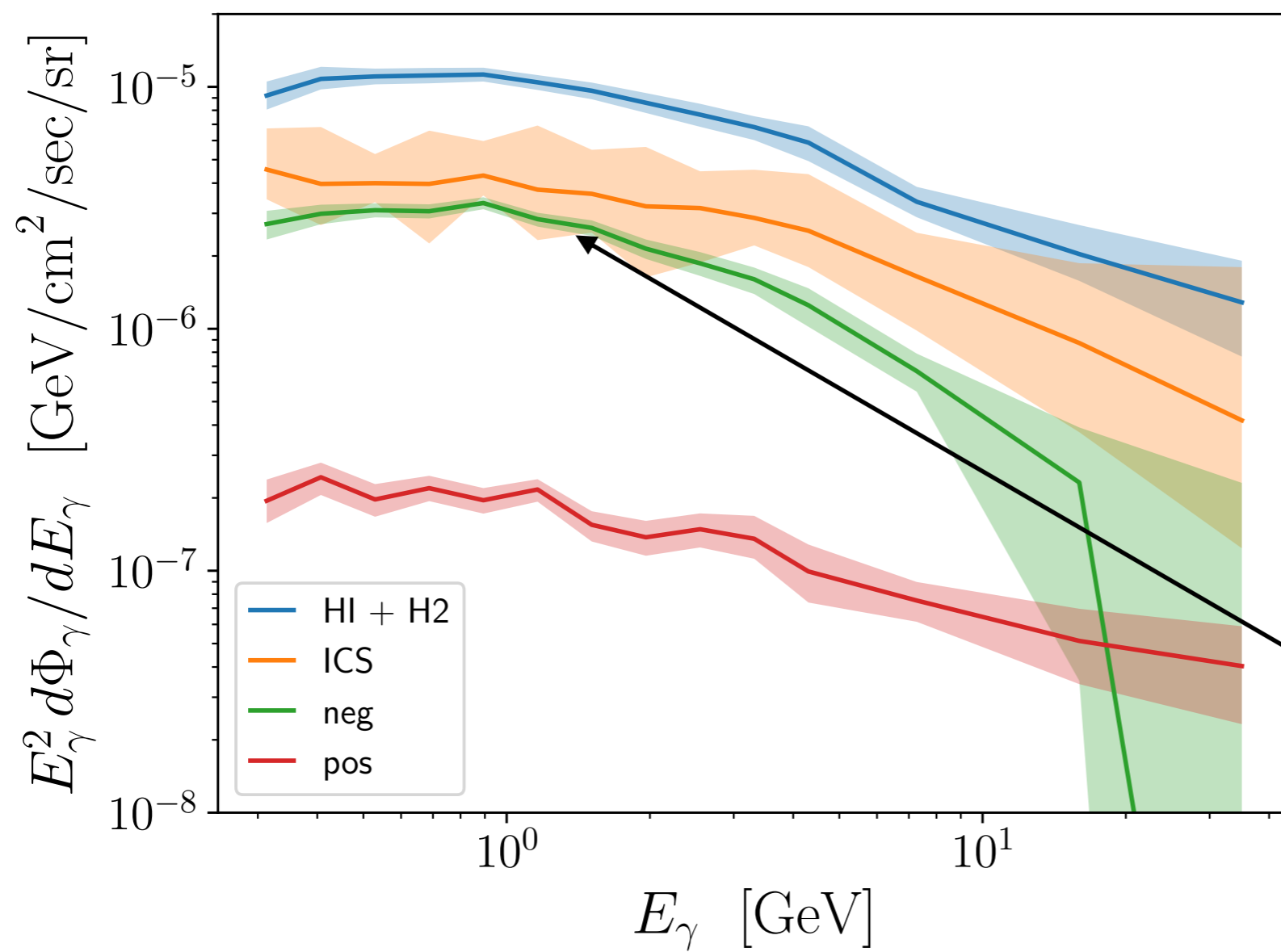


McDermott, Zhong, IC MNRAS Letters 2023

Figure 2. Best-fit spectra and 95% credible intervals of the flux of the ring-based templates that were fit alongside the boxy bulge excess template. For the negative residual component, we show its absolute value in the lower left panel.

Wide priors fit:

Excess Model	Bgd. Templates	$-2\Delta\ln\mathcal{L}$
No Excess	astrophysical - ring-based	1805
X-Shaped Bulge	astrophysical - ring-based	574
Boxy Bulge	astrophysical - ring-based	-52
Boxy Bulge “plus”	astrophysical - ring-based	-131
Dark Matter	astrophysical - ring-based	-942
DM + Boxy Bulge “plus”	astrophysical - ring-based	-1056

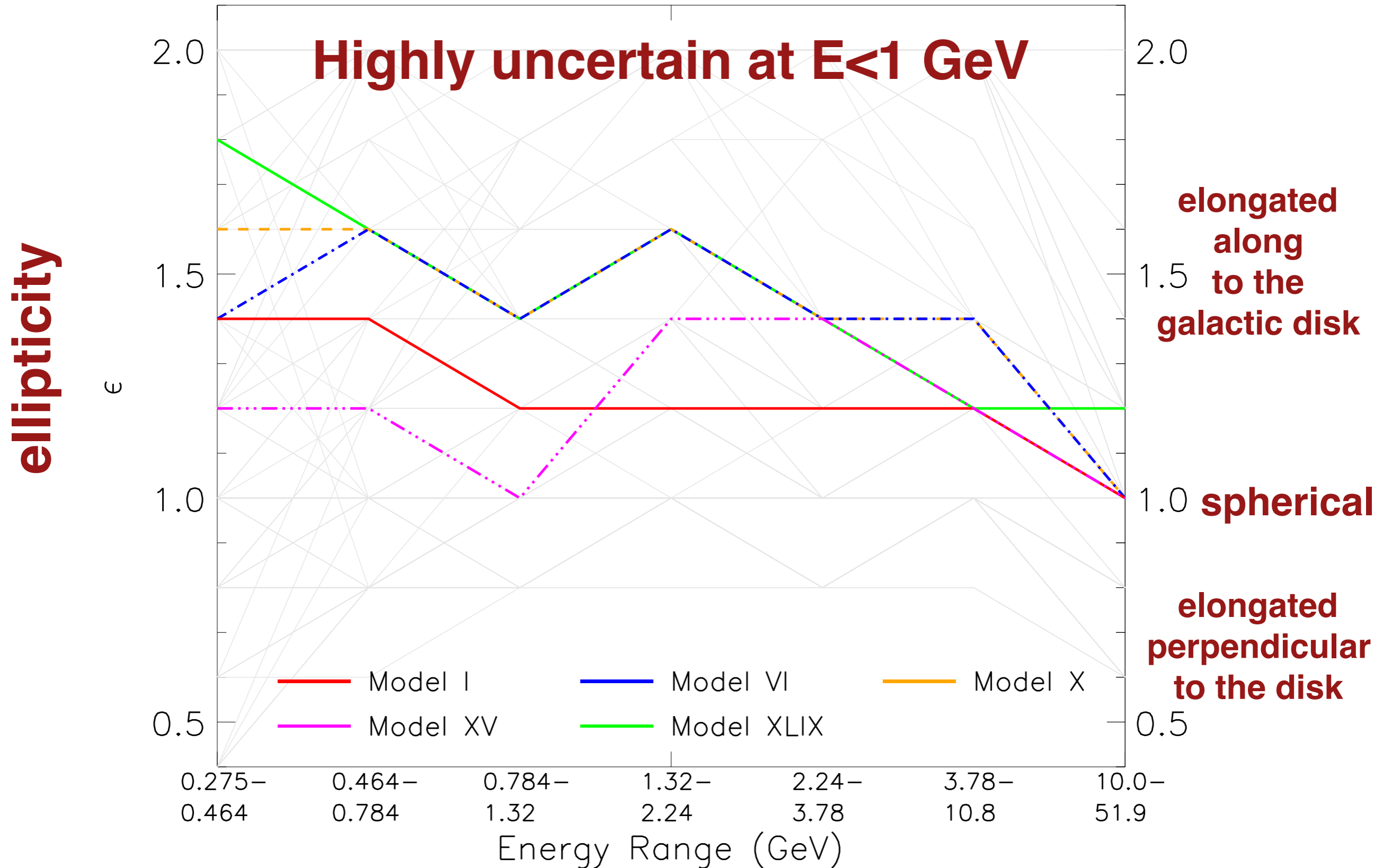


Lower is better

There is no physical justification for **negative** residual gas maps at the 20% level across the entire region (it should be a 0.1-1% correction).

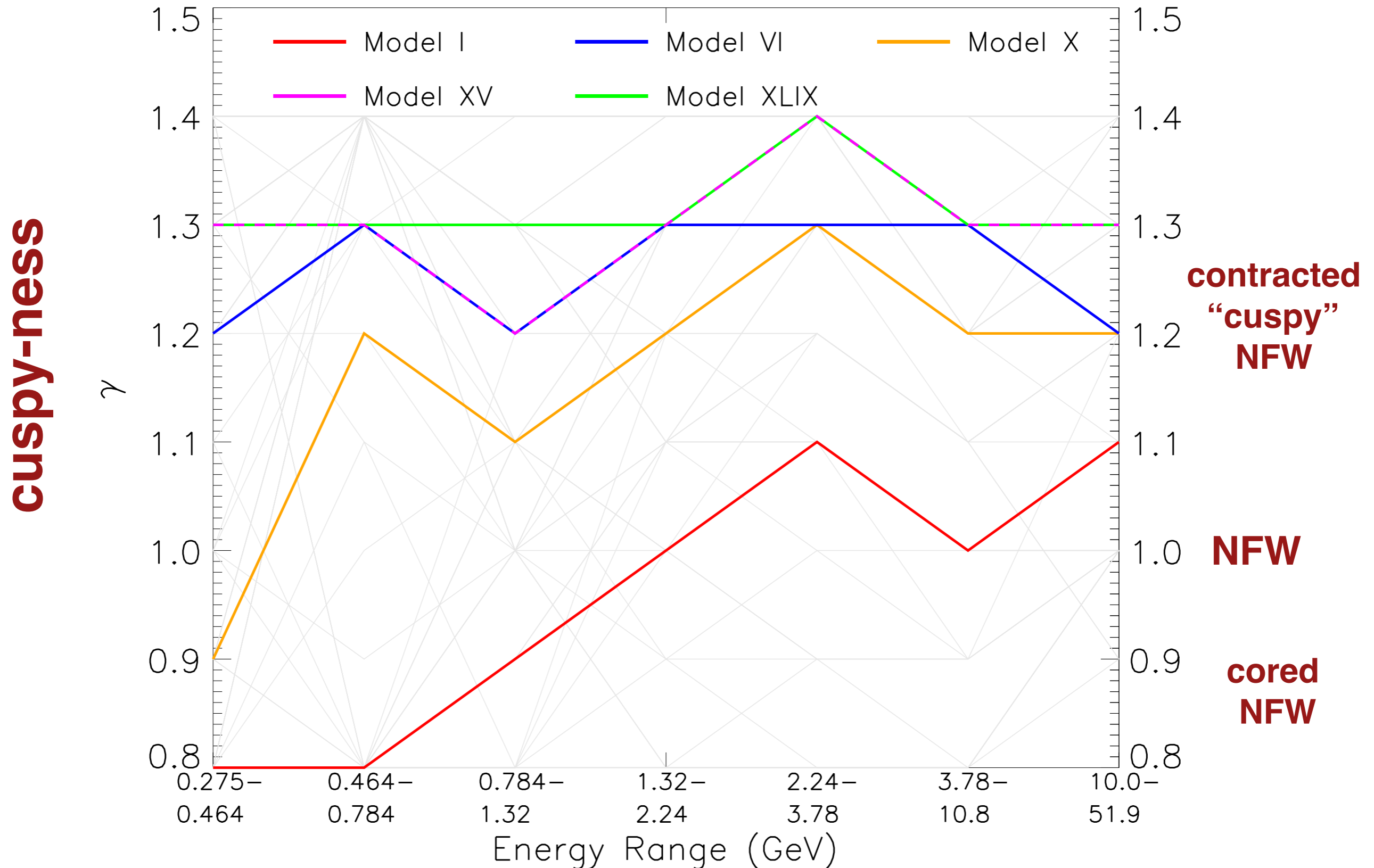
Testing how the morphology of the GCE depends on the energy of gamma-rays. Maybe it is more disk-like/bulgy at low energies?

Zhong, IC in prep. 2023



Testing how the morphology of the GCE depends on the energy of gamma-rays. Maybe it is more disky/bulgy at low energies?

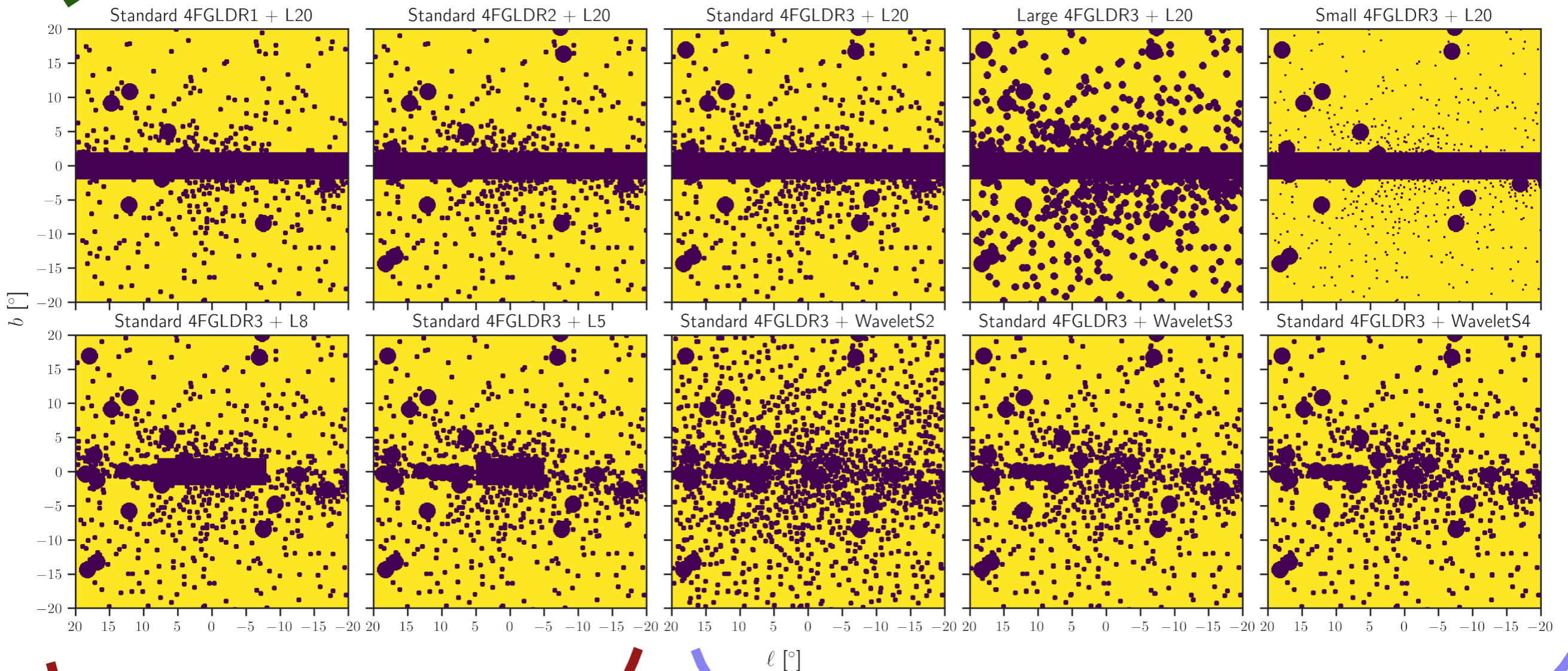
Zhong, IC in prep. 2023



Ongoing Preliminary: Zhong, IC 2023 in prep

Further Tests on the GCE morphology with Alternative Masks, including using wavelets to identify hot-spots:

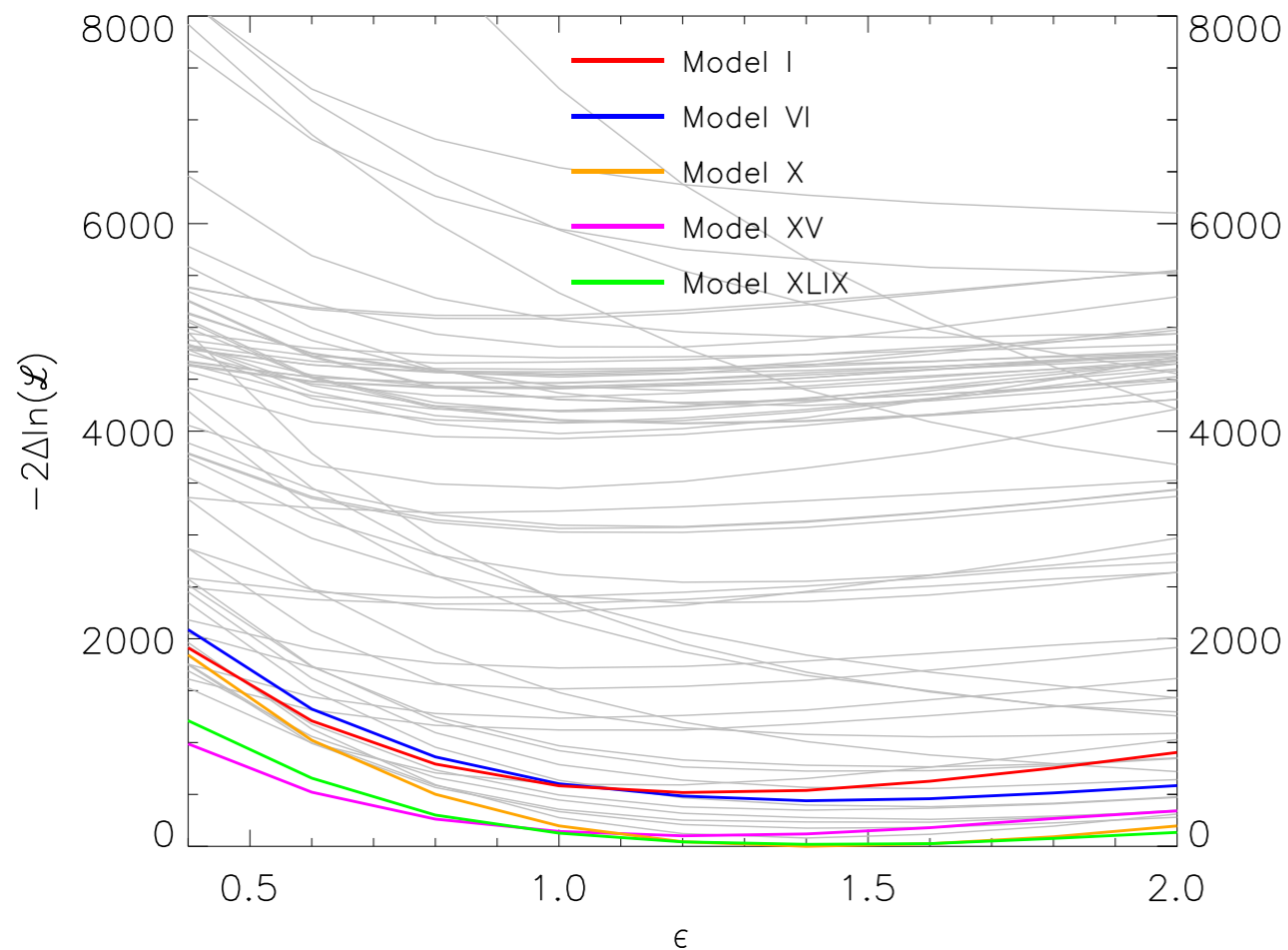
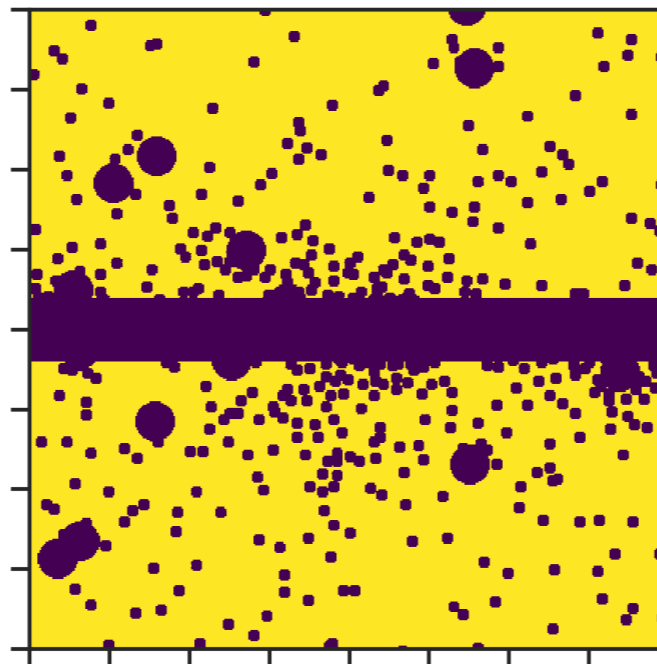
4FGL-DR1, 2 or 3 + all of the disk



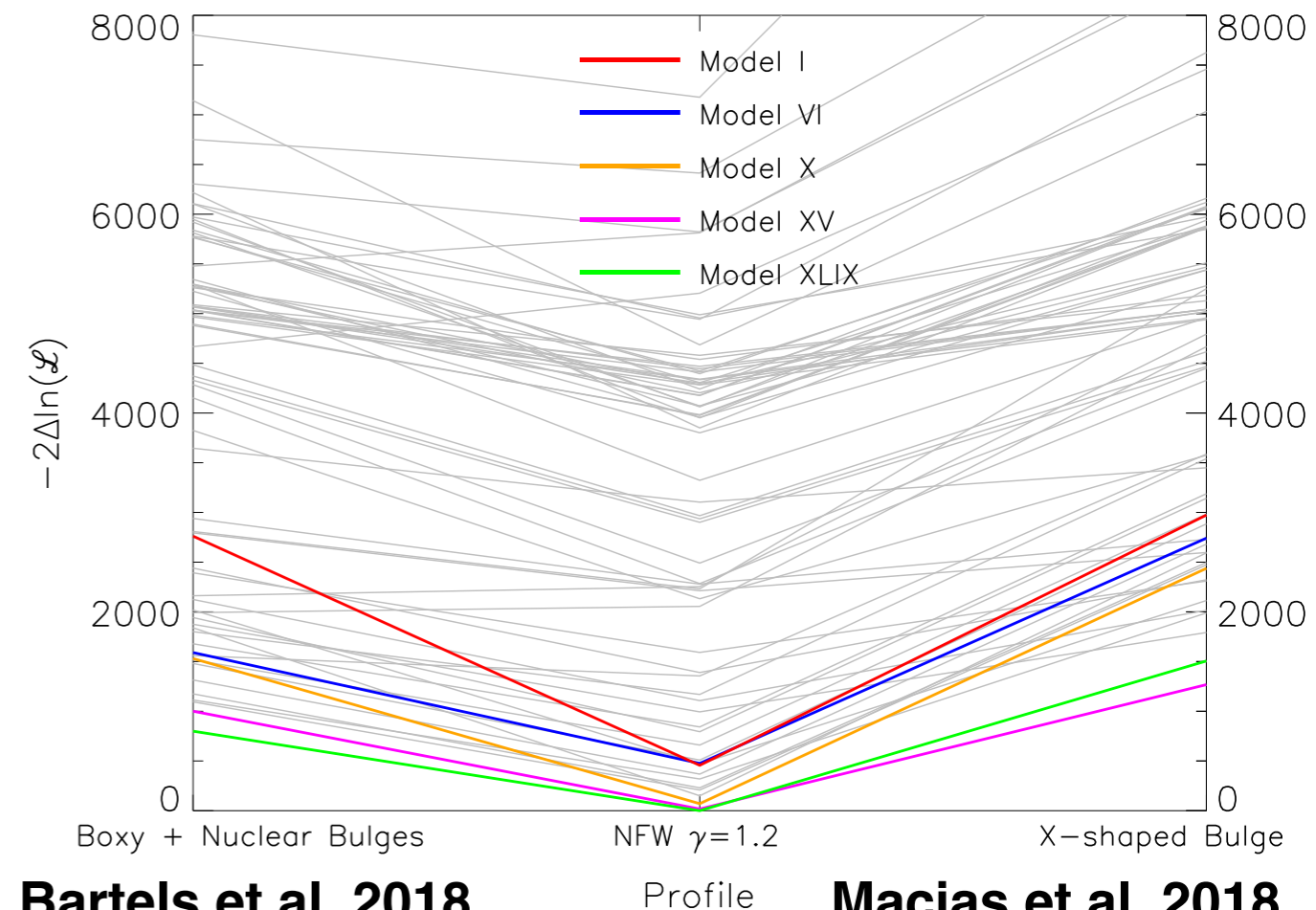
4FGL-DR3 + part of the disk

4FGL-DR3 + Wavelet-based

Standard 4FGLDR2 + L20



Ellipticity



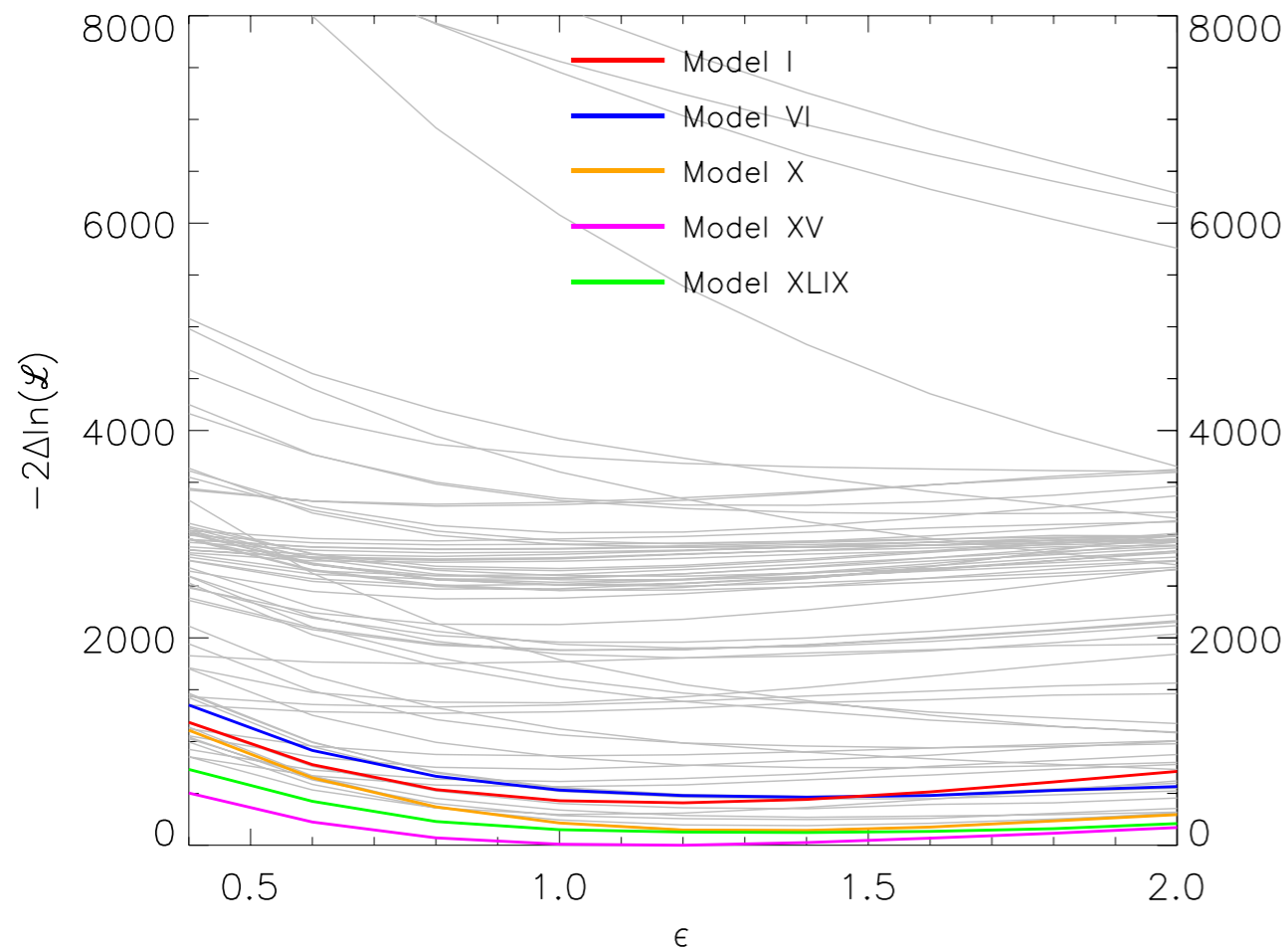
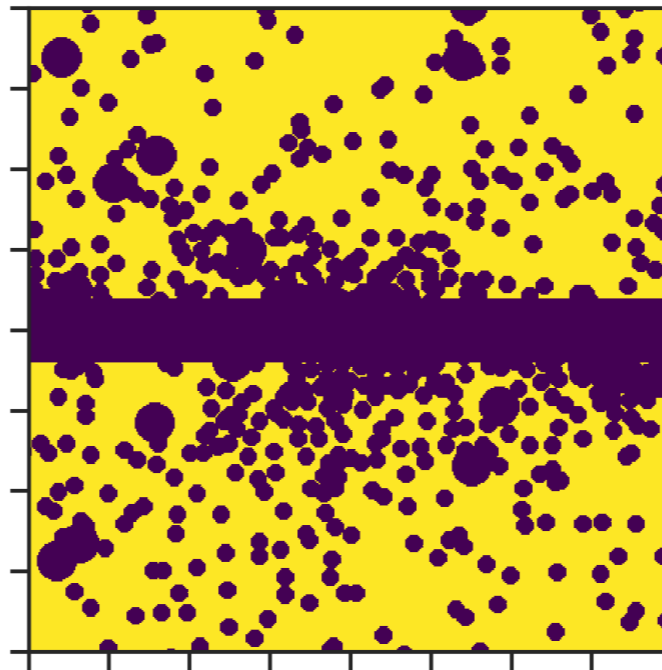
Bartels et al. 2018

Profile

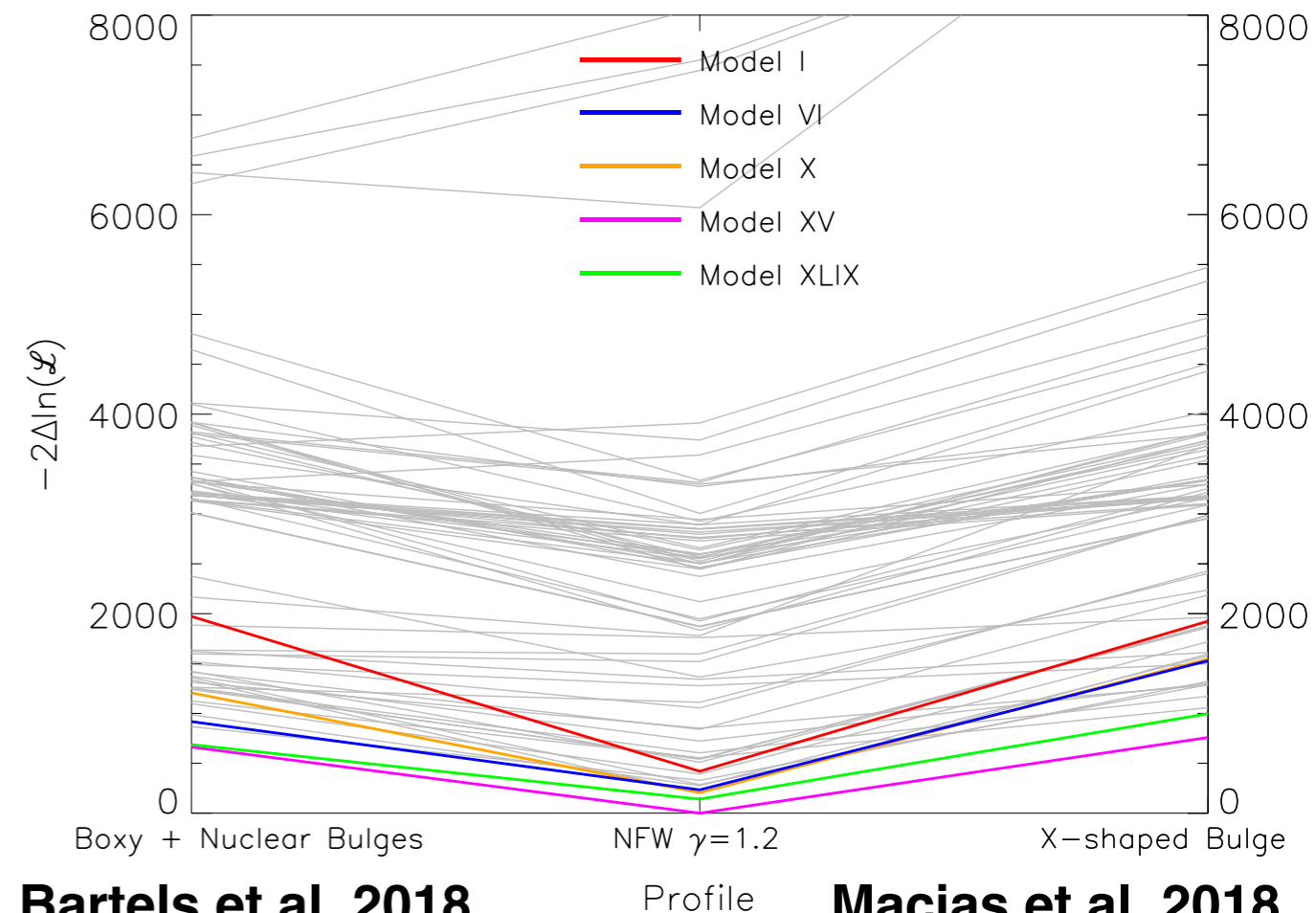
Macias et al. 2018

Spherical NFW vs Bulges

Large 4FGLDR3 + L20



Ellipticity



Bartels et al. 2018

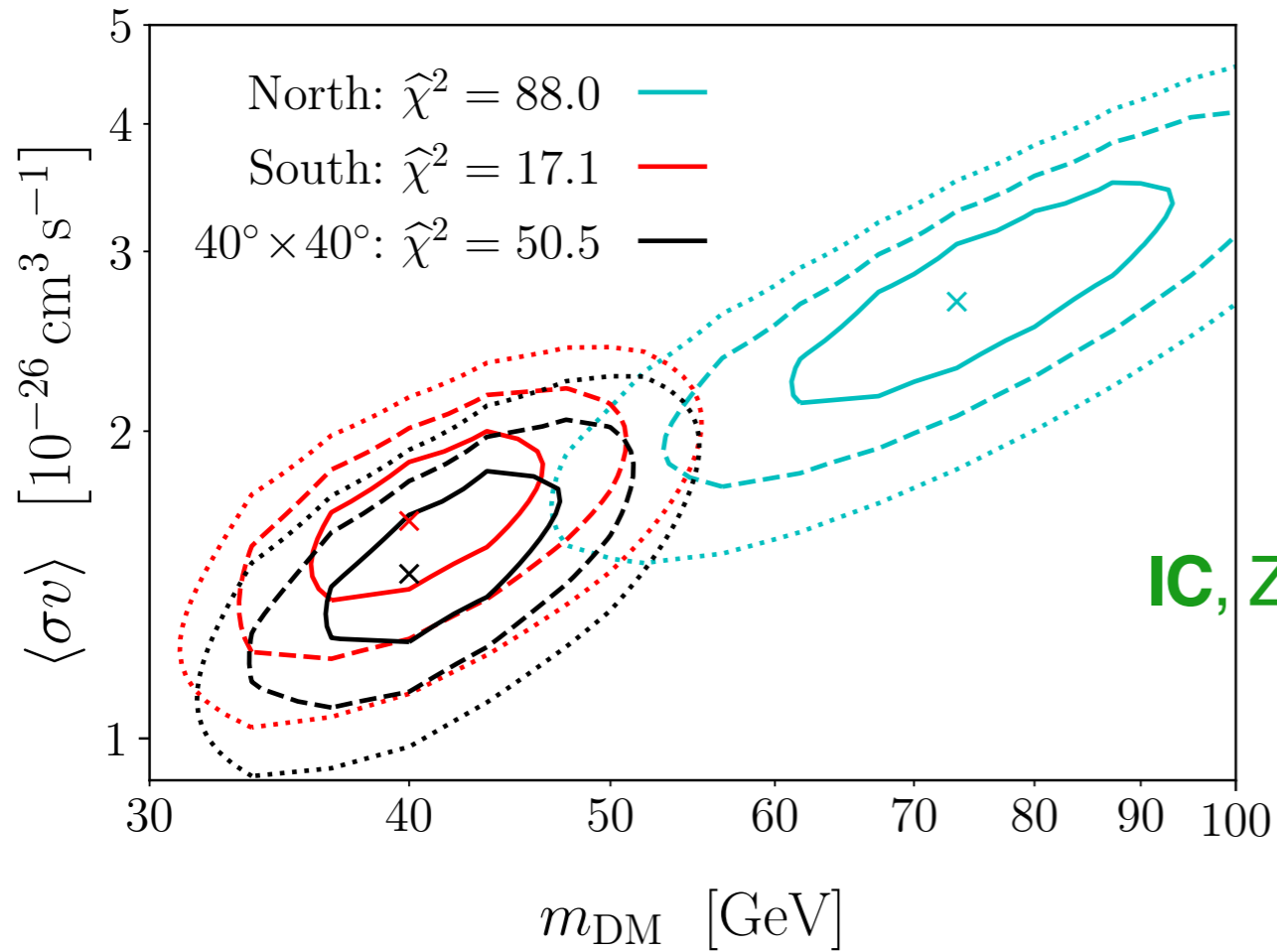
Profile

Macias et al. 2018

Spherical NFW vs Bulges

If this is a DM annihilation signal what do we learn about the particle physics?

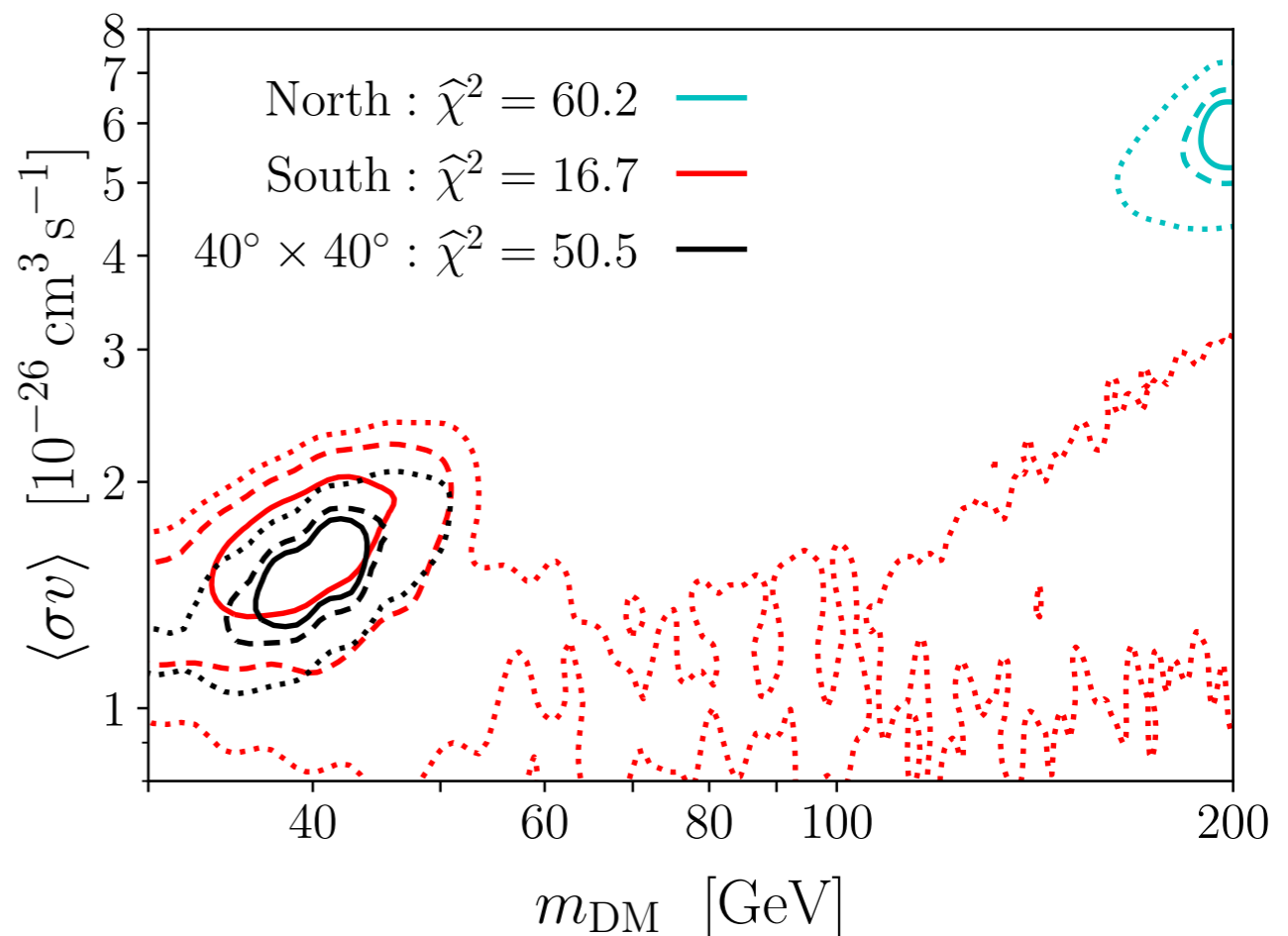
DM DM $\rightarrow b\bar{b}$



The mass range preferred very much within the WIMP range.

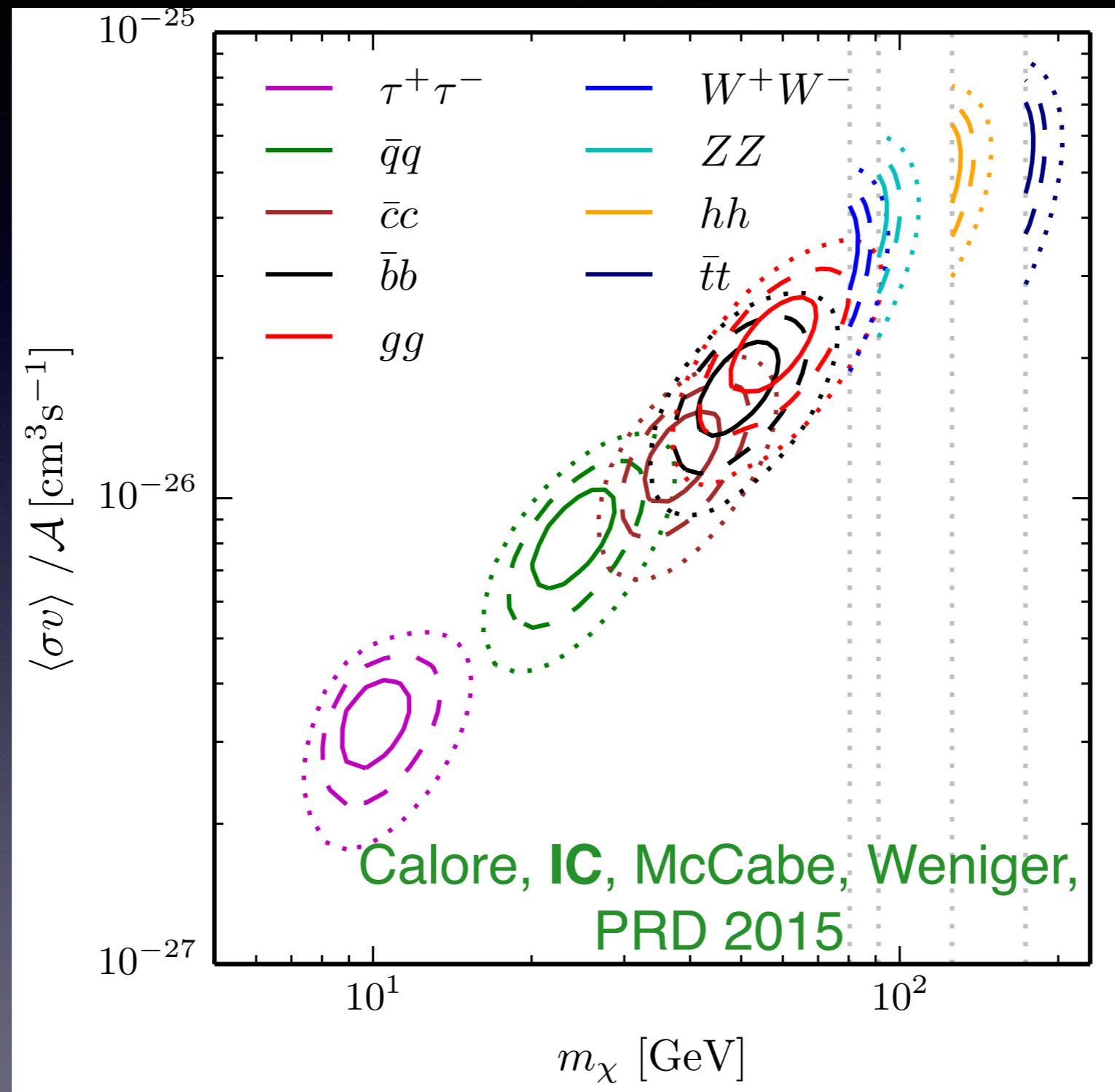
IC, Zhong, McDermott, Surdutovich, PRD 2022

MSPs + DM DM $\rightarrow b\bar{b}$



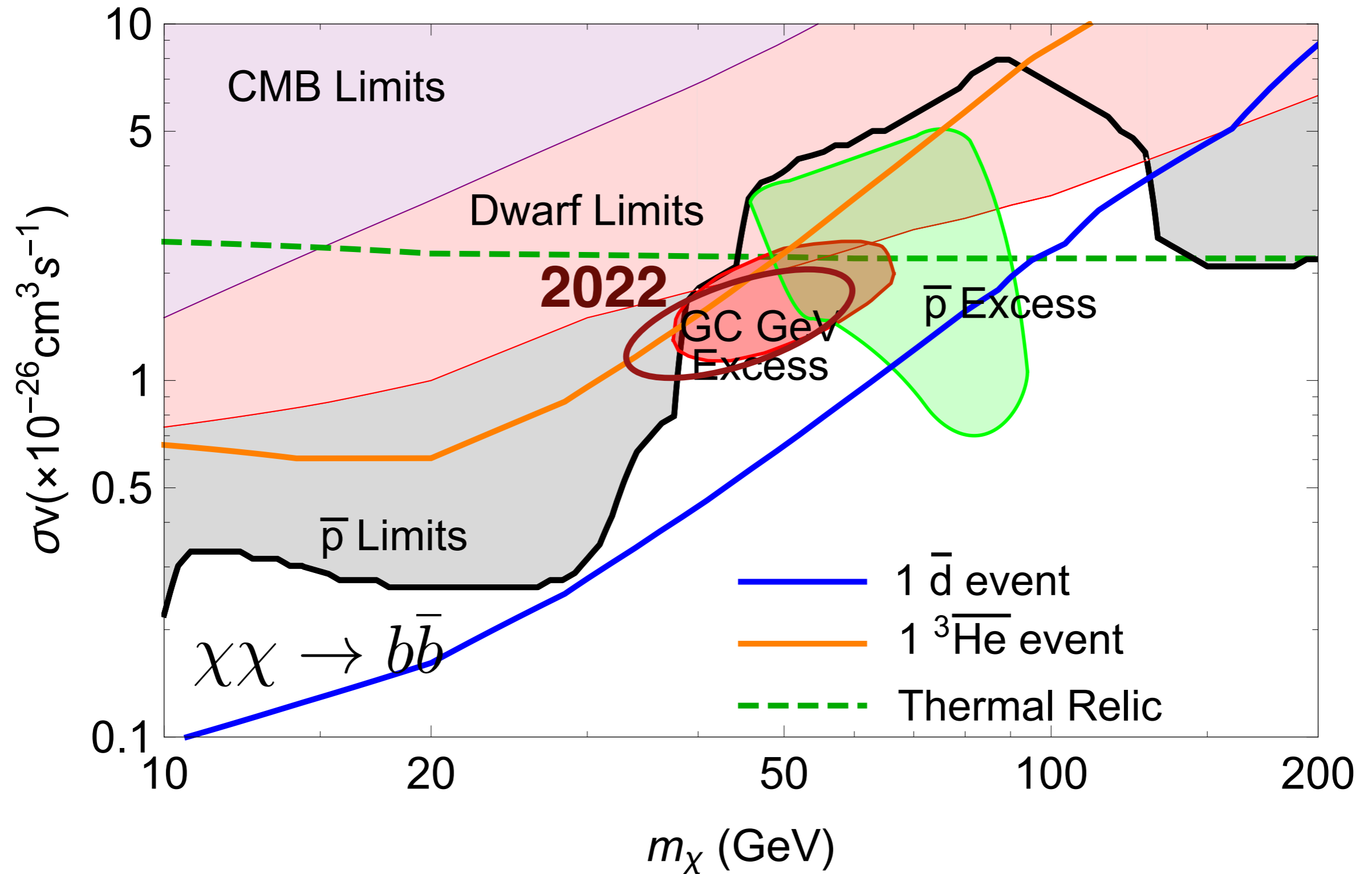
Adding an MSP component affects the fits on the more “dirty” (more galactic gas) Northern Hemisphere, but the Southern Hemisphere and the overall Inner Galaxy fit are fairly unaffected.

If this is a DM annihilation signal what do we learn about the particle physics?



The mass range preferred very much within the WIMP range.

Combining all Indirect DM searches



Acknowledgements

My Collaborators: Dan Hooper (Fermilab/U. Chicago), Tim Linden (U. Stockholm), Sam McDermott (Fermilab), Yi-Ming Zhong (KICP)

My Students: Iason Krommydas (NTUA—>Rice University),
Ian McKinnon (OU—>University of Oklahoma),
Osip Surdutovich (Carleton College—> Ohio State University)



MSGC, NASA No. NNX15AJ20H

MSGC, NASA No. 80NSSC20M0124

Oakland University Research Fellowship

Department of Energy, DE-SC0022352



Thank you!

Extra

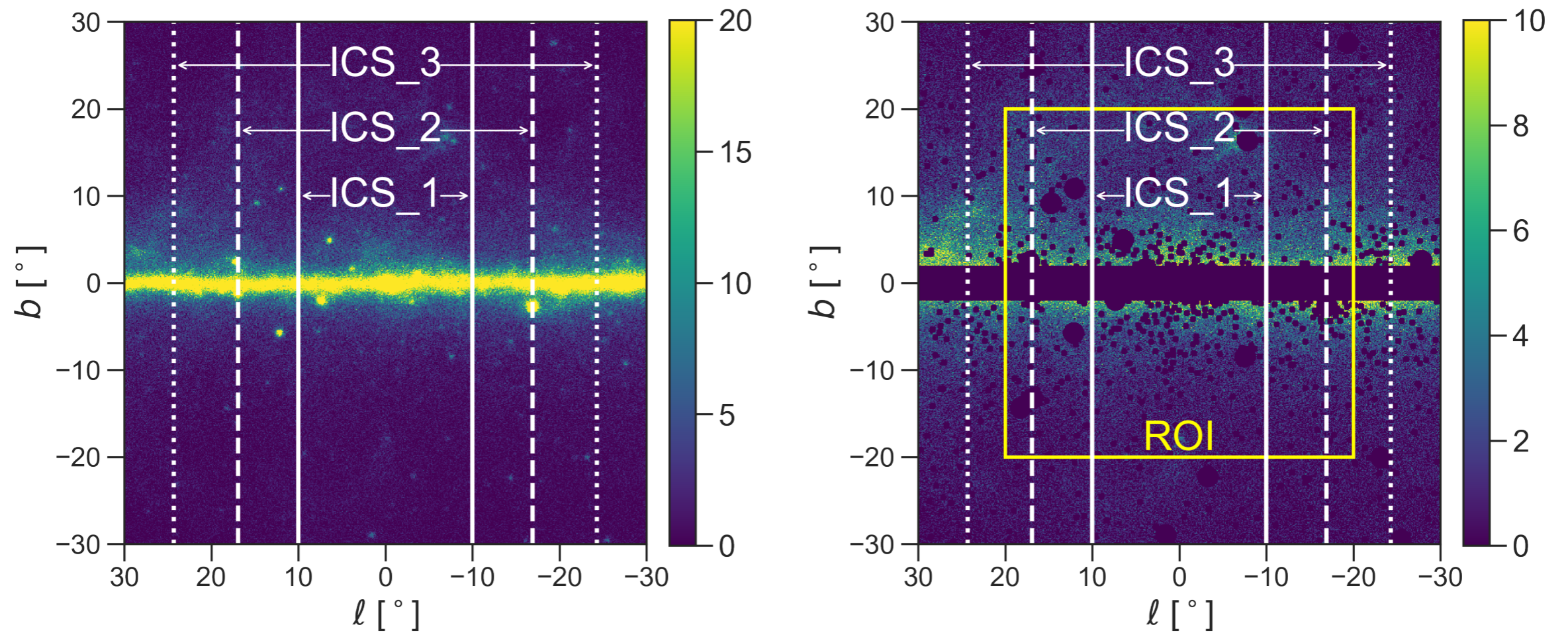
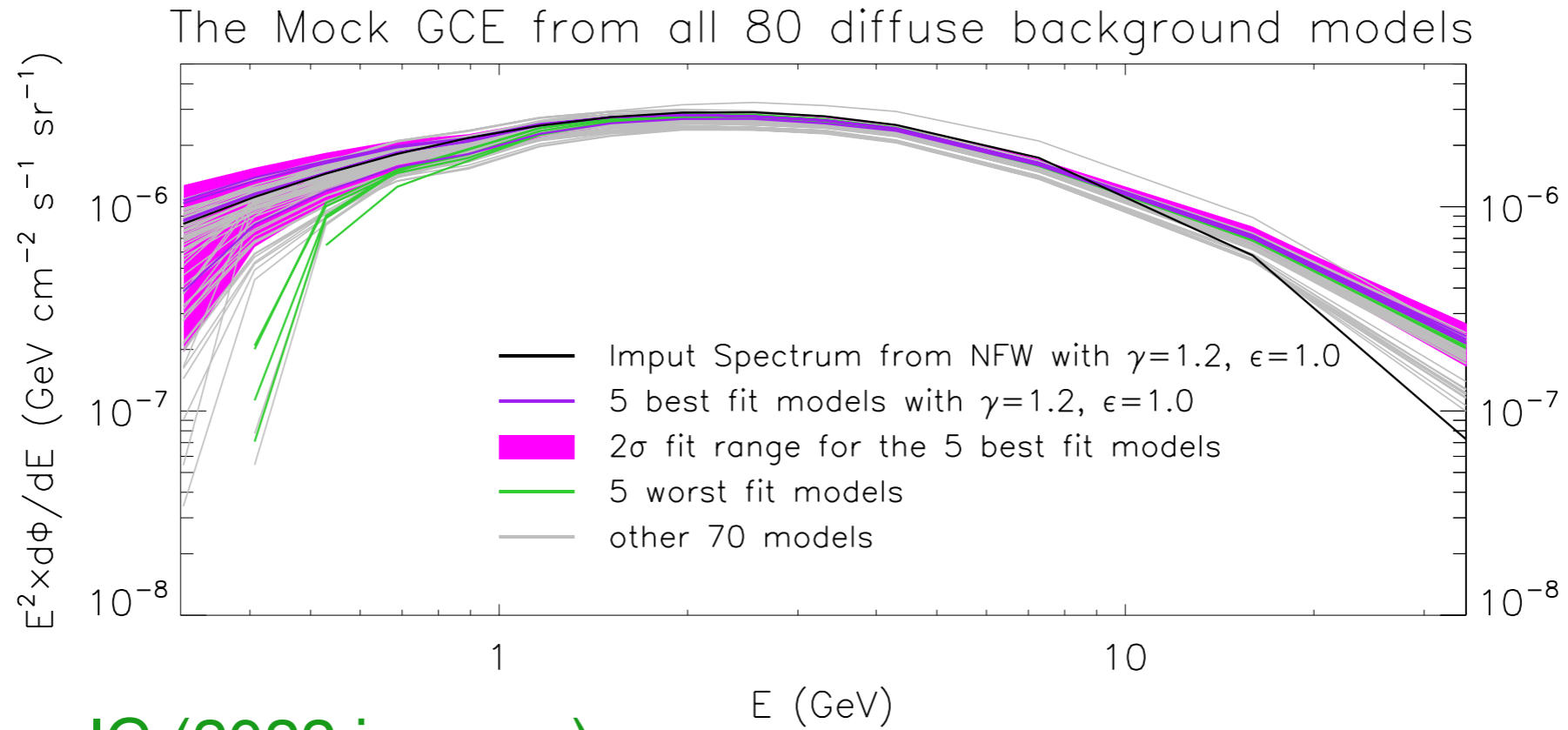


FIG. 2. Photons passing our cuts with energy $1.02 \text{ GeV} < E_\gamma < 1.32 \text{ GeV}$, without (left) and with (right) the mask that we use for our data. For illustration purposes, we show the boundaries of the ICS_1, ICS_2, and ICS_3 rings that vary independently in our fits. In the right panel, we show the region of interest in which we perform our fits.

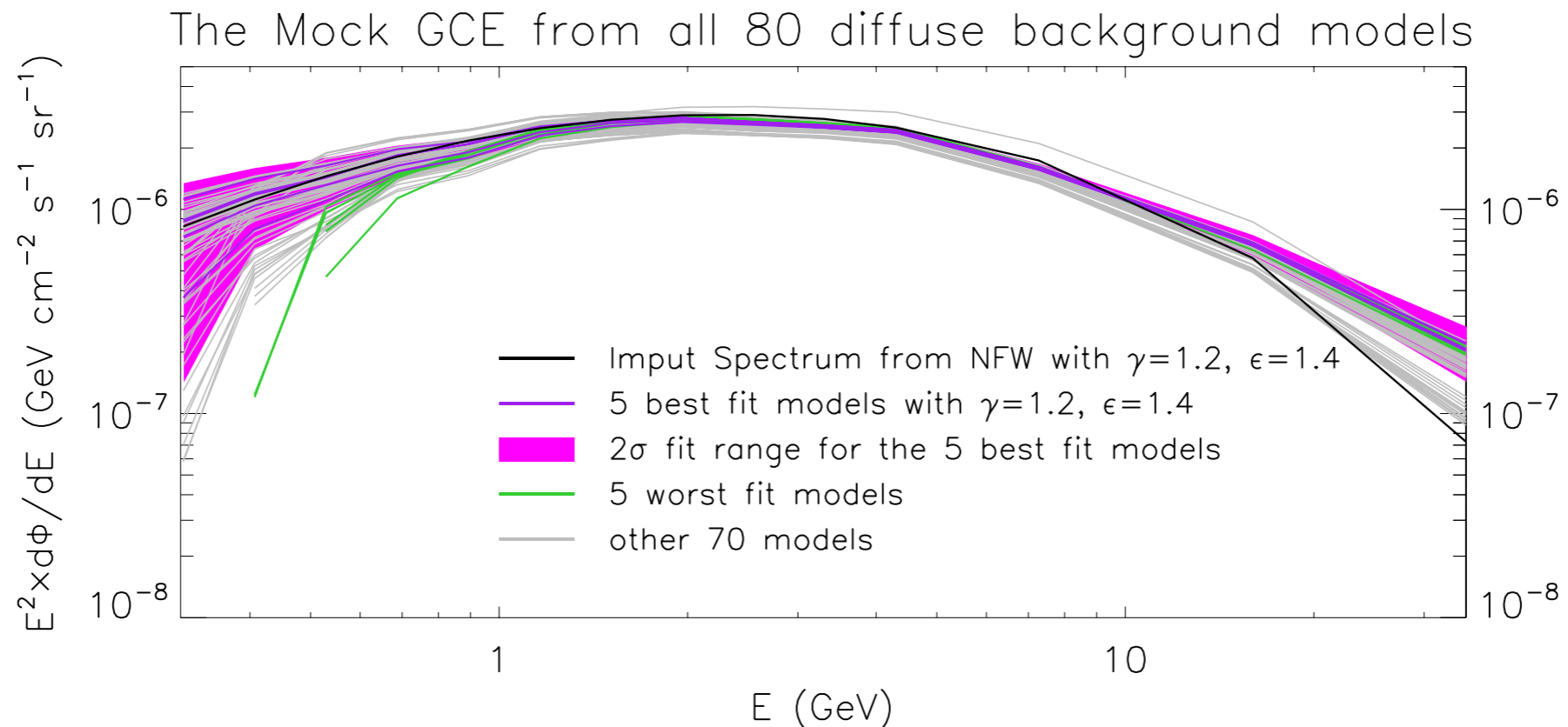
McDermott, Zhong, IC (arXiv:2209.00006)

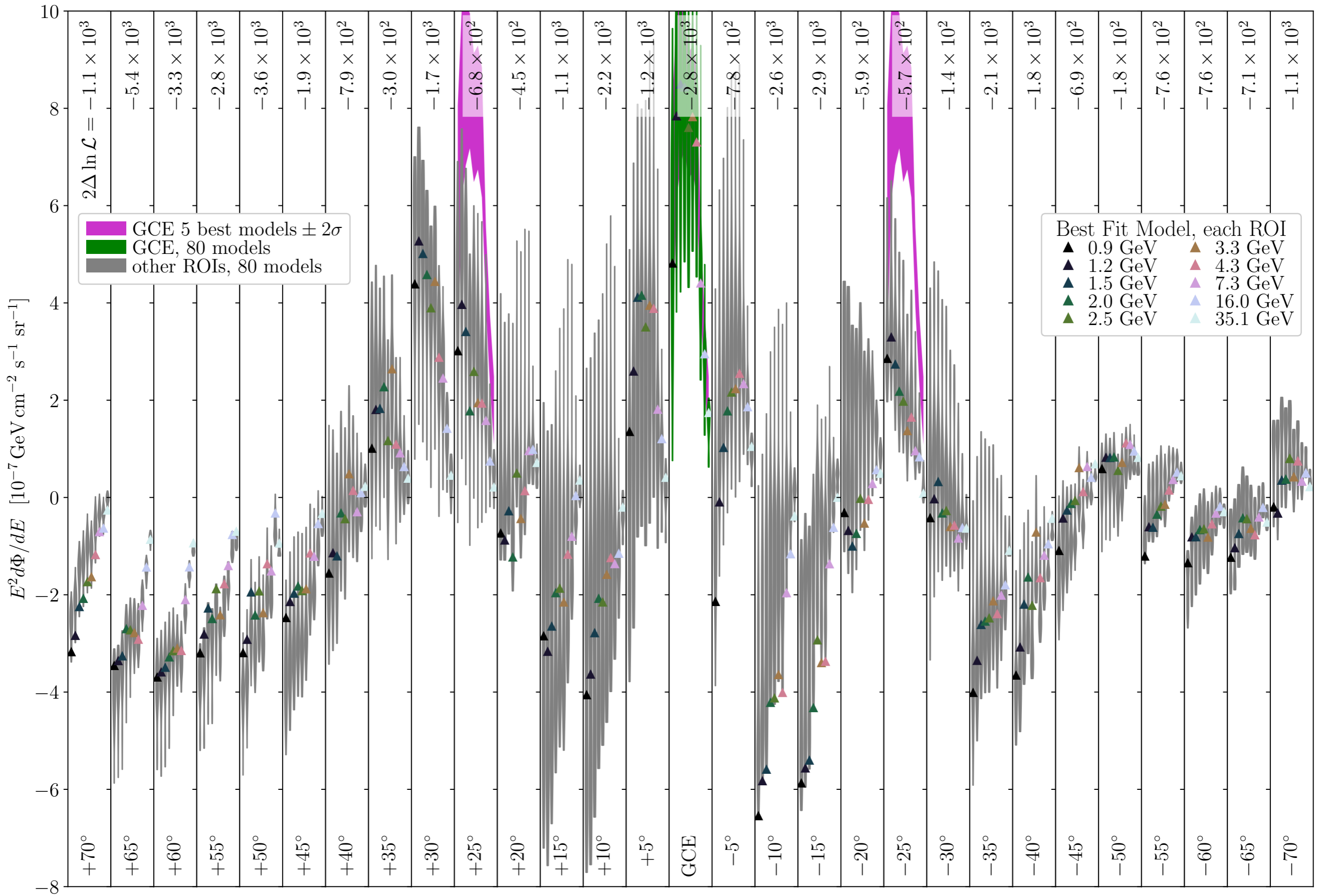
Ongoing Preliminary:

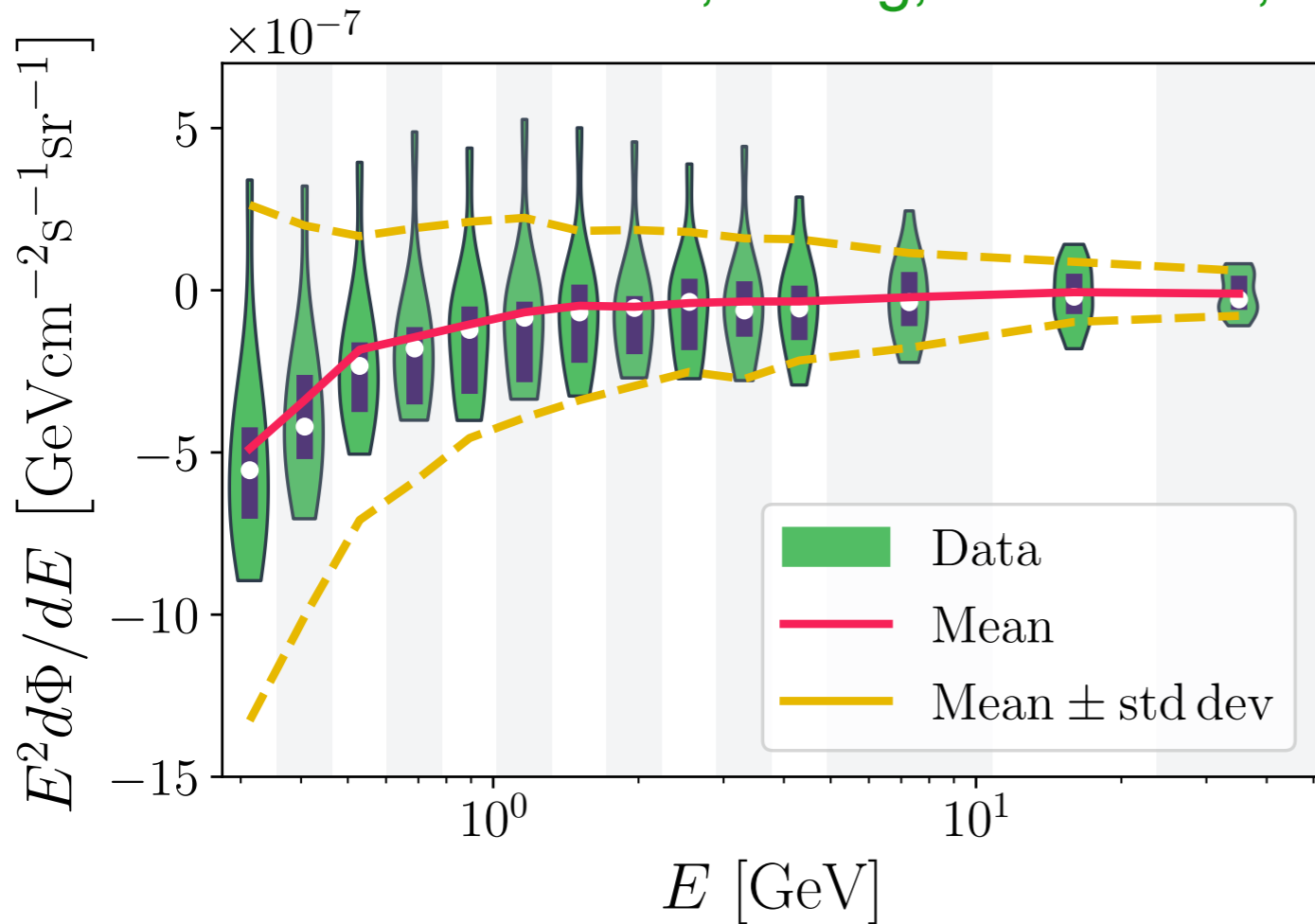
Further Tests of injected Mock Maps versus what we recover from the fits:



Zhong, IC (2022 in prep.)







The covariance matrix:

$$\Sigma_{ij,\text{mod}} = \left\langle E^4 \frac{d\Phi}{dE_i} \frac{d\Phi}{dE_j} \right\rangle - \left\langle E^2 \frac{d\Phi}{dE_i} \right\rangle \left\langle E^2 \frac{d\Phi}{dE_j} \right\rangle$$

Its truncated version:

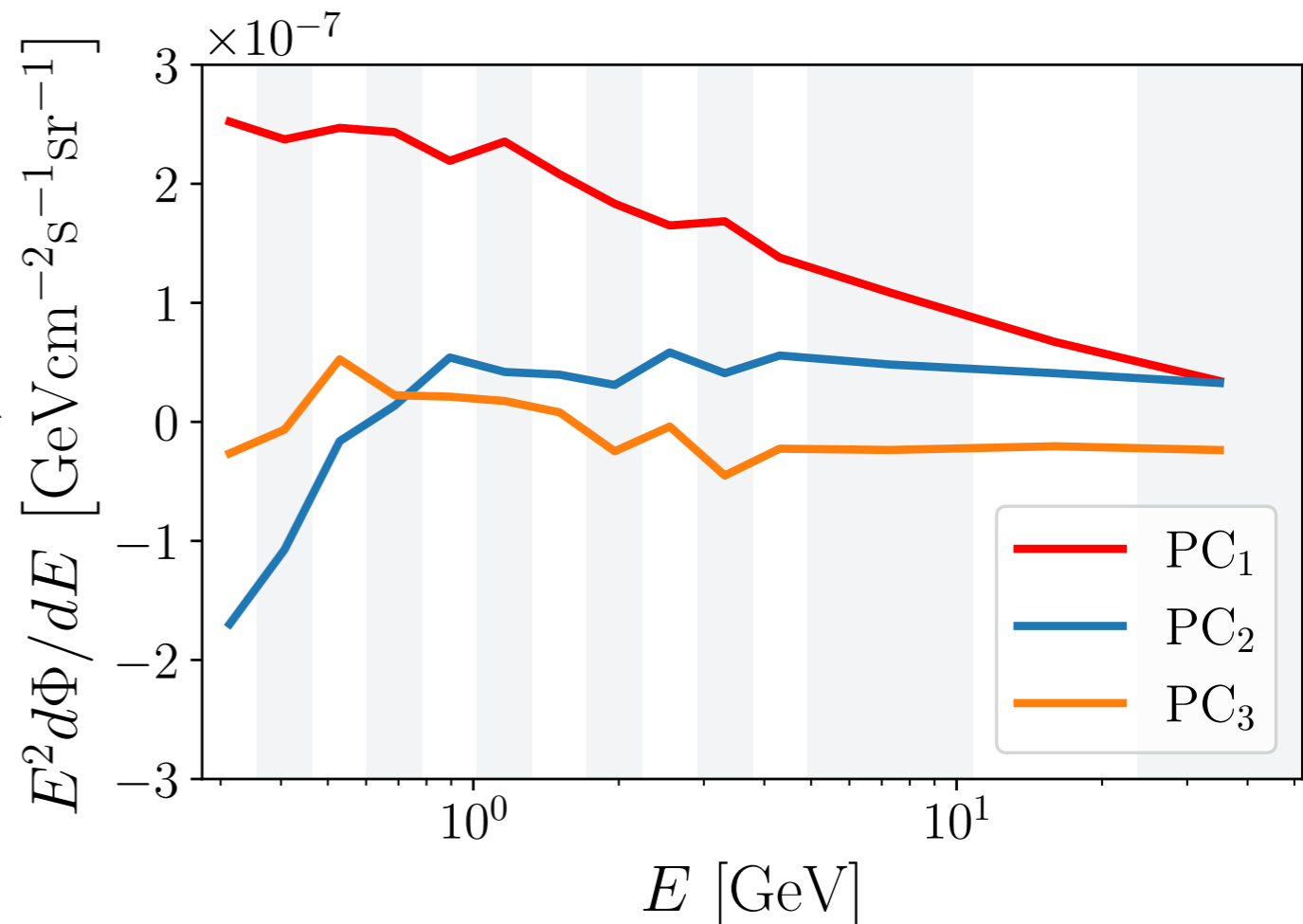
$$\Sigma_{jk,\text{mod}} \simeq \Sigma_{jk,\text{mod}}^{\text{trunc}} \equiv \sum_{i=1}^3 \text{PC}_{ij}^T \text{PC}_{ik}$$

The formal fit:

$$\chi^2 = \sum_{ij} \left(\text{GCE}_i - \sum_k f_{ik}(\theta_k) \right) C_{ij}^{-1} \left(\text{GCE}_j - \sum_\ell f_{j\ell}(\theta_\ell) \right)$$

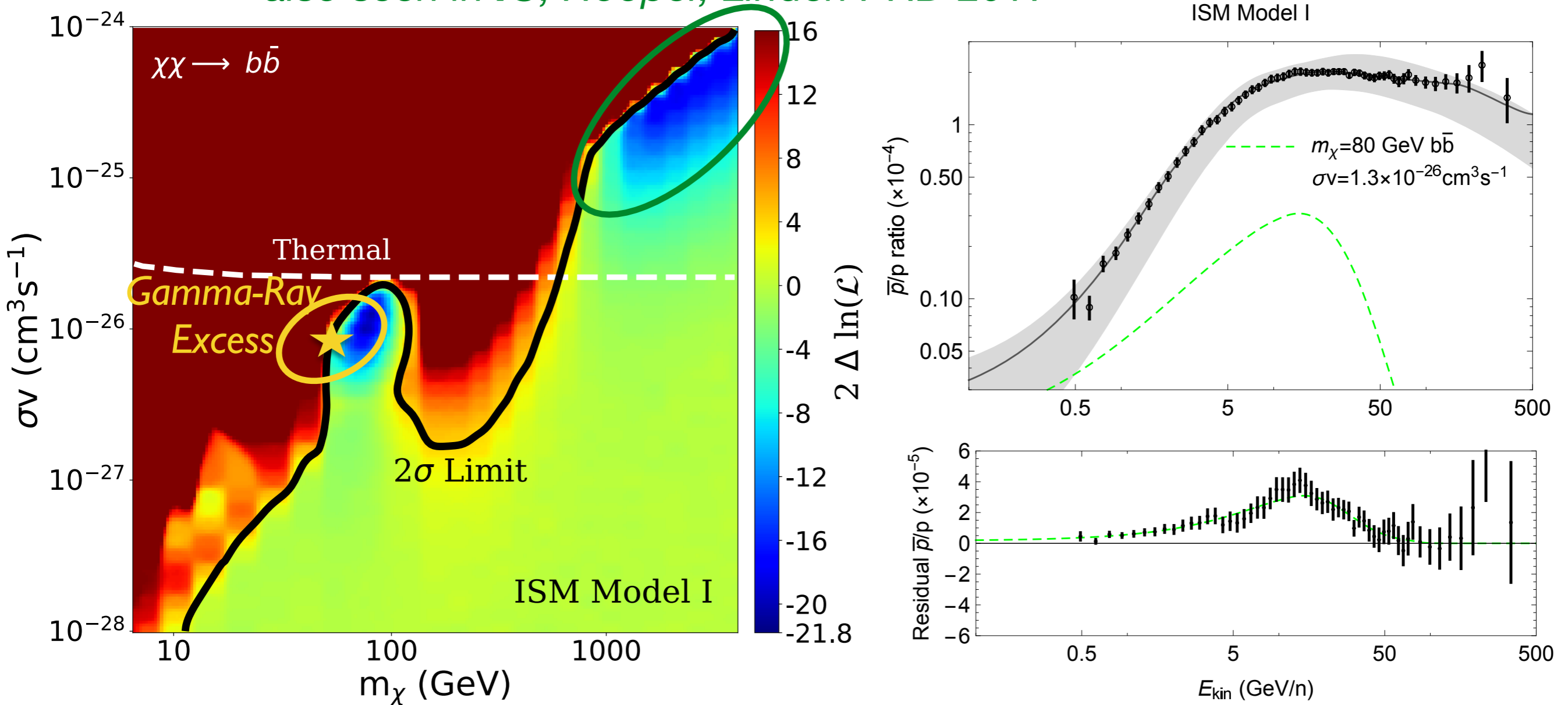
Where:

$$C_{ij} = \sigma_i^2 \delta_{ij} + \Sigma_{ij,\text{mod}}$$



Looking at the antiproton to proton ratio *find an the excess at ~ 3 sigma*

Supernova,
also seen in **IC**, Hooper, Linden PRD 2017



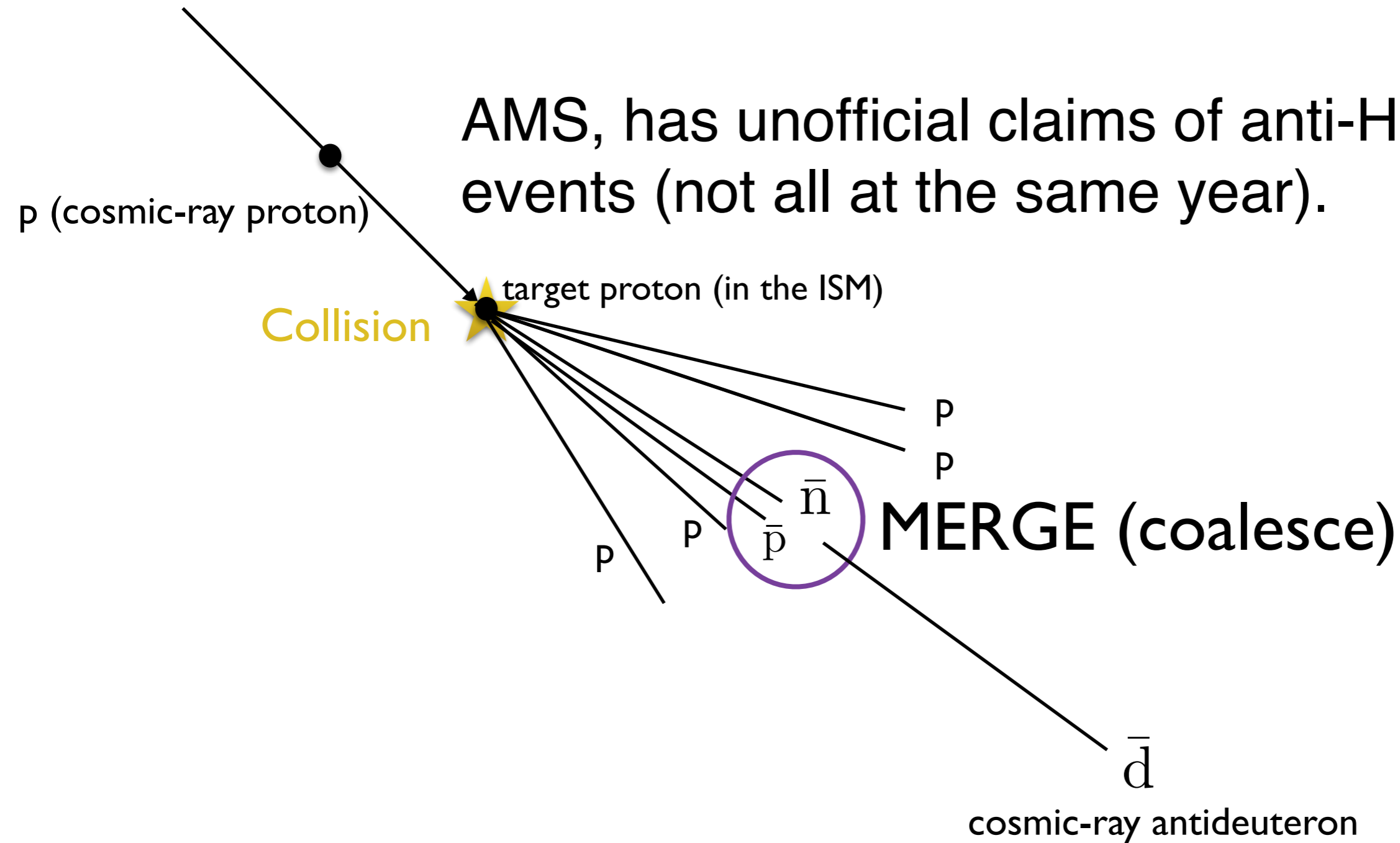
IC, Tim Linden, Dan Hooper PRD 2019

See also A. Cuoco et al. PRD 2019

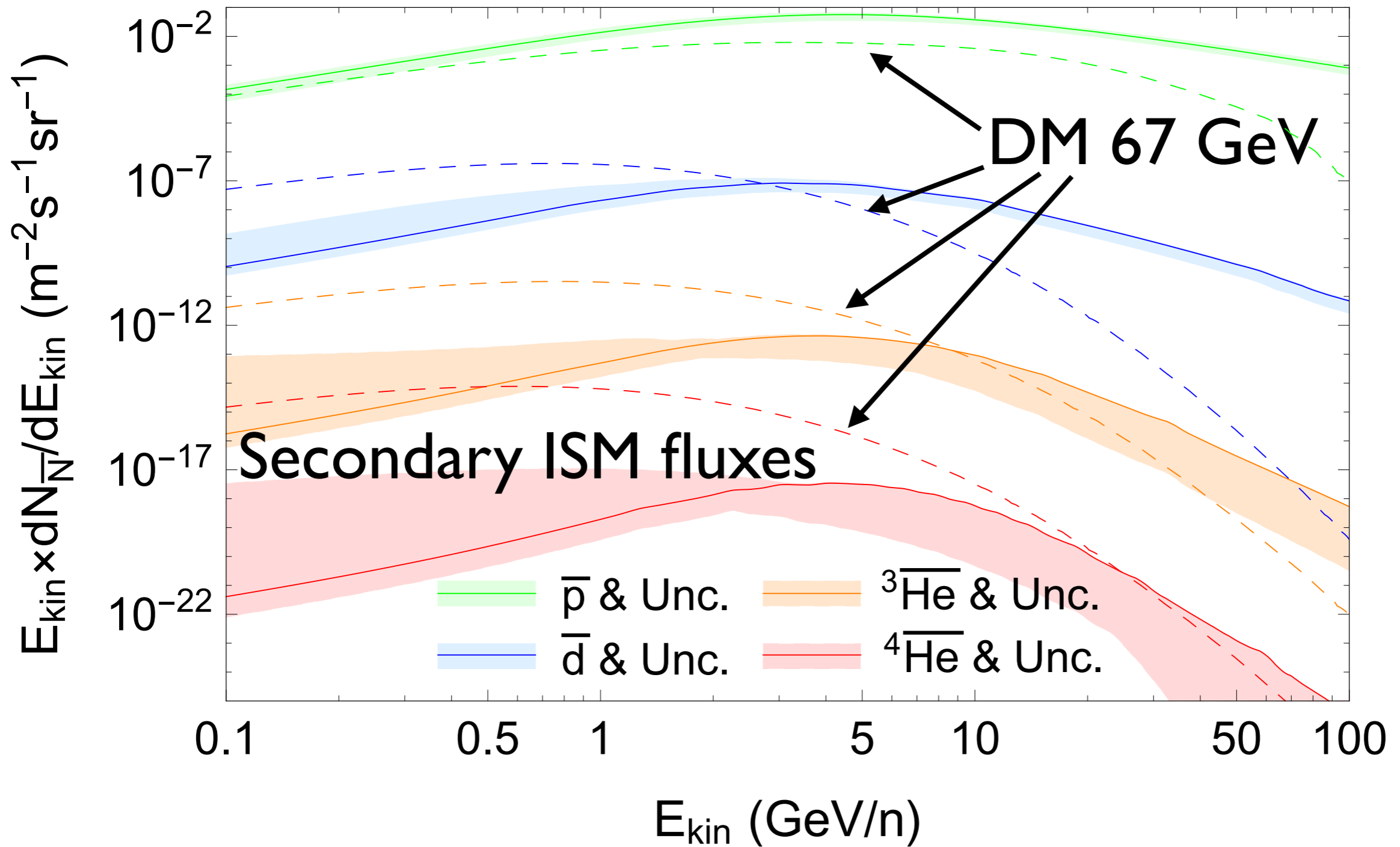
Earlier results: Cuoco et al. PLR 2017, Cui et al. PRL 2017

How about heavier nuclei?

AMS, has unofficial claims of anti-He CR events (not all at the same year).



Antimatter flux Uncertainties



And a little extra positrons....

Utilizing cosmic-ray positron and electron observations to probe the averaged properties of Milky Way pulsars

Ilias Cholis^{1*} and Iason Krommydas^{2†}

¹*Department of Physics, Oakland University, Rochester, Michigan 48309, USA*

²*Physics Division, National Technical University of Athens, Zografou, Athens 15780, Greece*

 (Received 19 November 2021; accepted 4 January 2022; published 14 January 2022)

Pulsars have long been studied in the electromagnetic spectrum. Their environments are rich in high-energy cosmic-ray electrons and positrons likely enriching the interstellar medium (ISM) with such particles. In this work we use recent cosmic-ray observations from the *AMS-02*, *CALET*, and *DAMPE*

and likely release $O(10\%)$ of their rotational energy to cosmic rays in the ISM. Finally, we find at ≈ 12 GeV positrons a spectral feature that suggests a new subpopulation of positron sources contributing at these energies.

